NASDA-TMR-950013T

NASDA Technical Memorandum

Study on Reference Trajectory for the Lunar Lander

March 1996

NASDA

NASDA-TMR-950013T

NASDA Technical Memorandum

Study on Reference Trajectory for the Lunar Lander

Yutaka Takano, Shigeaki Wada, Noriki Iwanaga

Future Space Systems Laboratory, System Engineering Department,
Office of Research and Development

National Space Development Agency of Japan

Contents

1. Preface

1.1 Introduction

NASDA is at present studying on the lunar exploration and development scenarios consisting of a progressive process of unmanned exploration, manned exploration, and exploitation. The scenario for unmanned exploration is composed of three missions: lunar orbiter, rover, and the sample return. While the systems/subsystems of a lunar orbiter and the specifications of onboard sensors have been studied, research and development efforts have focused on technologies for lander/ rover following orbital missions.

Although the Bus Unit of the lunar explorer can be applied on the existing technologies earth observation and geostationary satellites, some sensors and orbit insertion technologies need to be newly developed based on these satellites. In addition, various new developed technologies will be required for lander/rover, the sample return system, and human exploration. For example, NASDA does not have landing technology which is common to those missions. The progress from the orbiter phase to the lander/rover phase largely depends on development of the landing technology. It will be essential to continue R&D efforts on landing technology for its timely and appropriate availability.

In view of these issues, NASDA initiated to study the lunar precursor mission. It is a probe aboard the lunar orbiter, and will be launched before the development of lander/rover. This probe will be separated from the orbiter in lunar orbit, and autonomously descend down to the lunar surface. The four critical technological elements were identified through system study in fiscal 1994. For the development of the probe; the shock-absorbing mechanism (legs), the variable thrust engine, the navigation sensors, and the reference trajectory. Of these four elements, the reference trajectory is deeply interrelated with the other three; the performance requirements for the three elements determine the reference trajectory. In other word, reference trajectory must be revised if the performance requirements are not met. From this point, the reference trajectory is one of the core technological issues to development of the lunar lander.

This paper examines the landing trajectory of the lander. The resultant orbit will be a reference trajectory for future study and will help to establish the requirements for fuel consumption and for specification of the propulsion system and navigation, guidance, and control system.

1.2 History and Current Situation of Lunar Landing Technology

On September 14, 1959, Luna 2 of the former USSR achieved the first landing on the moon in the world. Although this landing is perhaps better described as "crash", it did demonstrate the technology for inserting a probe into lunar transfer orbit. Initial lunar orbiters (Luna 2 to 8/the former USSR and Ranger 6 to 9/NASA) were all collapsed at the moment of hard landing. However, these spacecraft took a number of photographic images of the lunar surface.

The first soft landing was achieved by Luna 9 on February 3, 1966. Luna 9 succeeded in taking panoramic photographs of the Oceanus Procellarum from its landing site. These photographs showed that the lunar surface was hard enough to support Luna 9 with a mass of 100 kg (at the landing). At the time, it was thought that the lunar surface was covered with layers of soft dust into which probes and astronauts would carried off their feet and be unable to move about.

Since the voyage of Luna 9, many lunar explorers equipped with various sensors have been developed by the United States and the former USSR and conducted their missions on the lunar surface. These are known as Surveyor 1 to 7/NASA and Luna 13 to 18, 20, 21, 23, and 24/the former USSR (though Luna 15 failed to make a "soft" landing) .

The Surveyor series technologically demonstrated navigation, guidance, and control systems (navigation sensors, guidance algorithms, etc,) and propulsion systems (variable thrust engine, etc.) for the landing and collected various data. The Apollo Project aimed at the first human exploration was eagerly promoted, and Apollo 11 finally succeeded on July 11, 1969 in landing in the vicinity of the Mare Tranquillitatis. The following Apollo missions 12-17 (excluding Apollo 13) landed in various mare and highlands on the lunar surface, conducted comprehensive exploration by using Luna and returned back to the Earth a total of 381 kg of samples from the lunar surface. However, the United States ceased all lunar missions, both manned or unmanned, following the Apollo 17 mission in 1972.

The former USSR, which had verified landing technology through the Lunar 9 mission, launched a number of lunar probes to the moon. While the unmanned Luna 16, 20, and 24 brought back samples of lunar resources, Luna 17 and 21 enabled the rover exploration to succeed in transversing tens kilometers across the moon. The former USSR had originally planned to carry out manned exploration, but canceled its projects.

After the acquisition of soft landing technology by these explorers, the major two spacefaring nations have not by far conducted space programs which could make the best use of the

technology. However, with the advent of the 1990s, the world has initiated to study new lunar exploration projects after a 20-year interval.

First of all, NASA launched Clementine on January 25, 1994. Clementine provided global mapping over two lunar months, and collected images of the moon's polar regions and detailed spectrometric data covering the entire surface. This data is the basis for mapping of the lunar resources and scientific study on the moon (the origin of craters, etc.). Lunar Prospector (planned launch in 1997) is being constructed to collect detailed data on the moon's polar regions for the search of water whose existence Clementine suggested.

European Space Agency (ESA) is under consideration to develop a lunar orbiter called MORO. This orbiter will separate two probes on the orbit, and the lunar gravitational potential will be measured from comparison of altitude and velocity of those orbiters.

Some concepts of lander/rover are being studied by the private and academic sectors in US. Under these concepts, the lander will be equipped with a rover which will carry out comprehensive probes in the vicinity of the landing site. Followings exemplify some of the concepts.

(1) Pele Project

This is a joint research project between McDonnell Douglas Corp. and the University of Hawaii. The project envisions the launch of modified Russia's rover to the lunar surface, where it plans to collect data on the lunar volcanoes and the topography.

(2) Interlune-One Mission

This is a joint research project between the University of Wisconsin and Space Industries International Corp. Using two rover vehicles, the mission is designed to analyze lunar regolith and search for Helium 3 and other mineral resources. One of the rovers will be a macro-rover with a mass of 163 kg, and the other will be a micro-rover with a mass of 10 kg.

(3) Jules Verne Rover Mission

This is a joint research project between the Johnson Space Center and the University of California. The mission will use a lunar rover to probe the lunar mantle and internal structure.

(4) LunaCorp's Rover

This is a research project of the LunaCorp. The objectives are to promote space-related education and to interest ordinary students in space by allowing them to manipulate a rover weighing approximately 400 kg. The project envisions the use of a landing device (with a 600 kg payload capability) proposed by ISE Co.

In Japan, the Institute of Space and Astronautical Science (ISAS) inserted the 13th scientific satellite 'Hiten' into a lunar transfer orbit in January 1990. At the same time, the ISAS succeeded in inserting 'Hagoromo' into a lunar orbit. These events demonstrated that Japan has established the insertion technology to lunar transfer/ polar orbit, and operational techniques. The next lunar probe will be the launch of the 17th scientific satellite 'Lunar-A' in fiscal 1997. This probe will strike three penetrators (exploratory probes) to conduct research of the internal structure. It is of the hard landing type, however, it will be Japan's first step on the moon.

Japan, being lagged behind the United States and the former USSR for 20 years, has thus taken its first step into the exploration of space near the moon. However, Japan has not developed technology required for the subsequent missions following the orbiter, and has not yet verified the soft landing technologies.

1.3 The Significance of Lander and Rover Mission

To us, who live on the earth, the moon is the closest heavenly body. Human beings has always explored unknown lands. Cultivating the habitable area widely has helped to advance the progress of civilization. Given the present situation that human beings live in most of lands on the Earth and enjoyed some benefits from space development activities, incentives for the lunar exploration and development simply spring from the human nature. In short, such explorations are most certainly the result of the intellectual curiosity about unknown lands and also reflect urge to gain deeper scientific understanding of far-away lands and our dream of going there.

The expansion of space activity to the moon involves verifying technological and economical feasibility. Small-scale but thorough probe will be required as a precursor mission before full development. One objective of our lunar missions will be to resolve a variety of questions, including how the moon can be developed, what resources are on the moon and what their potential uses are, what technologies will be needed to utilize the resources, and how much the activities will cost.

The exploration of the moon undertaken by the Apollo missions about 20 years ago demonstrated the technology for lunar landing on/off and the sample return. It was also confirmed that there existed titanium ore and other mineral resources as well as Helium 3, hydrogen gas, and other energy sources. The future lunar exploration will be conducted by using those resources, rather than consuming terrestrial resources. However, the explored lunar surface area is very small compared to its total surface area and data on the distribution of the lunar resources is quite insufficient.

Interest in the moon has recently reemerged, especially in the United States. While NASA developed and launched Clementine to collect precise optical images over the entire lunar surface in 1994, Lunar Prospector is being developed as the follow-on mission.

As with earth observation programs, remote sensing observation is the most suitable for collection of wide-area data, however the limited resolution of onboard sensor has disadvantage over the local observation. Moreover, data correction for accurate analysis requires in situ data. In other words, it is necessary to land on the lunar surface and explore the vicinity, combining with the orbiter mission.

The most recent lunar exploration initiatives in the United States focus largely on development of a miniature rover through application of the advanced miniaturization and robotics. This

rover will allow detailed exploration not only around the landing site, but also of a wide area of the vicinity. It world-widely appears to become aware of the importance of lander/rover mission.

Exploration through lander/rover has the significance not only for its collected data but also for technology verification. For example, soft landing technology is also critical to missions following lander/rover exploration, such as sample return and small-scale manned exploration. Moreover, it is also critical to the project of 'Lunar Astronomical Observatory', because of the necessity of transporting payloads to the moon, such as telescopes.

Therefore, it will be necessary to demonstrate the complete safe and high performance of soft landing technology in order to achieve future lunar development.

1.4 Required Technology for Lander and Rover Mission

The following four are considered to be key technologies for landing on the lunar surface.

(1) Shock-absorbing mechanism

Legs absorb the impact at the time of landing and protect electronics and payloads. For the US Surveyor and Apollo missions, the buckling of aluminum honeycomb legs absorbs the impact. Japan has no these domestic devices.

(2) Variable thrust engine

Variable thrust engines are required to control velocity during the descent and landing.

(3) Navigation sensors

The lander needs onboard altimeters and speedometers in order to accurately measure altitude and velocity of the lander. In the Apollo and Lunar missions, these sensors operated at the altitude of 10 km or less for correction of IMU data. Japan has developed such commercially developed components (including those manufactured under licensing agreement), rather than space-qualified ones.

In addition, there is likely to be a necessity of developing sensors that can automatically detect obstacles, such as lava boulders and craters on the landing site.

(4) Reference trajectory

The lander must safely land at the targeted site to ensure that required fuel is minimized and the functional requirements are met for each subsystems. In addition, it will be necessary to devise the specifications of each subsystem in order to meet the requirements of the reference trajectory.

For orbiter mission with exception of some onboard sensors and insertion technologies, it is basically feasible to apply the existing technologies used for earth observation and geostationary satellites. However, various newly developed technologies will be required for lander/rover. Neither has NASDA demonstrated landing technology which is common to those missions, nor developed the technologies that has the potential to be applicable. The successful progress from the orbiter phase to the lander/rover phase largely depends on development of the required system

technology. It will therefore be essential to continue R&D efforts on landing technology for its timely and appropriate availability.

In view of these issues, NASDA initiated to study the lunar precursor mission. It is a probe aboard the lunar orbiter, and will be launched before the development of lander/rover. This probe will be separated from the orbiter in lunar orbit, and autonomously descend down on the lunar surface. The probe is expected to demonstrate four critical technologies which were mentioned earlier.

Of these four technologies, the reference trajectory is deeply interrelated with thrust (maximum thrust, variable range, etc.), navigation sensors (imaging angle, precision, field of view, etc.), and impact tolerance at landing. In other words, these specification requirements are essential to evaluate propellant weight and landing precision which determine the reference trajectory.

If subsystem study proved that these specifications are not feasible, reference trajectory must be appropriately changed and the impact of its change on the entire system must be evaluated.

Since the reference trajectory plays an extremely important role in landing technologies, it should be carefully examined along with system study for precursor mission and its follow-on mission, or prior to their subsystem study.

This paper examines the landing trajectory of lander. The resultant orbit will be a reference trajectory for future study and will help to establish the requirements for weight of fuel consumption and for specifications of the propulsion system and navigation, guidance, and control system.

2. Outline of Lander System

2.1 Outline

The small lander is a demonstrator for soft landing technology which is a critical element for the future exploration missions. This system mounted on the lunar orbiter has autonomous propulsion and guidance systems, and softly lands on the surface after separation from the orbiter.

The onboard transmitter will be used to conduct Δ VLBI experiment mission for one year after landing.

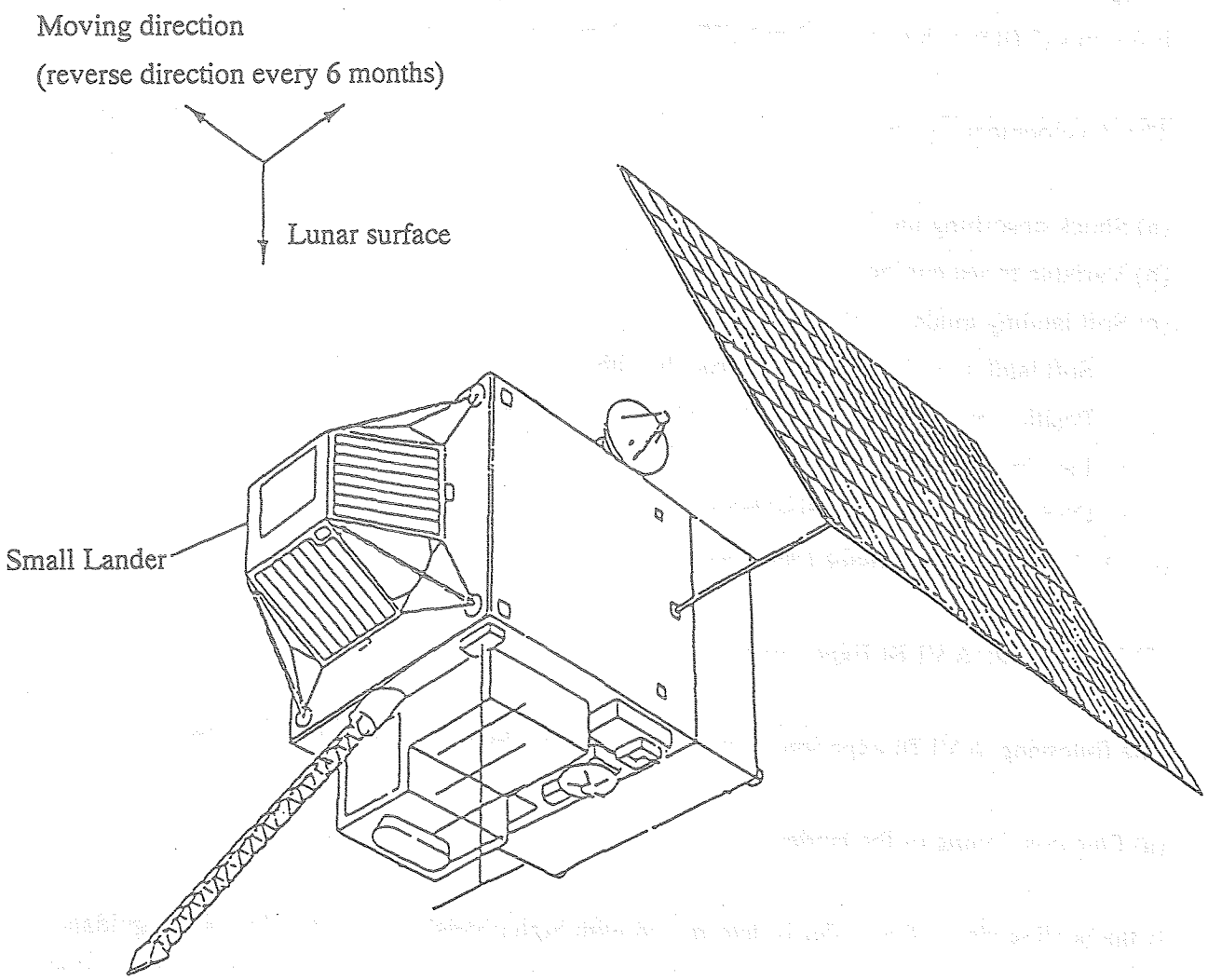

Figure 2.1-1 Configuration of the Small Lander (attached to the orbiter)

2.2 Mission of the Lander

The main purpose of the small lander mission is to demonstrate the technologies necessary for descent/ soft landing, through which it is expected that technical data for the development and operation of the future lunar lander (with a rover) will be gained. As optional missions, △ VLBI, including the fine positioning and the physical liberation of the moon, will be conducted by using the onboard transmitter for one year after landing.

(1) Mission #1: Descent and soft landing experiment

The small lander is separated from the orbiter in lunar orbit at an altitude of 100 km and softly and autonomously lands on the surface. Details of the reference trajectory for descent and soft landing will be discussed later in this paper. Here the conditions for soft landings are hypothesized as being similar to those of the Apollo missions; radial and horizontal velocity just before touchdown is 3.0 m/s (TBD) or less and 1.2 m/s (TBD) or less, respectively.

The development and operation of this lander is expected to verify the following technologies.

(a) Shock-absorbing mechanism
(b) Variable thrust engine
(c) Soft landing guidance and control
- Soft landing guidance and control algorithm
- Positioning and decent velocity computation through onboard navigation sensors
- Landing precision
- Obstacle detection and avoidance

(d) Optimization of reference trajectory

(2) Mission #2: Δ VLBI Experiments

The following Δ VLBI experiments will be carried out by using onboard transmitter.

(a) Fine positioning of the lander

If the landing site of the lander is determined with high precision, the precision of the guidance and control systems will be verified and the required technologies for positioning of rover shall be available.

(b) Collection of the lunar gravitational potential data

The lunar gravitational potential affects the orbit of the orbiter. Data on the relative positions of the orbiter and the lander through Δ VLBI experiments will improve an estimation of the gravitational coefficients with 4 to 5 digit precision. These data will help to enhance the precision of the landing guidance and control system in the future stages.

(c) Observation of the physical liberation of the moon

The position of the lander will be slightly affected by the physical liberation of the moon. Data on the physical liberation of the moon will be collected through highly precise measurements of the positional changes of lander. These data will improve the measurement of the lunar inertia moment and evaluate the internal structure of the moon, particularly the density of its core.

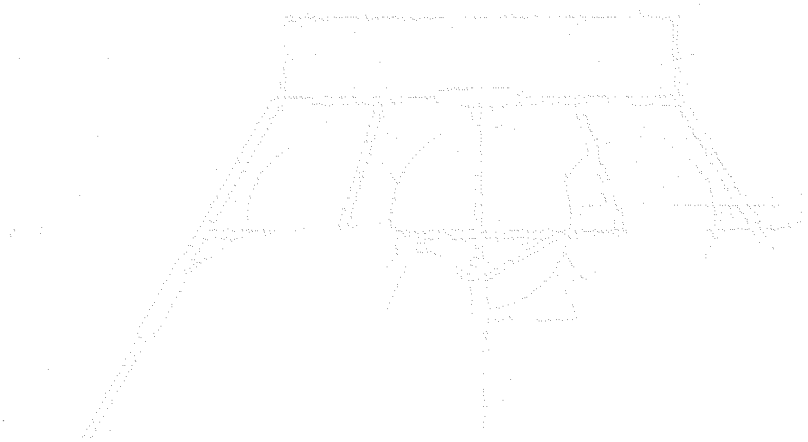

2.3 System Characteristics

Figure 2.3-1 and Tables 2.3-1 to -2 show a conceptual diagram of the small lander, its main characteristics, and its mass and electrical power distribution.

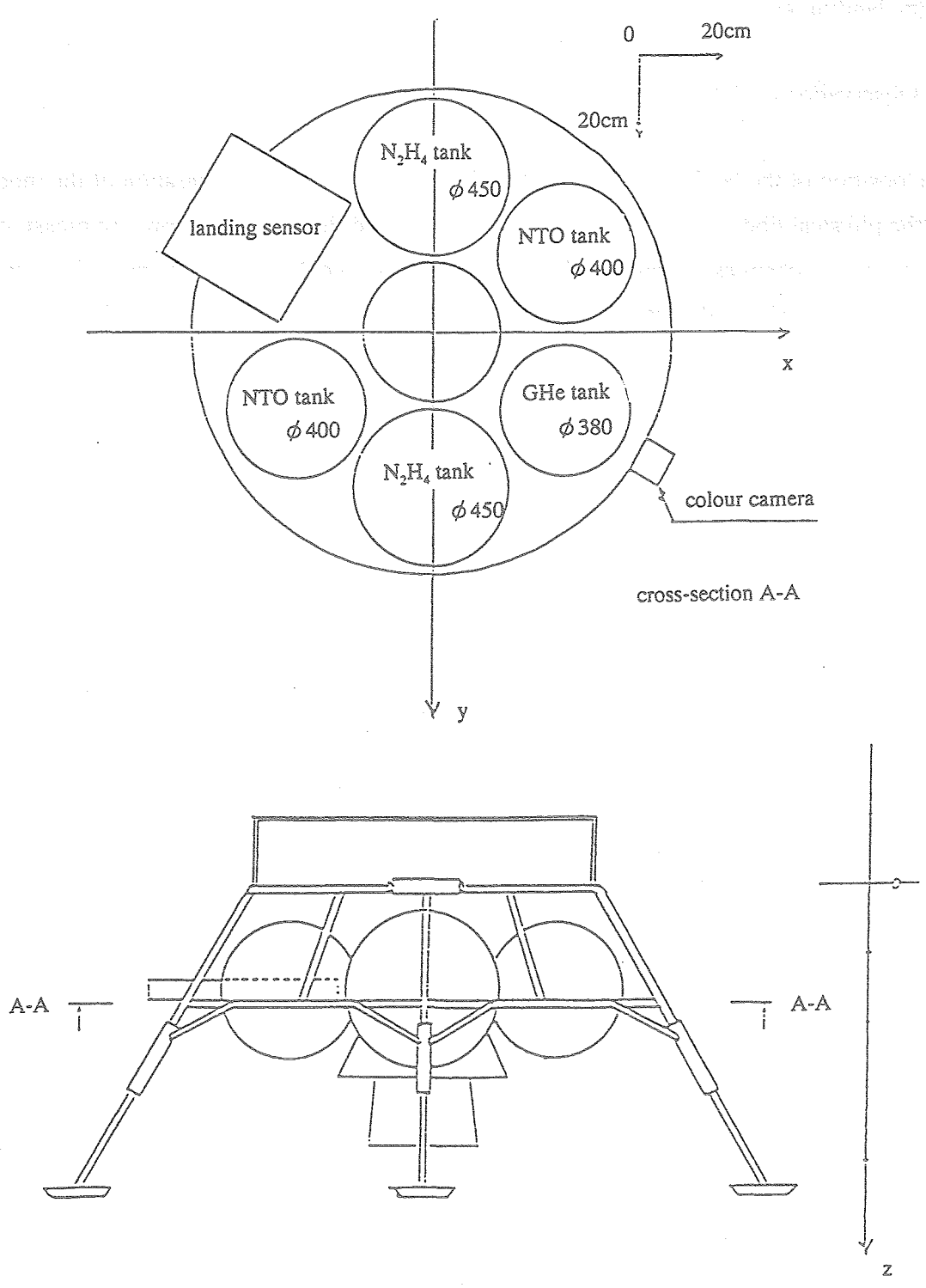

Figure 2.3-1 Overview of the Small Lander (planned)[*1]

Table 2.3-1 Main Characteristics of the Lander(planned)[*1]

Item	Main characteristics
Dimension	1,100mm (H), 2,200mm (distance between legs)
Mass (total)	350kg, 410kg (including VLBI mission)
Initial orbit	Separation at 100km altitude, 95° incl. and shift to descent/landing mode
Subsystem	
Structure	Panel/truss structure, Aluminum honeycomb 4-legged landing with shock absorber
Propulsion	Main thruster〔NTO/N_2H_4〕:1,000N x 1 (variable range: 250-1,000N) RCS (roll)〔NTO/N_2H_4〕:1N x 4 RCS (pitch)〔NTO/N_2H_4〕:50N x 2 RCS (yaw)〔NTO/N_2H_4〕:50N x 2 RCS (for separation)〔N_2H_4〕:1N x 4 〔Specific Impulse (Isp)〕 main thruster :300 seconds RCS : 210 seconds
Electric power	Secondary lithium battery Solar cells (when performing VLBI mission)
Navigation, guidance and control	IMU, mission sensors (radio altimeter/speedometer) 〔This IMU will be set up by navigation data (location, velocity) collected by the orbiter〕
Communication/data transmitting	Transmission and reception of S-band telemetry, command and images (except for transmitter for VLBI)
Mission	A set of colour camera Transmitter (when performing additional VLBI mission)

Table 2.3-2 Mass Distribution of the Lander[*1] (Unit:kg)

	Including VLBI mission	No VLBI mission
Structure	34.5	31.5
Thermal control	8.8	8.0
Propulsion	74.6	73.0
Navigation, guidance and control	26.0	26.0
Electric power	32.0	11.0
Communication/data transmitting	13.5	13.5
Mission	4.0	2.0
Integration hardware	11.0	10.0
Dry mass	204.4	175.0
Propellant weight	205.6	175.0
Total mass	410.0	350.0

3. Outline of Reference Landing Trajectory

The reference trajectory is defined here as the flight path from the initial powered descent after deorbit from the lunar orbit to the touchdown on the lunar surface.

This chapter outlines the premises and the orbit.

3.1 Premises

(1) Lunar model

Gravitational Potential model: Spherical (gravitational acceleration: 4.902778 x 10 km^3/sec^2)
Landing site model: Mare on the visible side of the moon. See 4.3.1 for details.
Others: a. Analysis as two-dimensional problems including lunar orbital plane
b. Two-body problems; Moon and the lander. No consideration to other celestial bodies.
c. No consideration to lunar rotation

(2) Lander model

Total mass: 350 kg (at the time of separation from the orbiter)[*1]
Specific impulse: 300 sec.
Main engine thrust: 250-1,000N (continuously variable)
Thrust axis: Roll axis, no gimbal mechanism
Attitude control: RCS (the analysis of propellant weight in this paper excludes fuel for attitude control by RCS)

(3) Orbit parameters

At start of descent: Lunar orbit
Altitude: 100 km (orbit radius: 1,838 km)
Inclination: 95 degrees
At touchdown: Target altitude: 0 km (1,738 km from center of moon)
Velocity just before touchdown: 3 m/s or less (radial), 0 m/s or less (horizontal)[*2]

(4) Orbit design concept

a) Minimum consumption of propellant

b) Optimally safe landing

Note 1: NASDA-GAF-94024B derived the total mass of 350 kg from the assumptions of (1) the dry mass of the lander at 175 kg and (2) ΔV of 2040m/s.

Note 2: NASDA-GAF-94024B specifies performance requirements for the structure systems (lander systems) at a horizontal velocity of 1.2 m/s or less.

3.2 Outline of Reference Landing Trajectory

The basic concept of the trajectory design is for the landing to be minimum-fuel and safe.

From the perspective of minimum-fuel use, the lander will first deorbit the lunar orbit and transfer to the Hohmann transfer orbit. It will then be guided into the minimum-fuel orbit derived from the optimum control theory. Compared with the direct entry into the minimum-fuel trajectory, the application of Hohmann orbit has a major advantage in a greater reduction in fuel consumption. This is partly because minimum-fuel trajectory only depends on powered descent with keeping thrust variable (See 4.1 for details). This guidance applied to the minimum-fuel trajectory is named E-guidance by an originator of Cherry and it will hereinafter be called E-guidance (See 4.2 for details).

E-guidance has the advantage over the guidance law, which was in 1993 derived from constant thrusting condition (bilinear tangent law), in providing viability and reducing computation time.

From the safe landing perspective, the lander will finally follow the vertical descent path by combination of a given constant velocity and constant acceleration descent. This descent approach will use simpler guidance and is expected to alleviate the load on the propulsion systems. Although this final descent phase will not necessarily contribute to minimizing fuel consumption, the difference of fuel consumption will be only less than 1 kg compared to E-guidance decent path.

Finally, it was proposed in fiscal 1994 that reference trajectory should consist of three orbits; Hohmann, minimum-fuel guidance, and vertical descent.

Figure 3.2-1 shows a flow of the reference trajectory design.

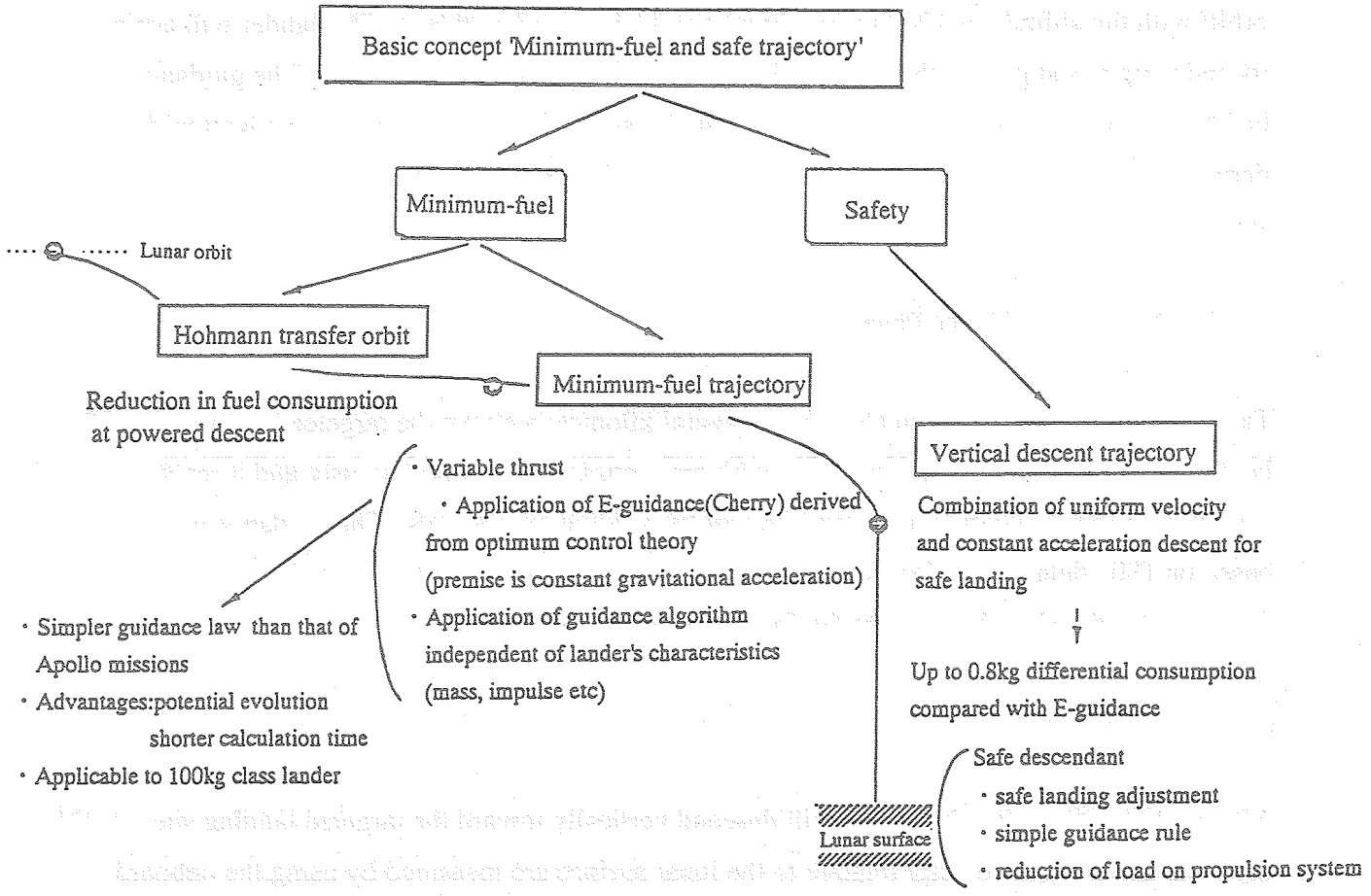

Figure 3.2-1 Reference Trajectory Design

An outline of each phase will be shown below.

(1) Hohmann Transfer Orbit Phase

The lander will be separated from the orbiter in lunar orbit, and move around the orbit at an altitude of 100 km. Then, it will fire its main engines and transfer to an elliptical orbit (Hohmann orbit) with the altitude of 100 km (perilune) and 15 km (pericynthian). The lander will again fire its main engines at pericynthian, and initiate the descent to the lunar surface. The guidance will be based on IMU data on acceleration and angular acceleration as well as the navigation data derived from the altitude and velocity input prior to the separation from the orbital navigation system.

(2) Fuel Minimal Guidance Phase

Target #1 will be located at an altitude of several kilometers above the targeted landing site. The lander will be guided toward Target #1, with main engines fired continuously and it reaches a (inertial) horizontal velocity of 0 m/s and a radial velocity of tens m/s. The guidance will be based on IMU data on acceleration and angular acceleration as well as the navigation data derived from the altitude and velocity input prior to the separation.

(3) Final Descent Orbit Phase

After passing Target #1, the lander will descend vertically toward the targeted landing site. At this time, the altitude and velocity relative to the lunar surface are measured by using the onboard landing sensors (radio altimeter and radio speedometer) in order to ensure the safe landing on an uneven surface. Based on IMU data and navigation data, the lander is appropriately guided to the targeted site.

This phase are subdivided into the following three phases.

a) Safe Landing Adjustment

After passing Target #1, navigation data is corrected so as to ensure the safe landing on the an uneven surface while the lander is descending vertically at a constant velocity. This phase will continue until the lander reaches Target #2 (an altitude of 1.4 km above the targeted landing site), which was derived in section 4.3.2.

b) Vertical Descent Phase

After passing Target #2, the lander will descend vertically at a given acceleration until it decelerates to the velocity of the final descent phase (1.5 m/s). This phase will continue until the lander reaches Target #3 (an altitude of 10 m above the targeted landing site), which was derived in section 4.3.2.

c) Final Descent Phase

After passing Target #3, the lander will descend vertically at a constant velocity to a point of 2 m above the targeted landing site, at which time the main engine will be cut off. The lander will fall to the landing site.

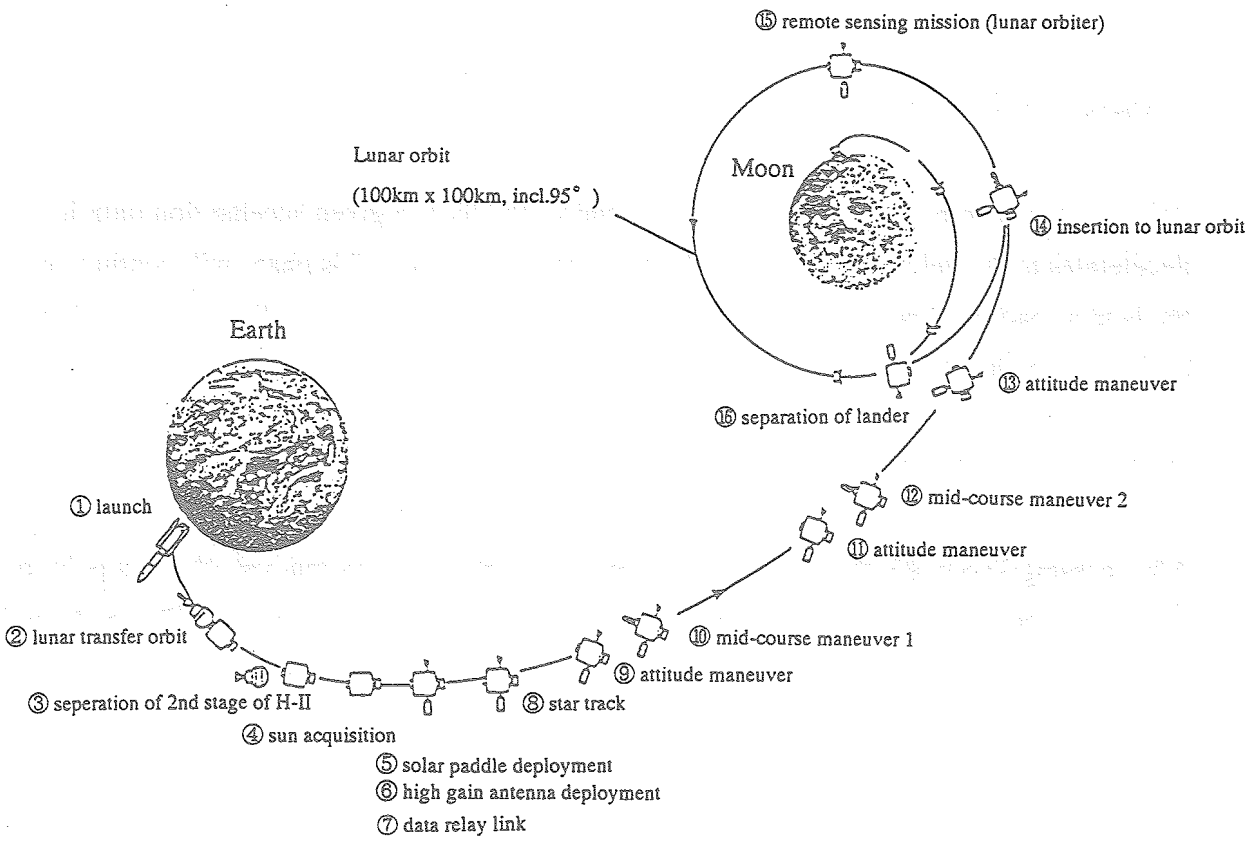

Figure 3.2-2 Mission Profile of the Lander

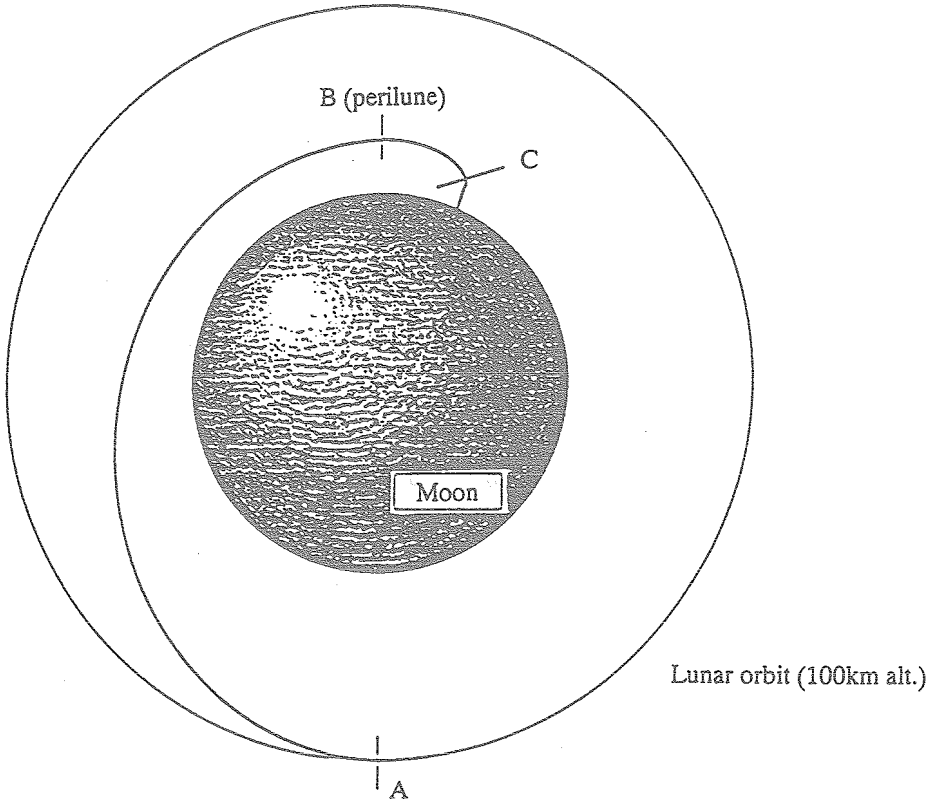

Figure 3.2-3 Mission Profile of the Lander 2

A～B: Hohmann transfer orbit phase (100 x 15km)

B～C: Minimum-fuel trajectory phase

C～lunar surface: Final descent phase

Reference (Chapter 1-3)

1. NASDA, Future Space Systems Laboratory; Reference Model of Lunar Lander Systems (planned) B-revised version, March 1995, GAF-94024B

2. NASDA, Future Space Systems Laboratory; Study on Lander Mission and System Concept (hands-out for presentation), October 1994

3. NASA; APOLLO 11 LUNAR LANDING MISSION -PRESS KIT-, (1969), pp33

4. Niclolas L. Johnson; Handbook of Soviet Lunar and Planetary Exploration, (1979); An American Astronautical Society Publication, pp54

5. Mori, Takizawa, Kaneko, Kawazoe, Takano, Namura; Feasibility Study on Lunar and Mars Exploration, NASDA Technical Memorandum (1995), NASDA-TMR-950001

6. NASDA, Future Space Systems Laboratory; Feasibility Study on Lunar and Mars Exploration (source material), (1994), RS-S94005

7. NASDA, Long-term Space Development Study Team, Lunar and Planet Study Working Group; Report on Lunar and Planet Working Group Study, March 1994, pp1-11

8. G.H. Heiken et al., Lunar Sourcebook: Cambridge Univ. Press, (1991)

9. SPACE NEWS, March 6-12, 1995

4. Details of Reference Landing Trajectory

4.1 Hohmann Transfer Orbit Phase

The lander will be separated from the orbiter in lunar orbit, and fly around the orbit at an altitude of 100 km. Then, it will thrust its main engines and transfer to an elliptical orbit (Hohmann orbit) with altitude of 100 km (perilune) and 15 km (pericynthian). The lander will again thrust its main engines at pericynthian, and initiate the powered descent to the lunar surface, by using E-guidance algorithm. The guidance will be based on IMU data related to the acceleration and angular acceleration data provided by the onboard IMU as well as the navigation data (position and velocity) derived from the location and velocity input prior to separation.

This chapter will focus on the effect of pericynthian altitude on the landing lander mass. Three cases were assumed with the altitude of pericynthian at 12, 15, and 18 km respectively, with one-degree shift of the orbit transfer angle from 13 to 20 degrees. In addition, the maximum landing mass was calculated in the range of 13-14 degrees. Moreover, calculations were made for another assumption that lander would directly transfer to E-guidance trajectory after deorbiting the lunar orbit. This objective is to ensure significance of application of Hohmann trajectory.

Figure 4.1-1 shows an outline of the four cases discussed in this chapter.

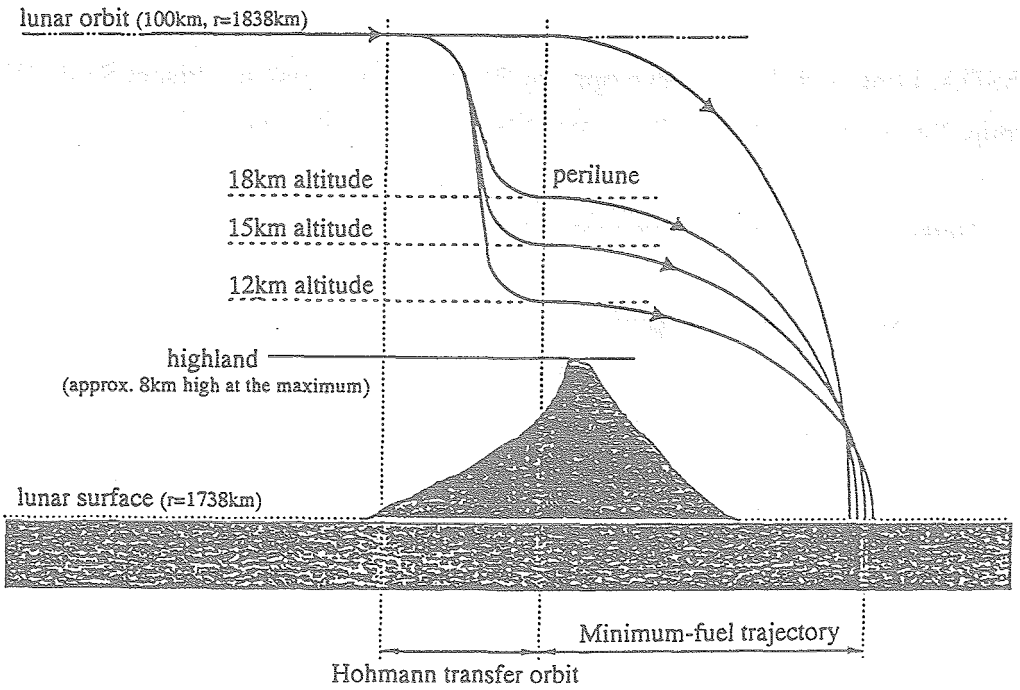

Figure 4.1-1 Overview of Reference Trajectory

In general, when the sweep angle is too small, the flight time to the lunar surface becomes too short to decelerate sufficiently. In other words, the minimum-fuel consumption theory is achieved when sweep angle is conditioned to be more than a given degrees. This study identified the threshold was 13 degrees or less.

The trajectory based on E-guidance is subject to the sweep angle (α) and the flight time (Ttg). In the case of the same sweep angle, the shorter flight time results in the greater landing mass. Table 4.1-1 shows flight time (Ttg) and the resultant maximum landing mass for each of the sweep angles in the four cases. From this Table, it can be understood that the smaller angle results in the greater mass and the shorter flight time. Moreover, the higher the starting altitude of powered descent (pericynthian), the smaller the sweep angle.

Table 4.1-1 Altitude of Pericynthian and Landing Mass (Flight time)

Sweep angle (deg)	12km alt.	15km alt.	18km alt.	Lunar orbit (100km)
	Mass (Ttg) kg (sec)	Mass (Ttg) kg (sec)	Mass (Ttg) kg (kg)	Mass (Ttg) kg (sec)
13	---	---	---	---
13.20	---	---	---	176.3 (525)
13.84	---	---	186.0 (509)	---
13.88	---	186.2 (511)	183.8 (537)	---
13.90	---	184.9 (526)	183.2 (545)	---
13.93	185.7 (519)	183.8 (540)	182.5 (555)	---
14	183.4 (549)	182.2 (562)	181.2 (573)	166.5 (743)
15	173.5 (707)	173.0 (712)	172.5 (718)	162.7 (846)
16	168.0 (808)	167.6 (813)	167.6 (818)	159.3 (934)
17	163.5 (895)	163.2 (899)	162.9 (903)	156.2 (1,014)
18	159.6 (973)	159.3 (978)	159.0 (982)	153.1 (1,090)
19	155.9 (1,048)	155.7 (1,052)	155.5 (1,056)	150.2 (1,163)
20	152.5 (1,119)	152.4 (1,122)	152.2 (1,126)	147.4 (1,233)

*Figure in parenthesis indicates flight time.

Based on Table 4.1-1, Table 4.1-2 shows the minimum-fuel consumption for each altitude of pericynthian, the resultant sweep angles and flight time.

Table 4.1-2 Minimum Fuel Consumption at Each Altitude and Other Interrelated Factors

Alt. of Pericynthian	12km	15km	18km	Lunar orbit (100km)
Landing Mass (kg)	185.7	186.2	186.0	176.3
Consumption (kg)	164.3	163.8	164.0	173.7
Sweep angle (deg)	13.93	13.88	13.84	13.20
Flight time (sec)	519	511	509	525

<Calculation Conditions>

(1) E-guidance[*1] is used as algorithm.
Engine thrust is limited to 250-1,000 N.

(2) Table 4.1-3 shows the mass at the point of pericynthian (before the start of powered descent) and horizontal velocity.

Table 4. 1-3 Mass and Velocity at Pericynthian

Alt. of Pericynthian (km)	Mass (kg)	Velocity (m/s)
12	347.6	1,694
15	347.7	1,692
18	347.8	1,690
100	350.0	1,633

Notice: Initial mass excludes necessary propellant weight (2.2~2.4kg) for deorbiting Hohmann transfer orbit from total mass (350kg) at separation.

(3) Terminal conditions
- Altitude: 0 km
- Velocity: 0 m/s (initial horizontal and radial directions)
- The sweep angle from the starting point of descent will be 13-20 degrees (by one-degree shift)
- Attitude: 0 degree (both landing legs and thrust vector are vertically oriented to the surface)

The results of the calculations are summarized below.

(1) The smaller the sweep angle, the shorter the flight time and the greater the landing mass.

(2) The lower the altitude of pericynthian, the greater the landing mass, under the condition of the same sweep angle.

(3) The landing mass achieves its maximum when the sweep angle is around 14 degrees. In these altitude conditions (12, 15, and 18 km), each maximum landing mass has no major differences when the sweep angle is shifted by 0.01 degrees.

---

*1 This is named based on the original paper which first formulated this guidance law. See section 4.2 for details.

(4) The landing mass is smallest in the case when the lander directly transfers to E-guidance trajectory after deorbiting the orbit at an altitude of 100 km.

The results proved that the reference trajectory had advantages in achieving greater landing mass. In these analyses (12, 15, and 18 km), each landing mass has no major differences. Therefore, altitude of pericynthian should be determined with emphasis on factors related to safe landing (ex. the uneven feature) rather than landing mass.

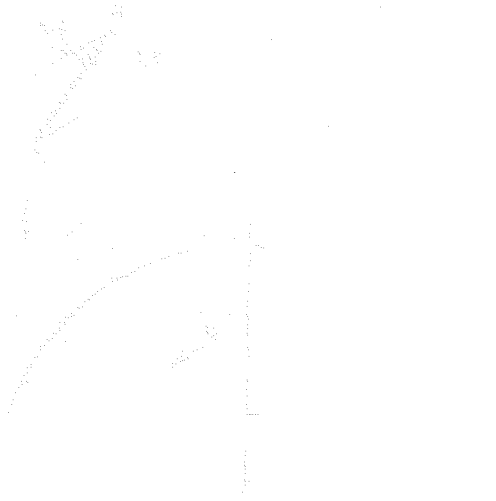

<Coordinate System>

Figure 4.1-2 shows a summary of the coordinate system used in the orbit analysis.

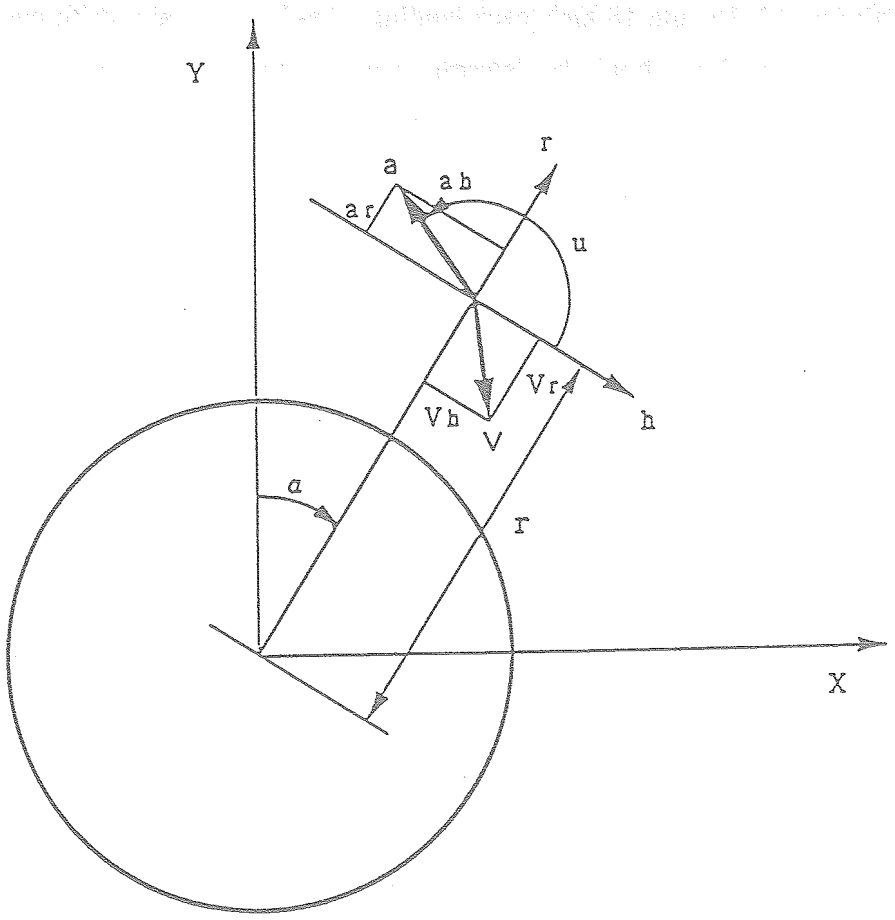

α : sweep angle
r : orbital radius
V: velocity of lander
Vh: horizontal (in inertial)
Vr: radial (in inertial)
a : acceleration of lander
a_h : horizontal (in inertial)
a_r : radial (in inertial)
u : control angle

Figure 4.2-1 Coordinate System in Analysis of Orbit

4.2 Minimum-Fuel Orbit Phase

4.2.1 Determination of Evaluation Functions

Let the initial mass of lander be $M(t_0) = M_i$, and the final mass be $M(t_f) = M_f$. To minimize M_f, we have

$$J_0 = M_f \quad (1)$$

The relation between mass increasing ratio per unit time and fuel consumption rate is

$$\dot{m} = -\dot{M}$$

Then, the mass of the lander at arbitrary time and at the termination is expressed by

$$M(t) - M_0 = \int_{t_0}^{t} \dot{M}\, dt \quad (2)$$

or

$$M_f = M_0 - \int_{t_0}^{t_f} \dot{m}\, dt \quad (3)$$

From (2) and (3), the following equation should have the minimum value, instead of (1).

$$J_1 = \int_{t_0}^{t_f} \dot{m}\, dt$$

In view of the equation of motion in the lander,

$$\frac{dP}{dt} = K$$

the right hand side of the equation can be expressed in a different form.

$$(M+dM)(v+dv)+(-dM)(v-v_e)-Mv=Mg$$

yields

$$Mv = T + Mg \quad (4)$$

$$T = -Mv_e = mv_e$$

or

$$\dot{v} + \frac{\dot{M}}{M} v_e = g \quad (5)$$

The engine velocity is constant in a vacuum. Thus, by denoting to

$$v_e = \text{Const.}$$

and integrating formula (5) over time, we obtain

$$(v_0+\Delta v_0) - v_0+v_e \int_{M_0}^{M_0-\Delta M_1} d(\ln M) = \int_{t_0}^{t_0+\Delta t_1} g\, dt$$

and furthermore

$$\Delta v_D = -v_e \ln\left(1+\frac{\Delta M_0}{M_0}\right)+g\Delta t_0$$

Therefore, the increase in mass after the first pulse is given by

$$\Delta M_1=M_0\left[-1+\exp\left\{-\frac{v_{e1}}{{v_{e1}}^2}(\Delta v_1-g\Delta t_1)\right\}\right]$$

and then the fuel consumption is

$$\Delta m_1=M_0\left[1-\exp\left\{-\frac{v_{e1}}{{v_{e1}}^2}(\Delta v_1-g\Delta t_1)\right\}\right]$$

After the second pulse, we have

$$\Delta m_2=(M_0-\Delta m_1)\left[1-\exp\left\{-\frac{v_{e2}}{{v_{e2}}^2}(\Delta v_2-g\Delta t_2)\right\}\right]$$

$$\Delta m_3=(M_0-\Delta m_1-\Delta m_2)\left[1-\exp\left\{-\frac{v_{e3}}{{v_{e3}}^2}(\Delta v_3-g\Delta t_3)\right\}\right]$$

Thus, after the Nth pulse, the fuel consumption is given by

$$\Delta m_{TOT}=\Delta m_1+\Delta m_2+\cdots+\Delta m_N$$

$$=M_0\left[1-\exp\left\{-\sum_{k=1}^{N}\frac{v_{ek}}{{v_{ek}}^2}(\Delta v_k-g\,\Delta t_k)\right\}\right]$$

Therefore, the following function is the minimum value for the total fuel consumption.

$$J_2=\int_{t_0}^{t_f}\frac{v_e}{{v_e}^2}\cdot dv_T$$

Here it should be noted that the formula

$$dv_T=dv-g\,dt$$

is the acceleration relative to thrust.

The relation between the engine velocity and thrust acceleration is

$$V_e\propto -dv_T,$$

which yields

$$J_2=-\int_{t_0}^{t_f}\frac{1}{v_e}dv_T$$

Substitution of the formula defining specific impulse

$$Isp=\frac{T}{\dot{m}g}=\frac{v_e}{g}$$

yields the formula

$$J_2=-\int_{t_0}^{t_f}\frac{dv_T}{Isp\cdot g}$$

Since v_e = Const. as noted above, it is possible to introduce Isp=Const. as an assumption.

Thus, the resultant function can be expressed by the formula

$$J_3 = \int_{t_0}^{t_f} d\, v_T$$

This is equivalent to determining the trajectory which allows less thrust acceleration or input energy for each time.

Therefore, the final form of the evaluation function is

$$J_4 = \frac{1}{2}\int_{t_0}^{t_f} a_T^2\, dt \qquad (6)$$

4.2.2 Derivation of E-Guidance

Formula (4) can be also rewritten as

$$\dot{r} = v$$

$$\dot{v} = a_T + g$$

Thrust acceleration of the lander is expressed by

$$a_T = -\frac{\dot{M}}{M} v_e \left(= -\frac{\dot{m}}{M} v_e\right)$$

Applying the lunar-centered coordinate system, the initial conditions are

$$r(t_o)=r_o,\ v(t_o)=v_o \quad (7\text{-}1)$$

and the final conditions are

$$r(t_f)=r_D,\ v(t_f)=v_D \quad (7\text{-}2)$$

To satisfy the boundary conditions and equation of motion, we want to minimize the fuel consumption, which is equivalent to find the minimum value of the equation below.

$$J = \frac{1}{2}\int_{t_0}^{t_f} a_T^2\, dt \qquad (6)$$

According to the optimal control theory, using Hamilton's equation which is defined as

$$H = \frac{1}{2} a_T^2 + \lambda_1 \cdot v + \lambda_2 \cdot (v_T + g) \qquad (8)$$

we need to solve the following equations of motion,

$$\dot{\lambda}^T = -\frac{\partial H}{\partial \lambda} \qquad (9)$$

$$\frac{\partial H}{\partial a_T} = 0 \qquad (10)$$

First, formulas (8) and (9), and (8) and (10) yield

$$\dot{\lambda}_1 = -\lambda_2 \cdot \nabla g \qquad (11)$$

$$\dot{\lambda}_2 = -\lambda_1 \qquad (12)$$

$$a_T + \lambda_2 = 0 \qquad (13)$$

Obtaining an undefined coefficient from (11) and (12), the substitution of the coefficient to (13) yields

$$a_T = -\tilde{\lambda}_2$$

which in turn yields

$$\dot{v} = -\tilde{\lambda}_2 + g$$

To simplify, the lunar gravitational acceleration is assumed constant, then

$$g(x) = g_0$$

Then, we have

$$a_T = \tilde{C}_1 t + \tilde{C}_2 \qquad (14)$$

$$\dot{v} = C_1' t + C_2' \qquad (15)$$

However, using

$$C_1' = \tilde{C}_1$$

$$C_2' = \tilde{C}_2 + g_0$$

and the Time-To-Go formula

$$t_{GO} = t_o - t \qquad (16)$$

then (14) and (15) can be rewritten as,

$$a_T = C_1 t_{GO} + C_2 - g_0 \qquad (17)$$

$$\dot{v} = C_1 t_{GO} + C_2 \qquad (18)$$

where,

$$C_1 = -C_1' = -\tilde{C}_1$$

$$C_2 = C_1' t_d + C_2' = \tilde{C}_1 t_d + \tilde{C}_2 + g_0$$

The defined vector coefficients that meet the initial and terminal conditions are determined here.

The definition formula for velocity and position vectors

$$v = \int dv = \int \dot{v}\, dt$$

$$r = \int dr = \int v\, dt = \int \left(\int \dot{v}\, dt \right) dt$$

can be closely approximated by

$$a = \dot{v}$$

$$v_D = v + a\, t_{GO} + \frac{1}{2} \dot{a}\, t_{GO}^2$$

$$r_D = r + v\, t_{GO} + \frac{1}{2} a\, t_{GO}^2 + \frac{1}{6} \dot{a}\, t_{GO}^3$$

$$= r + (v_D - a\, t_{GO} - \frac{1}{2} \dot{a}\, t_{GO}^2)\, t_{GO} + \frac{1}{2} a\, t_{GO}^2 + \frac{1}{6} \dot{a}\, t_{GO}^3$$

$$= r + v_D\, t_{GO} - (a\, t_{GO} - \frac{1}{2} \dot{a}\, t_{GO}^2)\, t_{GO} + \frac{1}{2} a\, t_{GO}^2 + \frac{1}{6} \dot{a}\, t_{GO}^3$$

By substituting (18) to the above and using

$$\Delta V_D = V_D - V$$

$$\Delta r_D = r_D - r - v_D t_{GO},$$

yields

$$\Delta v_D = C_2 t_{GO} + \frac{3}{2} C_1 t_{GO}^2$$

$$\Delta r_D = -\frac{1}{2} C_2 t_{GO}^2 + \frac{3}{2} C_1 t_{GO}^3$$

Solving this yields

$$C_1 = -\frac{1}{t_{GO}^3}(12\Delta r_D + 6\Delta v_D t_{GO})$$

$$C_2 = \frac{1}{t_{GO}^2}(18\Delta r_D + 10\Delta v_D t_{GO})$$

Substituting them into (17) and (18), we obtain

$$\dot{v} = \frac{6}{t_{GO}^2}\Delta r_D + \frac{4}{t_{GO}}\Delta v_D \qquad (19)$$

$$a_T = \frac{6}{t_{GO}^2}\Delta r_D + \frac{4}{t_{GO}}\Delta v_D - g_0 \qquad (20)$$

These are the desired guidance formulas and were derived by G. W. Cherry (1964)[1,2]. They are named E-guidance by Cherry, and guidance derived from the formulas is therefore called E-guidance in this paper.

4.2.3 Methodology of Trajectory Determination

The guidance is controlled under the conditions given below.

> Desired thrust acceleration vector

$$a_T = 6\frac{r - r_D - v_D(T_D - t)}{(T_D - t)^2} + 4\frac{v - v_D}{T_D - t} - g_0 \qquad (1)$$

where;

r : present position vector

v : present velocity vector

t : present time (flight time from the beginning of powered descent)

r_D : terminal (required) position vector

v_D : terminal (required) velocity vector

$T_D = t_f$: required flight time

g_0 : lunar gravitational acceleration vector

> Fuel consumption

$$\Delta m = m_0 \left\{ 1 - \int_{t_0}^{t} \exp\left(-\frac{a_T}{Isp \cdot g_0} dt \right) \right\}$$

where;

m : initial mass

Isp : specific impulse

> Required thrust vector

$$T = Ma_T$$

where,

$$M = M_0 - \Delta m$$

> Mass flow

$$\dot{m} = \frac{T}{Isp \cdot g_0}$$

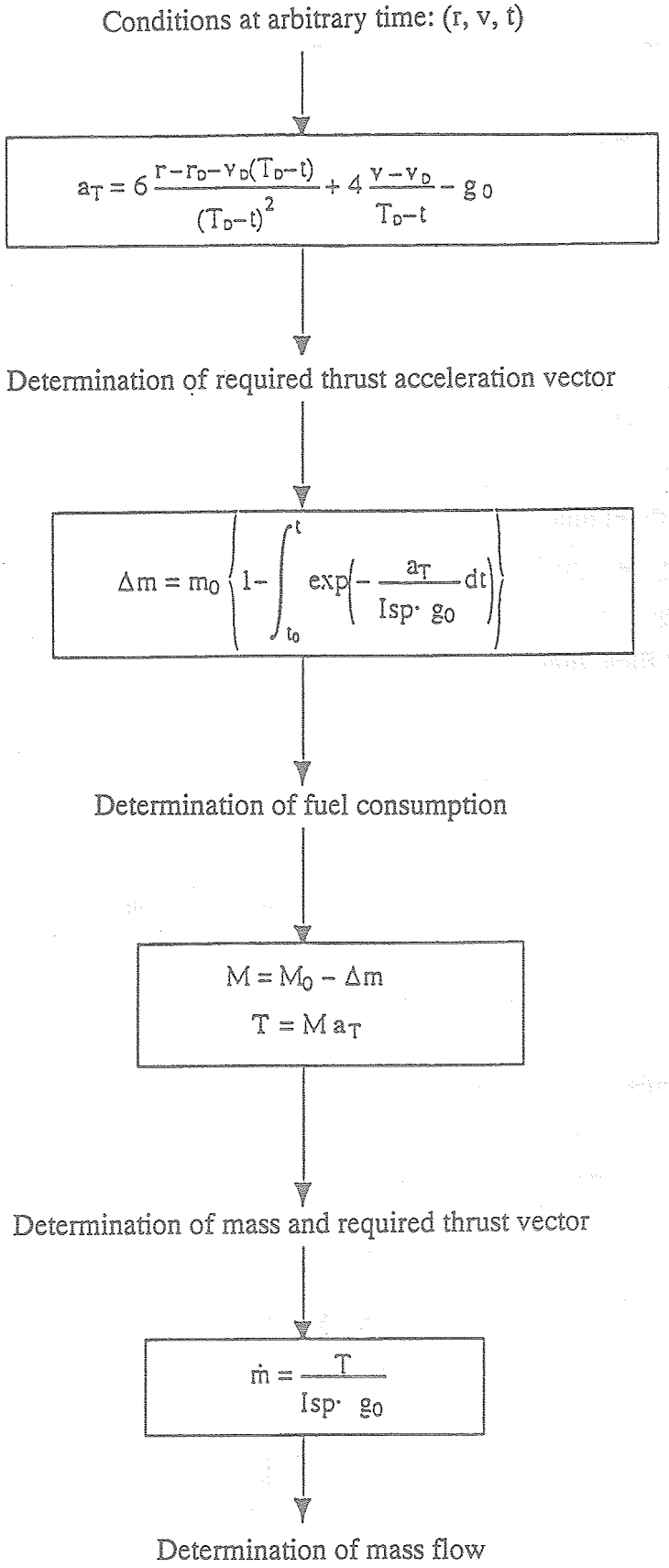

Figure 4.2.3-1 Determination of Five Factors

As seen from formula (1), the determination of E-guidance trajectory requires predetermination of terminal conditions (r_D, v_D, T_D). Since E-guidance, namely minimum fuel trajectory, is derived from the specified terminal conditions, the trajectory changes in response to targeted landing site and the descent velocity. Therefore, some trajectories are figured out under various assumptions of the terminal conditions, and it is necessary to select out the trajectory and its terminal conditions that best meet the requirements for the minimum fuel consumption. These conditions may be divided into

(1) vertical decent vector to the targeted landing site (r_D) and the velocity at that point (v_D)
(2) the (required) flight time (T_D) to the target.

According to the section 4.1, the position vector (r_D) in formula (1) selects an altitude of 1.4 km above the lunar surface.

Then, decent velocity (v_D) is determined by the requirements of the final descent phase;

v_{Dr} = -50 m/s (vertical downward composites)
v_{Dh} = 0 m/s (no horizontal composites).

Among the selected trajectories to meet those requirements, the first optional trajectory will have to provide the flight time which minimizes the fuel consumption. However, this nominal trajectory does not meet the requirements other than those of fuel consumption. These are:

(1) Thrust requirements

(a) Force

$$T_{min} \leqq T \leqq T_{max} \qquad T_{min} = 250N \qquad T_{max} = 1{,}000N$$

(b) Thrust change rate

$$T_{min} \leqq T \leqq T_{max} \qquad T_{min} = \text{T.B.D.} \qquad T_{max} = \text{T.B.D.}$$

The maximum thrust of RCS is subject to these requirements.

(2) Terminal attitude requirements

$$\varphi(T_D) = \tan^{-1}\frac{v_r}{v_h} = \frac{\pi}{2}$$

(c) The lander will vertically approach the targeted landing site. In other words, the terminal roll

axis will be vertical to the lunar surface.

(d) The lander will have no rotating angular velocity at termination.

$$\dot{\varphi}(T_D) = 0$$

Of the trajectories derived on the basis of the conditions r = 1.4 km, V = (-50 m/s, 0 m/s), the selected nominal trajectory meets requirements (a) through (d), and the flight time which minimizes the fuel consumption. The following diagram illustrates the above procedures.

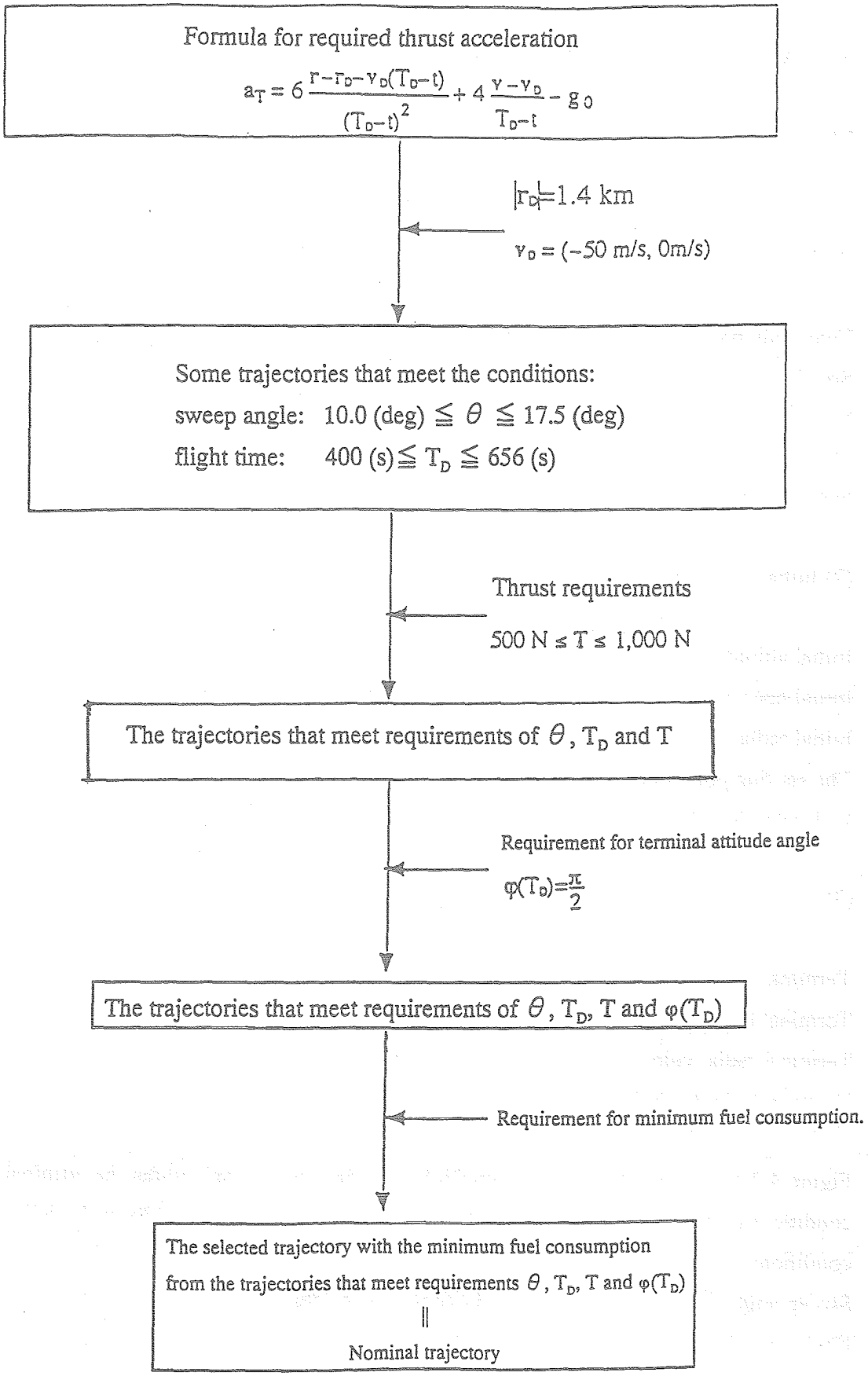

Figure 4.2.3-2 Methodology of Nominal Trajectory Determination

4.2.4 Analysis of by E-guidance Trajectory

The motion model used in the analysis as well as the initial and terminal conditions are shown below[4,5].

(1) Motion model

Two-body problem that assumes the spherical moon. μ = 4902.778 km^3/sec^2
Specifc impulse: Isp = 300 sec
Mass flow: calculated by the following equation

Initial mass: M = 350 kg

(2) Initial conditions

Initial altitude: h = 14 km
Initial horizontal velocity: v_h = 1.692 km/s
Initial radial velocity: v_r = 0 km/s
The starting point of powered descent will be pericynthian in an elliptical orbit with an altitude of 15 km (pericynthian) and 100 km (perilune).

(3) Terminal Conditions

Terminal altitude: h_D = 0 km
Terminal horizontal velocity: v_{Dh} = -50 m/s
Terminal radial velocity: v_{Dr} = 0 m/s
Terminal attitude angle:

Figure 4.2.4-1 shows relation between flight time and sweep angle under the terminal conditions (r_D,v_D). From this Figure, the trajectory should be selected from the following conditions.
Sweep angle θ_D: 12 (deg) ~ 18 (deg)
Flight time T_D: 420 (sec) ~ 720 (sec).

Figure 4.2.4-2 shows the relation between flight time T_D and the terminal attitude angle φ_D under the above angle conditions. From this Figure, the attitude angle of 90 degrees is limited to the cases shown in Table 4.2.4-1. The larger the attitude angle, the longer the flight time.

Table 4.2.4-1 Characteristics Option

	1st option	2nd option	3rd option
Sweep angle (deg)	14	14.2	14.4
Flight time (sec)	548	595	625

Figure 4.2.4-3 shows the terminal payload under the selective conditions from Figure 4.2.4-2. As a result, the terminal payload as the first option is largest, and calculated as

$$M_D = 187 \text{ kg}.$$

Accordingly, when the following flight time and transfer angle are selected,

$$T_D = 548 \text{ (sec)}$$

$$\theta = 14^\circ$$

the mass of fuel consumption and the fuel mass ratio are:

$$\Delta m_{TOT} = M_0 - M_D = 163 \text{ kg}$$

$$\eta = \frac{\Delta m_{TOT}}{M_0} = \frac{163}{350} = 0.465$$

Adding the marginal mass (170 x 0.1 = 1.7 kg) to the fuel mass, the mass ration is;

$$\eta = \frac{163+1.7}{350} = 0.53$$

This ratio validates the determination of E-guidance trajectory which is derived from above characteristics.

Figure 4.2.4-4 shows the trajectory profile derived from the above-mentioned characteristics. Its major feature is that the lander once ascends up to 2 km above an altitude of pericynthian. This is mainly because the terminal attitude angle was specified at 90 (deg).

Figure 4.2.4-5 shows the relation between altitude and the angle between radial and roll axis.

Figures 4.2.4-6 and 4.2.4-7 show the relation between the positions and the velocity in inertial.

Figure 4.2.4-8 shows the relation between the flight time(t) and the thrust(T). It appears that the largest thrust force is required during 69% of the total flight time (380/548). This is the time frame in which the guidance deviated from E-guidance will take place. This leads us to consider a new guidance law, as noted in the section of Future Studies.

Figure 4.2.4-9 shows the changes in payload mass against flight time.

As can be seen from the above, the E-guidance trajectory proves its effectiveness which is quite similar to that verified in the previous study.

Reference

1. Kato; Engineering Optimal Control, Tokyo University Press (1988)

2. C.W.Cherry, Prog in Astro and Aeronautics, Guidance and Control, II, vol13, New York, Academic Press, 1964

3. Yamanaka; Material belongs to NASDA Control Technology Laboratory, January 1995

4. Nakajima; MSS Service Support Data, PP22-0406-0003, March 1995

5. Nakajima; MSS Service Support Data, PP22-0406-0001, January 1995

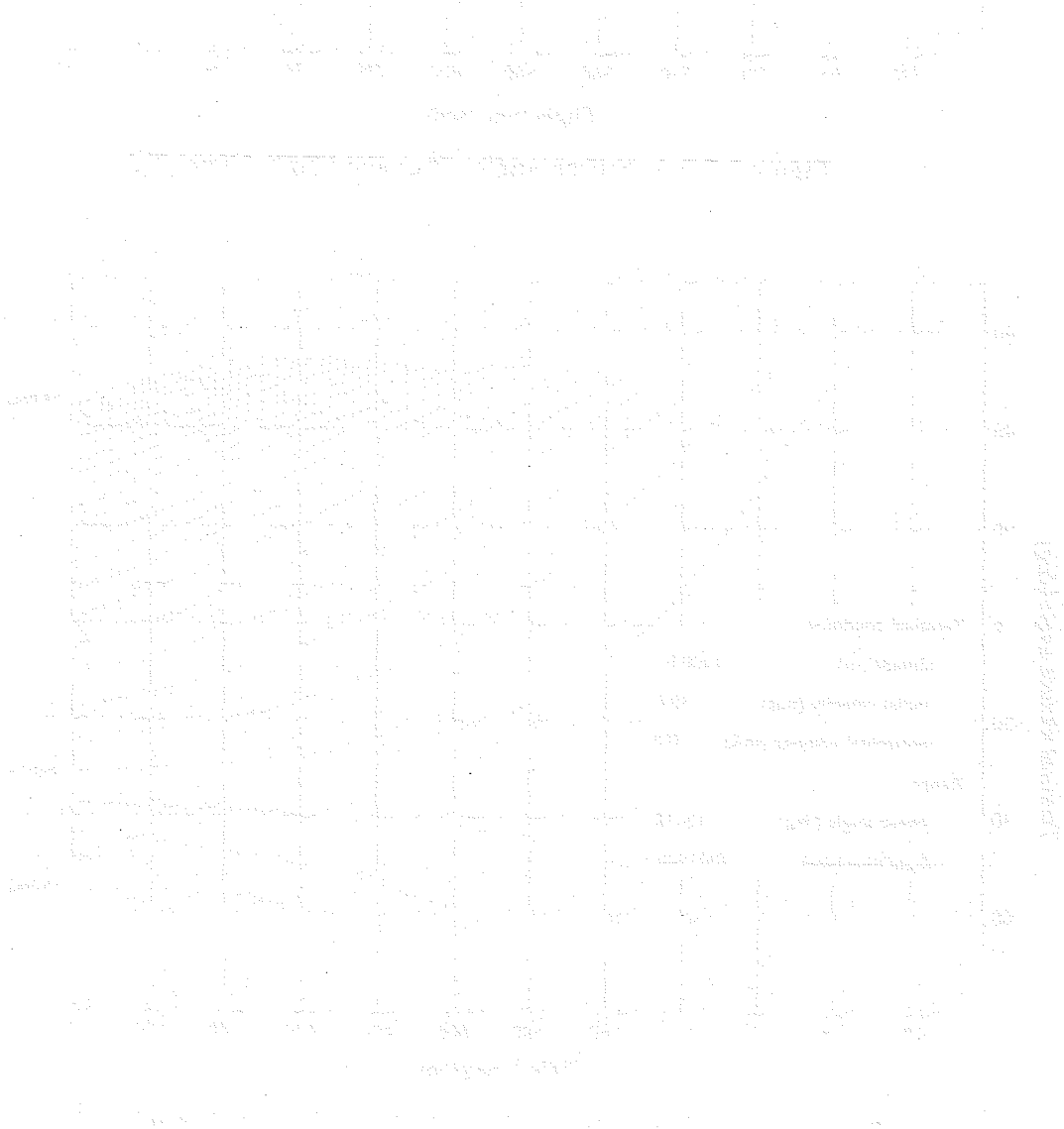

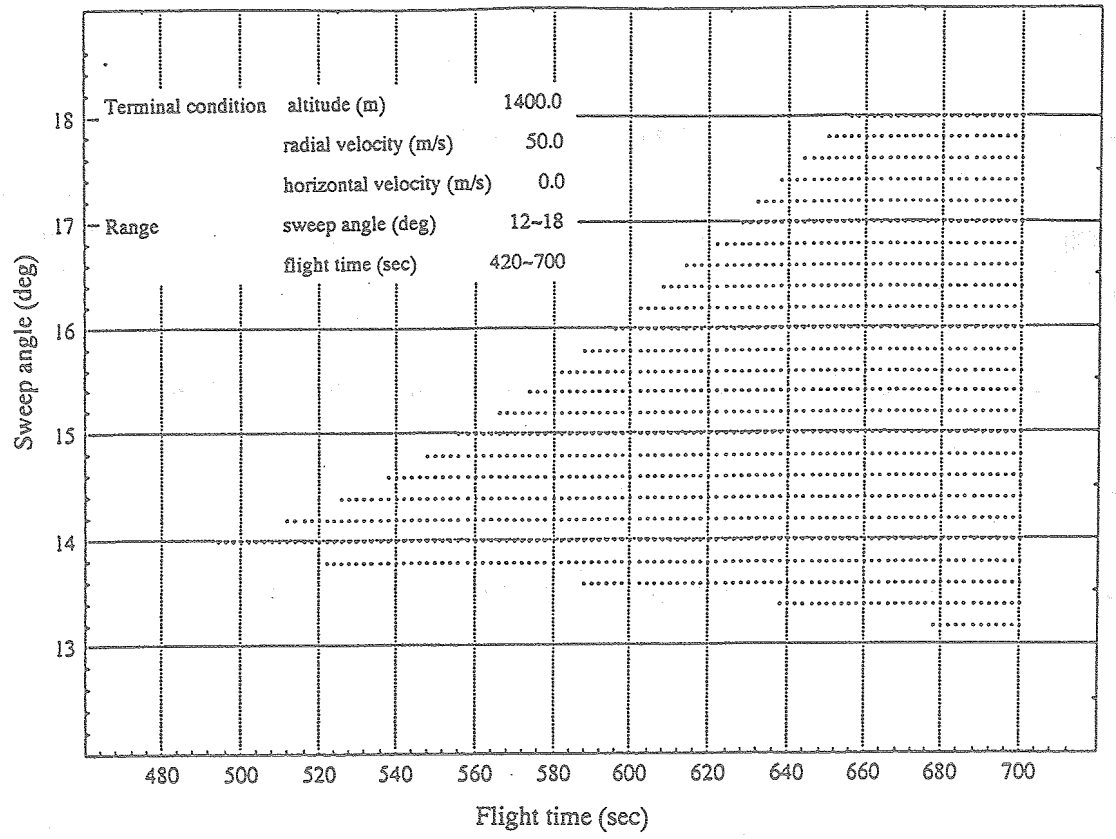

Figure 4.2.4-1 Sweep angle (θ_D) and Flight Time (T_D)

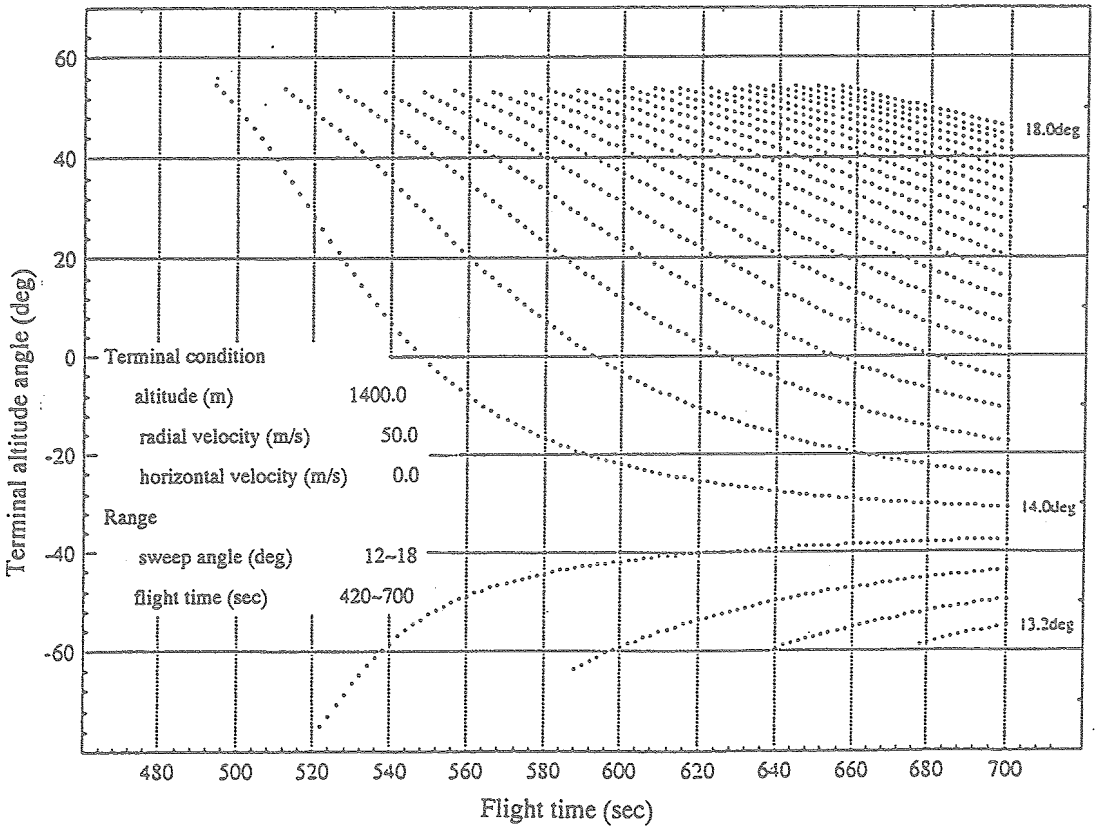

Figure 4.2.4-2 Flight Time (θ_D) and Terminal altitude angle (ϕ_D)

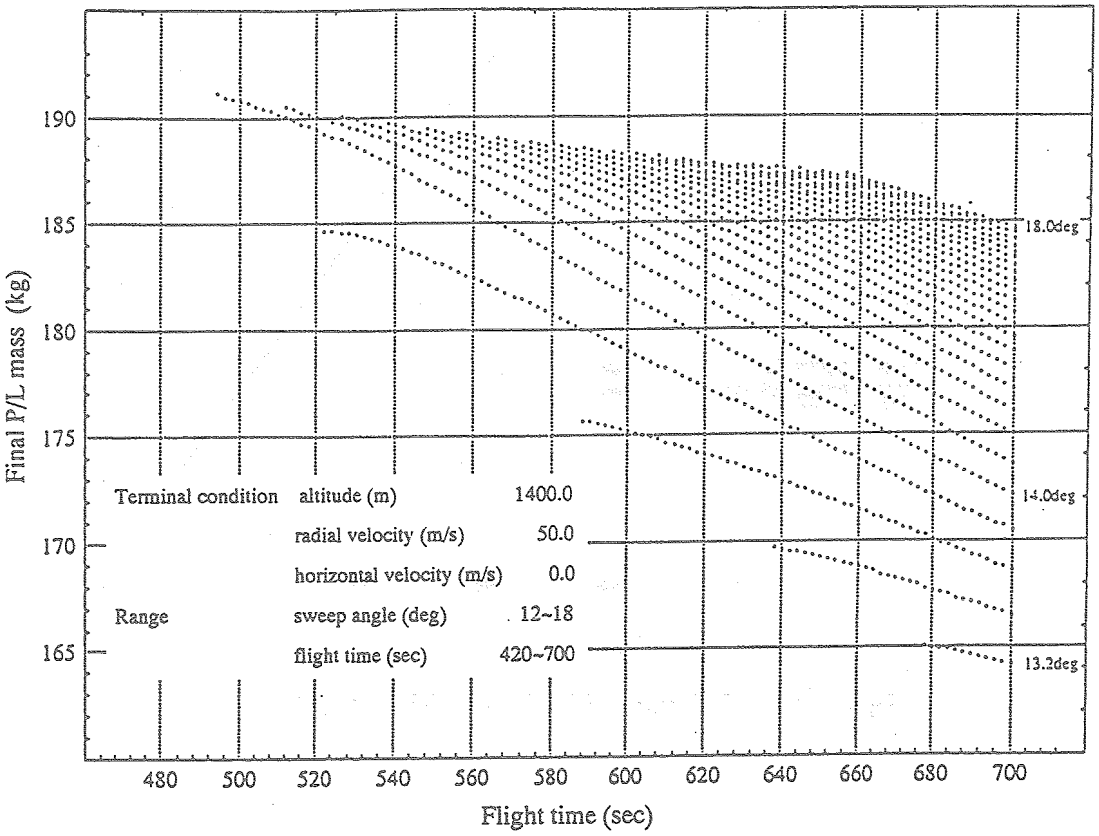

Figure 4.2.4-3 Flight Time (T_D) and Sweep angle (M_f)

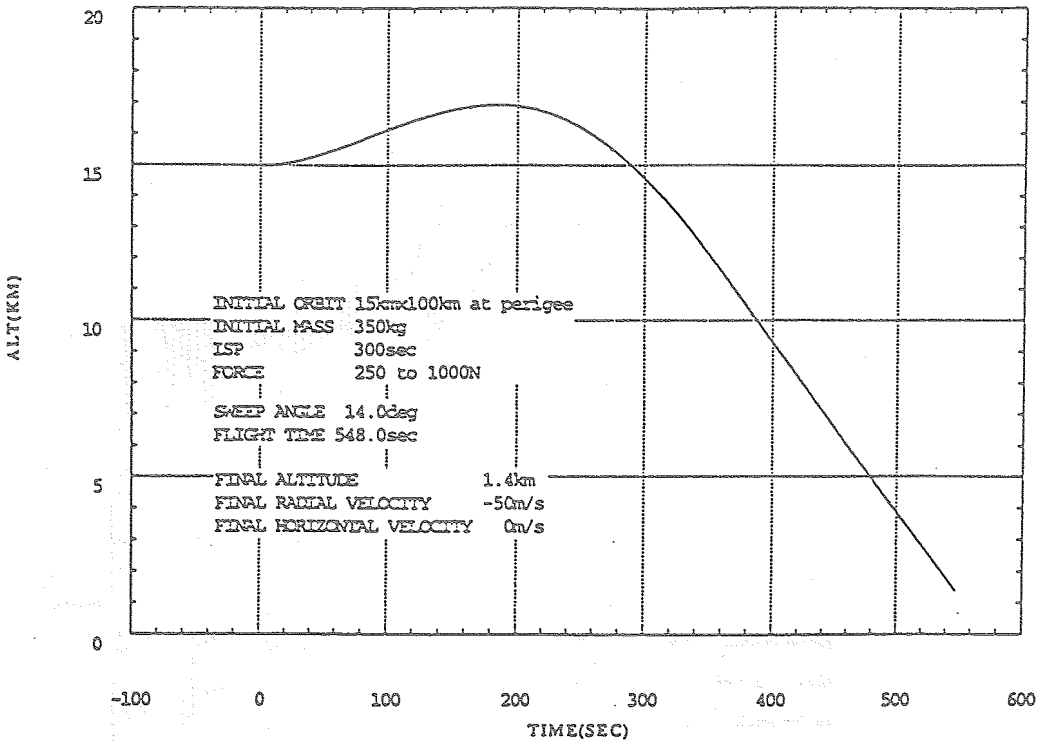

Figure 4.2.4-4 Flight Time (t) and Altitude (h)

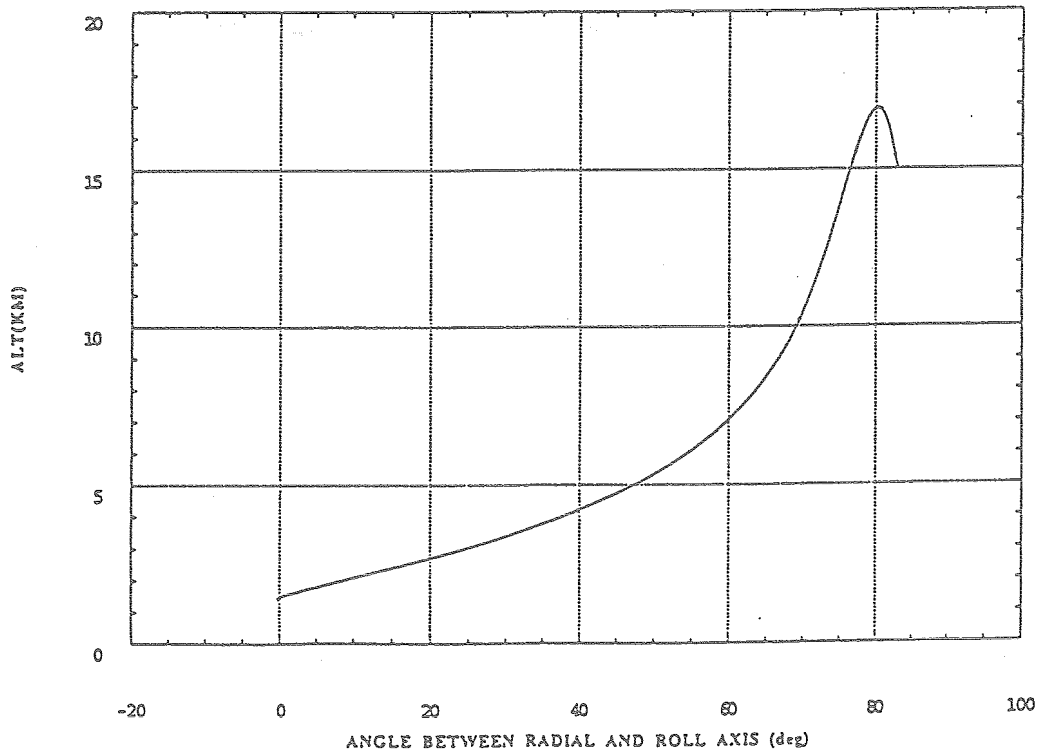

Figure 4.2.4-5 Altitude (h) and Angle Between Radial and Roll Axis (β)

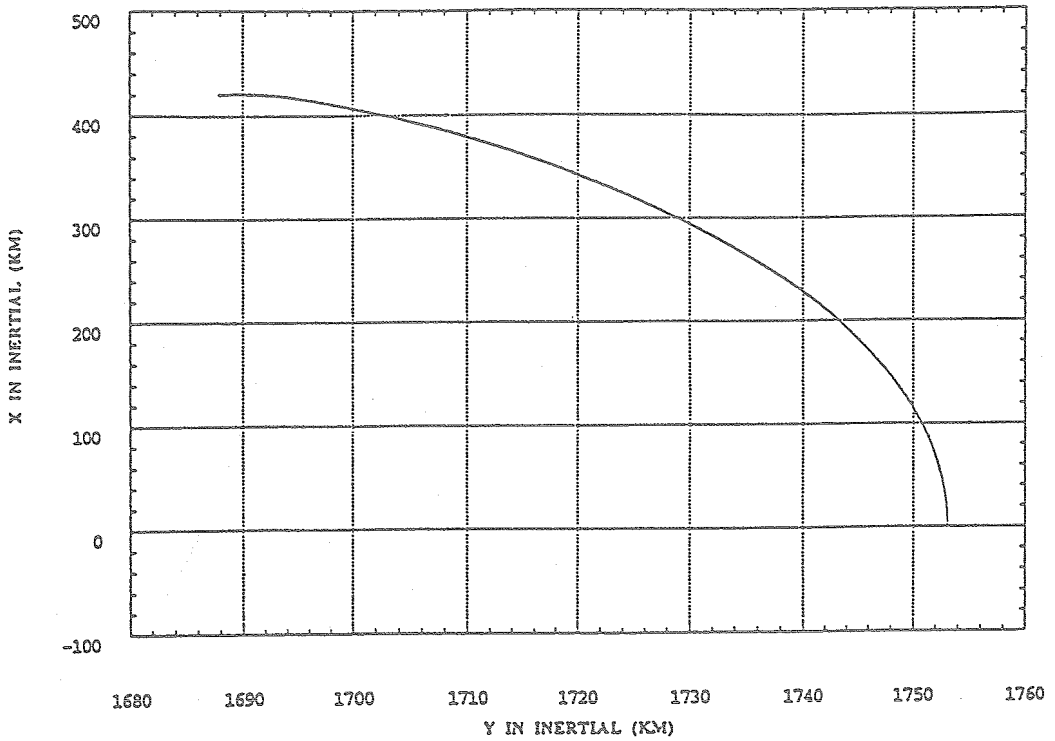

Figure 4.2.4-6 Altitude of Inertial Coordinate System

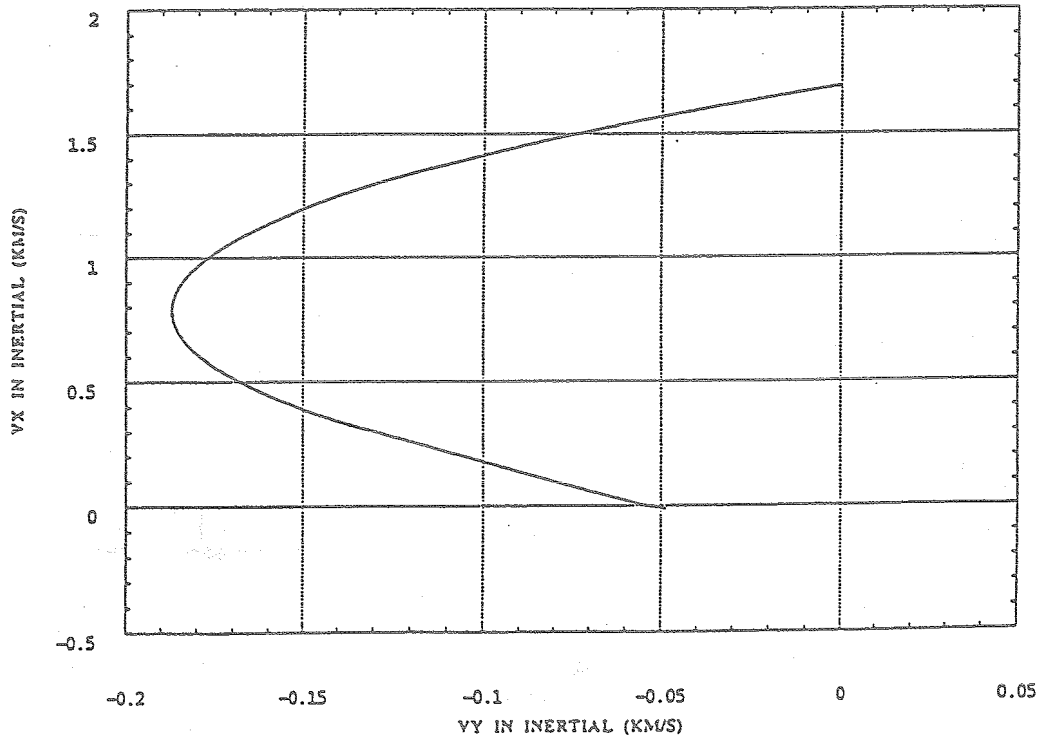

Figure 4.2.4-7 Velocity of Inertial Coordinate System

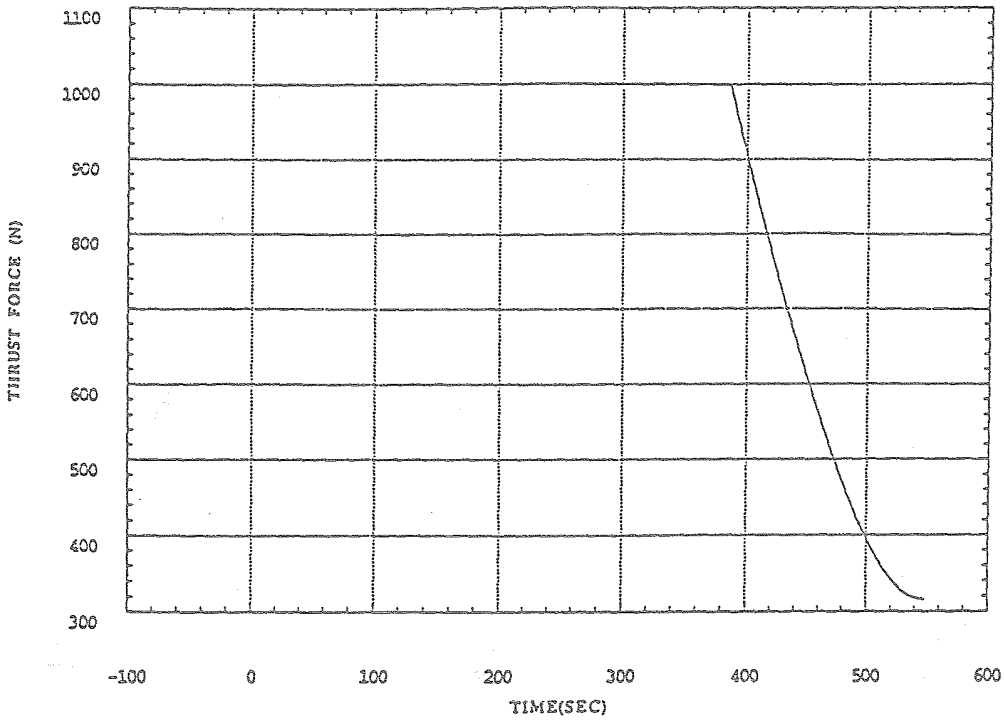

Figure 4.2.4-8 Flight Time (t) and Thrust (T)

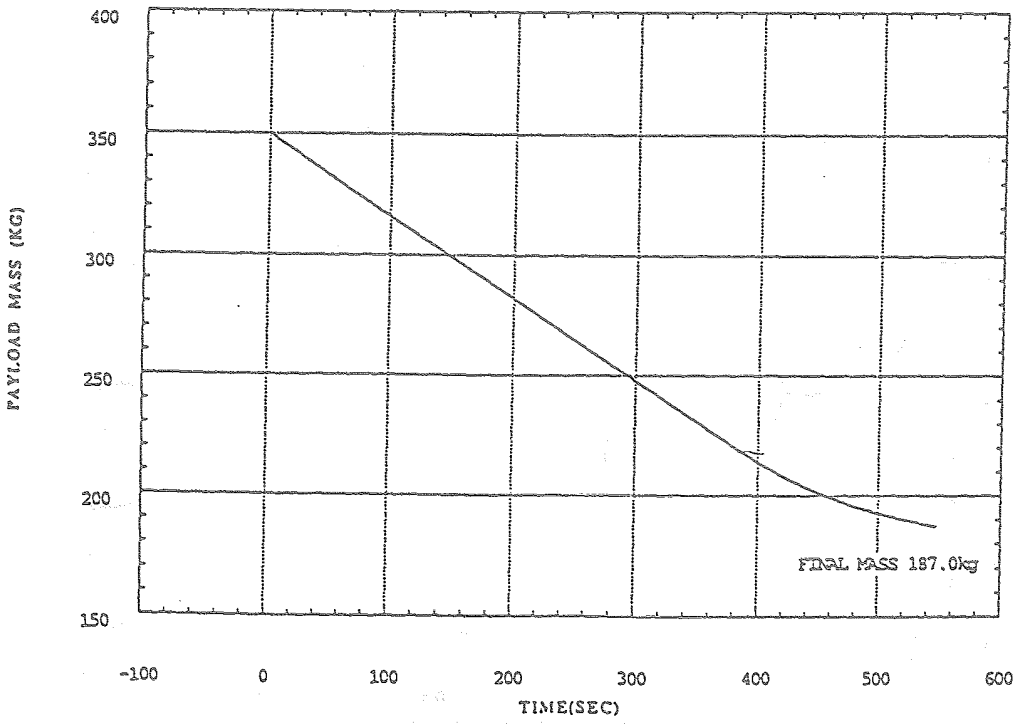

Figure 4.2.4-9 Flight Time (t) and P/L Mass (M)

4.3 Analysis of the Final Descent Phase

This section will discuss an inevitable factor, targeted landing site modelling, to the planning of the final descent phase of the reference trajectory.

4.3.1 Modelling of the Landing Site

Given various conditions and requirements for operation and mission, the landing site should be selected in determining the reference trajectory. However, there will be a possibility of different site being selected after the detailed mapping of the lunar surface by lunar orbiter. Consequently, the modelling of the landing site should be carried out in such a way that it will be as widely applicable as possible. This section describes a simple modelling method with emphasis on uneven topography rather than dimension of the lander (no consideration is given to the modelling of craters).

(1) Optional Landing Sites

The desirable conditions are that:

- the start point of the powered descent for landing is trackable from the ground stations,
- the landing site is trackable, and
- the landing site is as even as possible (mare).

From these conditions, the following four mares located on near side of the moon (earthward side) could be optional (See Figure 4.3-1).

1 Mare Imbrium
2 Mare Serenitatis
3 Mare Vaporum
4 Mare Nubium

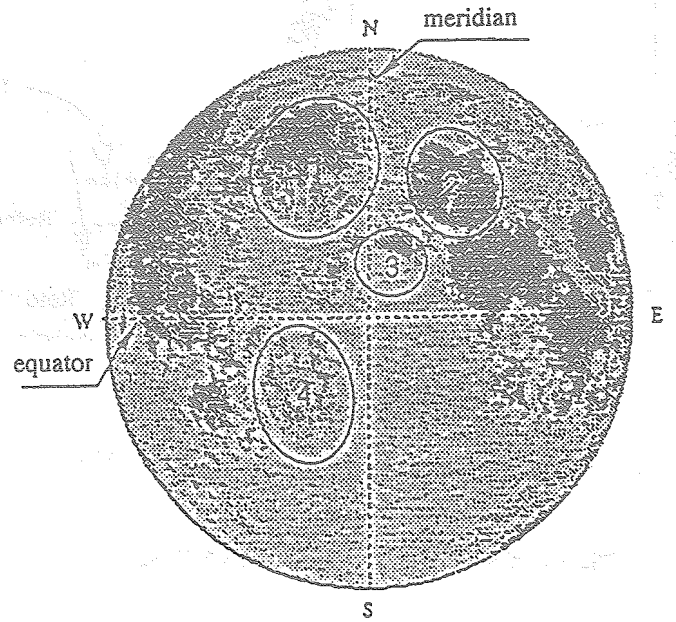

Figure 4.3-1 Location of Optional Four Mares

Although maps of a portion of the Mare Imbrium and Mare Serenitatis are currently available (issued by NASA), detailed data is not completely sufficient. Therefore, we will consider a landing somewhere in the Mare Serenitatis as an example.

(2) Landing Site Model

The elevation of the Mare Serenitatis is 5,673 m at its highest and 3,370 m at its lowest. This is measured from peak to valley, thus it is not suitable to use them as the true values. It reasonably assumes the highest elevation to be 5,500 m and the lowest to be 3,500 m, with 2 km differences. Since this could be applied to the other three mares, the selected landing point (area) is common to four mares.

As seen from Figure 4.3-2, there are two lunar radiuses; 1738 km and 1730 km from the center of the Moon (center of lunar mass). The former was used to determine the most appropriate Hohmann transfer elliptical orbit at altitude of 100 km x 15*1. In this section, this radius is

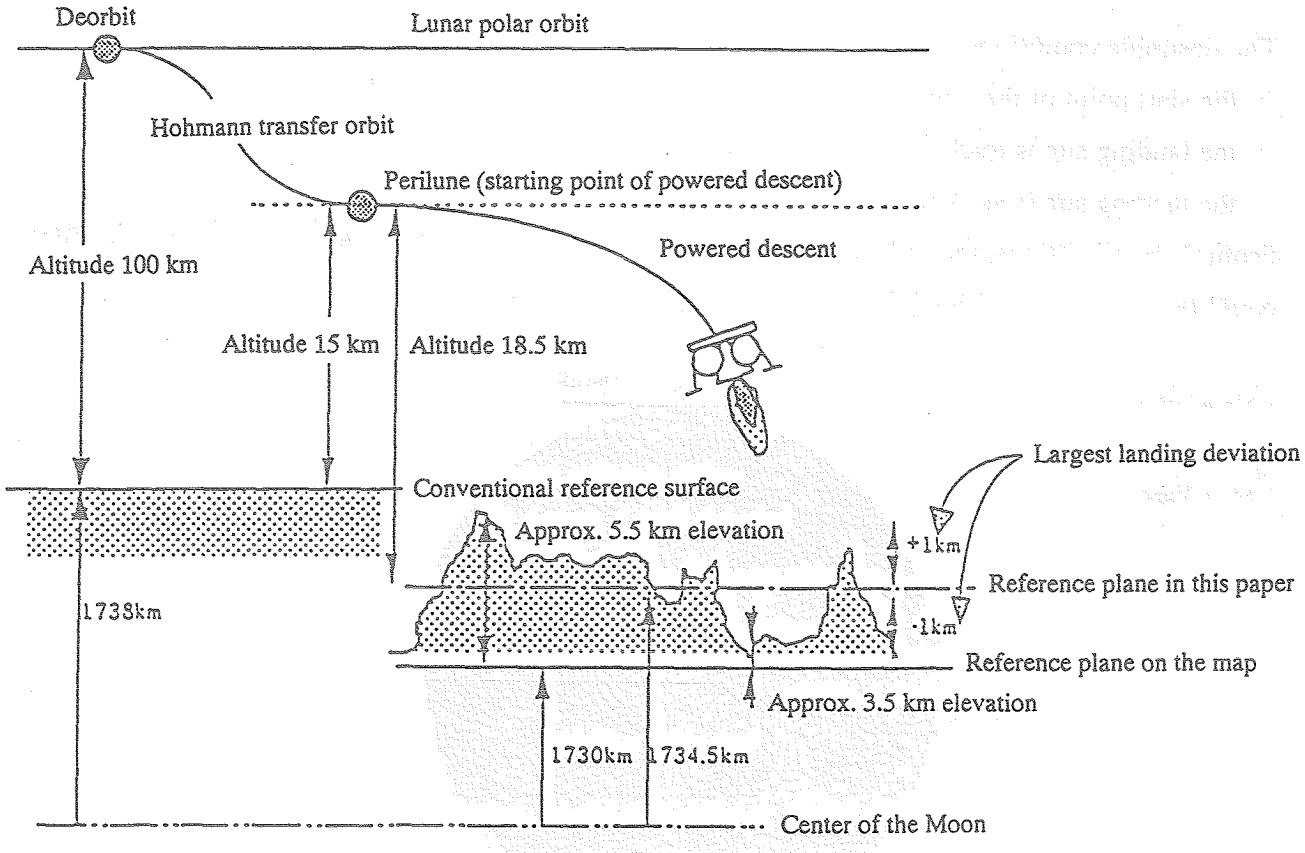

Figure 4.3-2 Landing Site Modelling

*1: See Section 4.1

applied as reference from deorbit to pericynthian because it is necessary to avoid confusion and to consider change of the landing site without changing the setting of the elliptical orbit. Then, the reference radius is set as 1734.5 km from the pericynthian to landing, which is derived from average of the largest and lowest elevations ((1730 + 5.5) + (1730 + 3.5))/2). Thus, the largest landing deviation is to be ± 1 km. See Figure 4.3-2 in detail.

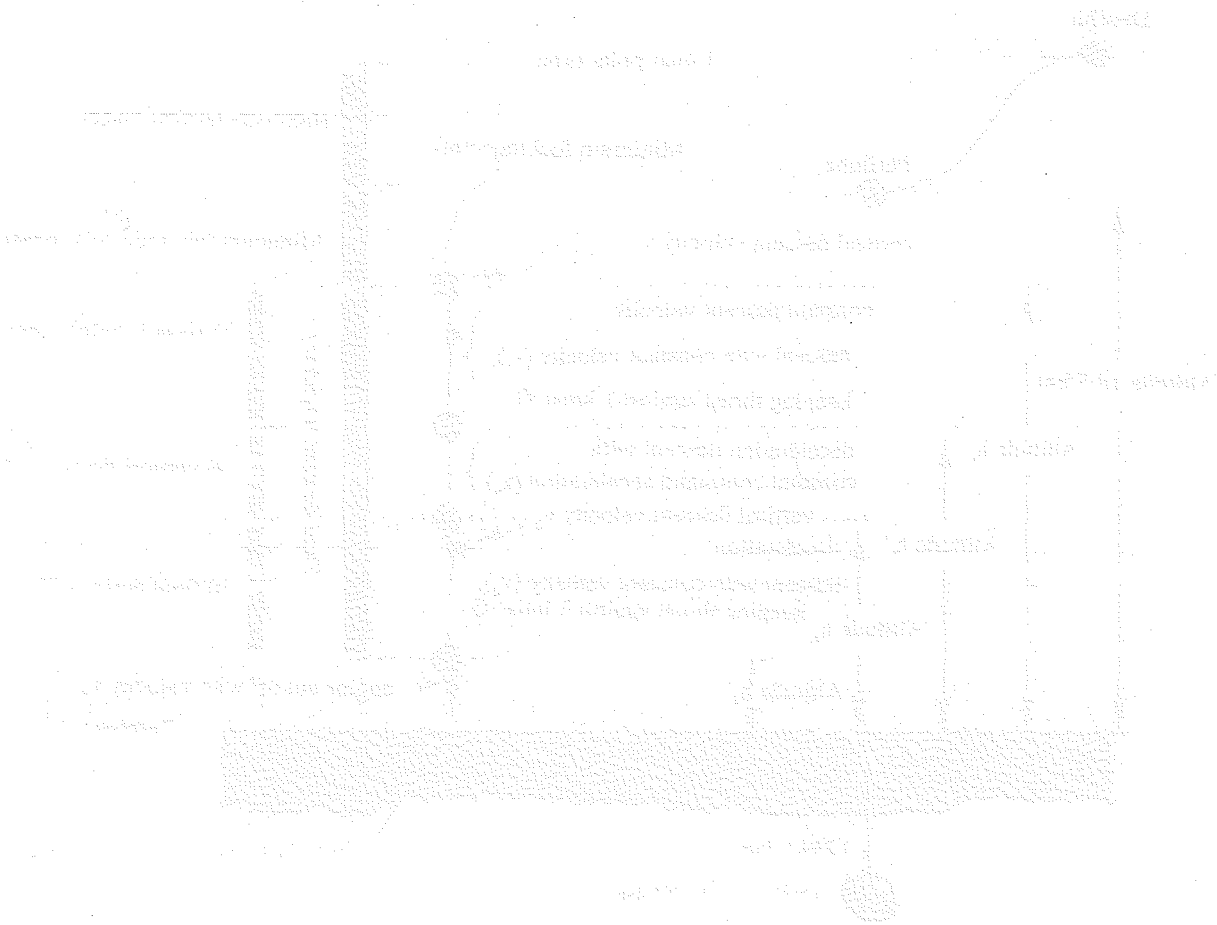

4.3.2 Final Descent Trajectory

The term "final descent trajectory" used here refers to the vertical descent path for landing on the lunar surface after the trajectory from deorbit to the targeted point where minimum-fuel orbit was passed. This trajectory is devised to ensure that the lander will successfully land on the lunar surface via minimum-fuel and safe trajectory. The final descent phase has three subphases.

1) Surface height adjustment
2) Vertical deceleration
3) Final descent

An outline of the phasing is shown in Figure 4.3-3, and a profile of the vertical velocity and altitude is shown in Figure 4.3-4.

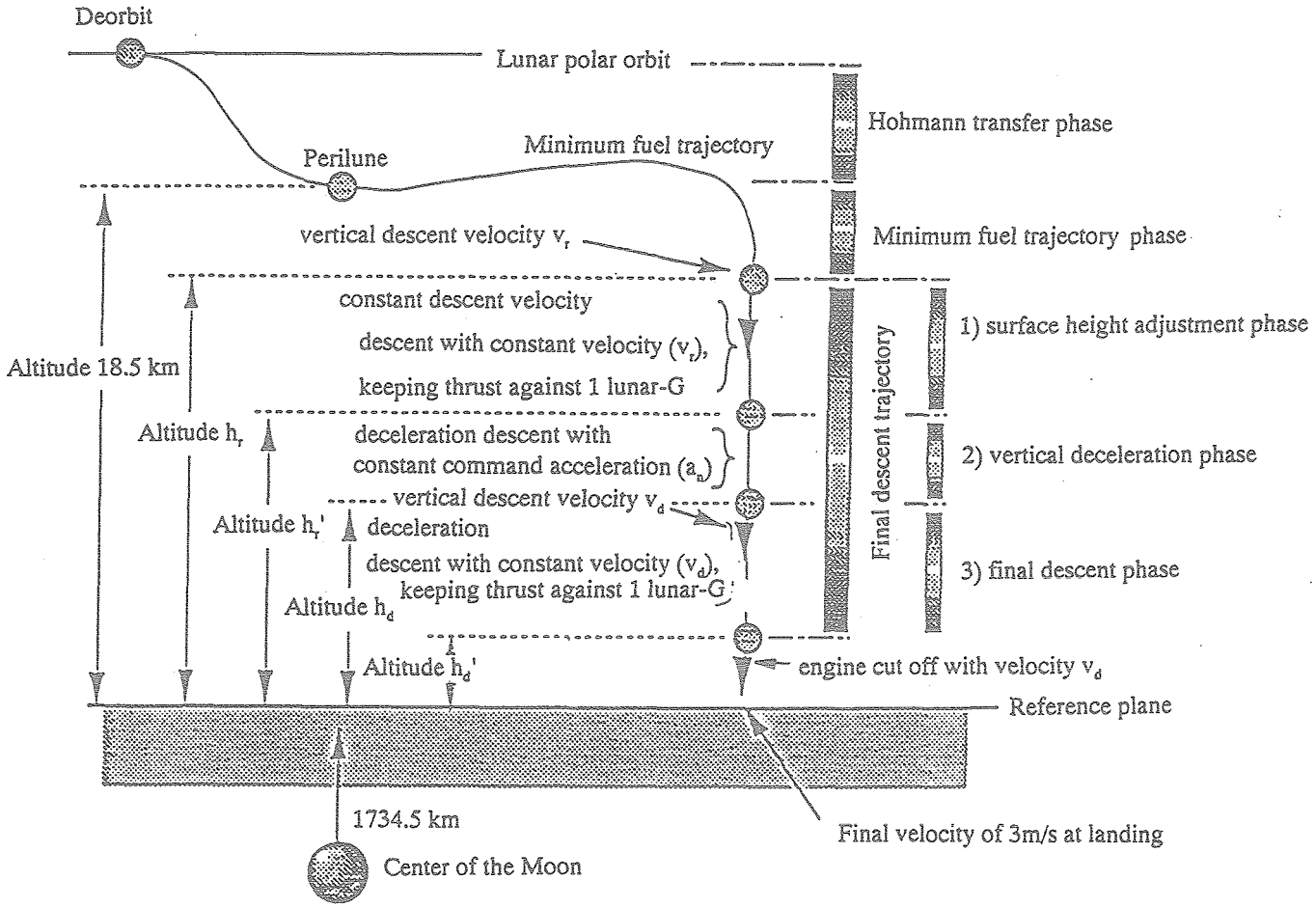

Figure 4.3-3 Phasing Outline

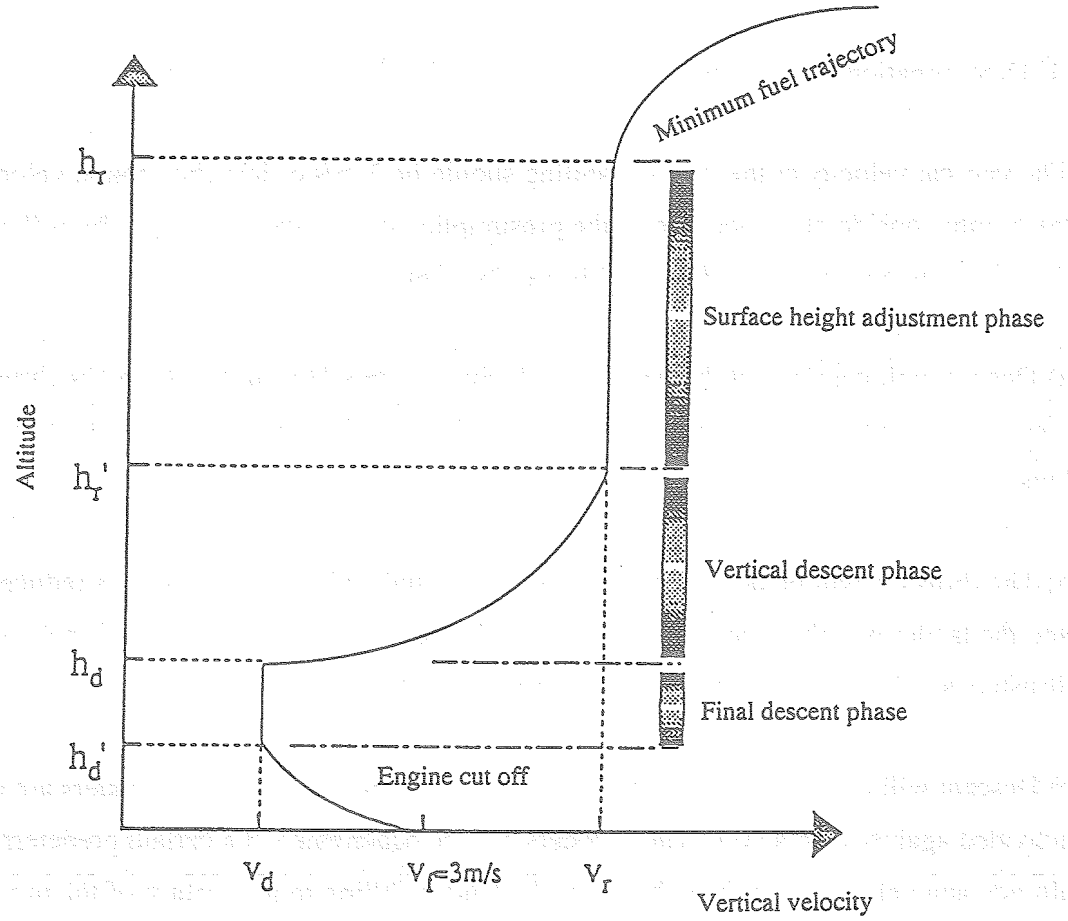

Figure 4.3-4 Profile of Velocity and Altitude

Below will be in detail discussed the development of the vertical descent trajectory and its related conditions, taking into the above-mentioned landing site model. Since the first priority is put on validity of overall landing trajectory, it is necessary to determine the targeted point as the final destination of minimum fuel trajectory, and the various conditions in the vertical descent orbit (backwards in time from the landing point).

① Determination of Landing Requirements and the Final Descent Phase

The vertical velocity at the time of landing should be 3 m/s or less (horizontal velocity will not be taken into consideration because of the presumption of vertical descent). The following typical three landing approaches will meet this requirement.

a) Descent will continue at the constant velocity of 3 m/s (during that time, the thrusters are continuously activated against 1 lunar-G), and they are deactivated at the same time when the lunar surface is contacted.

b) The thrusters will be deactivated at a certain altitude where the velocity is reduced to 0 (zero) and the lander will fall freely. In this approach, the final velocity of 3 m/s is achieved when thrusters are deactivated at an altitude of approximately 3 m.

c) Descent will continue at the constant velocity (during that time, the thrusters are continuously activated against 1 lunar-G). The thrusters will be deactivated at a certain predetermined altitude and velocity, and the velocity of the lander, falling to the surface of the moon, will be 3 m/s at the time of landing. There are an infinite number of combinations of velocity and altitude in this particular case.

In approach (a), the thrusters are continuously activated vertically until the lunar surface is contacted. It is quite likely that the environment of the landing site may deteriorate due to the piling up of disturbed regolith or may become destabilized due to the creation of craters. Therefore, this approach can obviously not be recommended simply as it is. Let us then give consideration to approach (b). There are two approaches to reduce velocity to 0 (zero) at a certain altitude: (1) to reduce gradually to 0 (zero) while throttling down thrust, or (2) to reduce suddenly to 0 (zero) while decelerating at high level of thrust. Approach (1) is safe but not economical because its gravity loss is sizeable. Sub-method (2) is likely to be economical but dangerous because of various conceivable situations due to an incorrect timing of the thrusters deactivation at velocity 0 (zero). For example, if the thrusters are deactivated too early, the lander could crash on the lunar surface at a higher than tolerable velocity. Or if the thrusters are deactivated too late, the lander could crash into the lunar surface after rising up for an instant. In approach (c), if we properly select velocity and altitude to deactivate thrusters, there is little danger because the velocity does not reach 0 (zero), and disturbances from scattering regolith can be also avoided because the thrusters will be deactivated at a certain altitude.

Table 4.3-1 illustrates the tradeoff study for three approach.

Table 4.3-1 Tradeoff in Three Landing Method

	Scattering regolith	Safety		Economy
a	X	○		△
b	○	1	○	X
		2	X	○
c	○	○		△

From the above Table, it is likely to determine that approach (c) is the most appropriate of the three methods. Velocity and altitude will be determined as indicated below in approach (c). Following the terminology used in Figure 4.3-4, the initial altitude of the final descent phase will be h_d, the terminal altitude will be h_d', and the intervening constant descent velocity will be v_d. The relation between altitude h_d' and velocity v_d, assuming v_f (velocity at time of contact) is 3 m/s, can be expressed in accordance with the energy conservation, and shown below.

Altitude h_d' 3 m -> velocity v_d 0.0 m/s
2 m -> 1.5 m/s
1 m -> 2.4 m/s.

It is better for h_d' to be higher and v_d to be slower from a safety point of view. Therefore, it will be appropriate to select here $h_d' = 2$ m and $v_d = 1.5$ m/s. The value of h_d is also better to be higher from the view point of safety. However, the lander descends at the constant velocity (thrust against 1 lunar-G) from h_d to h_d', and a higher altitude will be uneconomical. The relation between the altitude and ΔV during the constant velocity descent ($v_d = 1.5$ m/s) is:

Altitude h_d 10 m -> ΔV 8.7 m/s
20 m -> 19.6 m/s
30 m -> 30.4 m/s.

These terms v_d and h_d are the terminal conditions of the vertical deceleration phase immediately before the final descent phase and are also guidance targets. Therefore, their conditions will be contingent on the precision of the guidance in the vertical deceleration phase. Here, the followings are developed as target values.

- initial altitude h_d of the final descent phase: 10 m
- initial velocity v_d of the final descent phase: 1.5 m/s (the velocity does not change till the lander arrives at the terminal altitude)
- terminal altitude h_d' of the final descent phase: 2 m

Here the values of v_d and h_d' were devised from view point of safety, but the final determination of these conditions fully consider the regolith issue. For evaluation of this issue, priority is likely to be put on the relation between (1) disturbances due to scattering regolith and the creation of craters and (2) thrust, altitude, and descent velocity. It will be necessary to analyze these relation quantitatively by using CFD (one of numerical fluid simulations) and regolith simulant. Moreover, the value of altitude h_d will also have to be optimized by tradeoff study on various related factors, including guidance precision.

② Deceleration Approach and Initial Altitude in the Vertical Deceleration Phase

It is necessary to develop deceleration approach in the vertical deceleration phase.

In this phase, it is be critical to decelerate efficiently by accelerating at a certain level of high thrust. The question then arises as to which condition, thrust or acceleration, should be selected in devising acceleration. No matter which condition is selected, the use of fixed value will be beneficial in keeping the guidance approach simple and in alleviating the load on the propulsion systems. However, even if force of the thrust is firmly fixed, mass of a lander is not. This is because the mass depends on weight of residual fuel, and in turn, acceleration produced by the propulsion system will likewise be depending on the case. It appears that at the present stage, determination of the nominal trajectory under such conditions would require more time than is available and would not be efficient. At the same time, deceleration at the fixed thrust level would require the propulsion system being continuously throttled down so as to achieve variable in response to the dwindling mass of the lander. However, it will be feasible to control velocity and altitude by determining acceleration, and to determine the nominal trajectory easily. Moreover, the application of this approach will likely keep the guidance law simple and also be beneficial to future analyses. In view of the above points, we will adopt deceleration at constant acceleration in the vertical deceleration phase.

The following formula will express the curve shown in Figure 4.3-4 in regard to the nominal acceleration and altitude profile.

$$v(h)=\sqrt{2(a_n-g_L)(h-h_d)+v_d^2} \qquad (4.1)$$

v; vertical velocity
h; altitude
a_n; nominal acceleration
g_L; lunar-G

It is necessary to determine the value of a_n. a_n is desirably as high as feasible, however, the acceleration is to be 5 m/s^2 when the mass of the lander and the thrust at the initial stage of this phase are assumed to be 200 kg and 1000 N respectively. In fact, the mass of the lander at that time will be less than 200 kg (according to the result of detailed simulations, it is to be around 190 kg), so the potential acceleration will increase by around 5% of 5 m/s^2. The mass of the fuel will thereafter gradually decrease, thereby increasing the potential acceleration. Therefore, it is to be feasible to produce acceleration of 5 m/s^2 even in the worst case, and it will likewise be possible to keep about 5% margin for guidance at the minimum (the margin will increase over time). In view of the above points, it will be appropriate to fix the value of a_n at 5 m/s^2 for deceleration. (Note that 5 m/s^2 is the acceleration produced by the propulsion system; this value will actually be decreased by lunar gravitational acceleration (around 1.62 m/s^2), which will yield about 3.4 m/s^2 for deceleration purposes)

Applying a_n = 5 m/s^2 in formula (4.1) above, the relation between velocity and altitude in the nominal trajectory will be as shown in Figure 4.3-5. The dotted lines in that Figure show one example to illustrate the nominal trajectory of two phases; minimum-fuel and surface height adjustment.

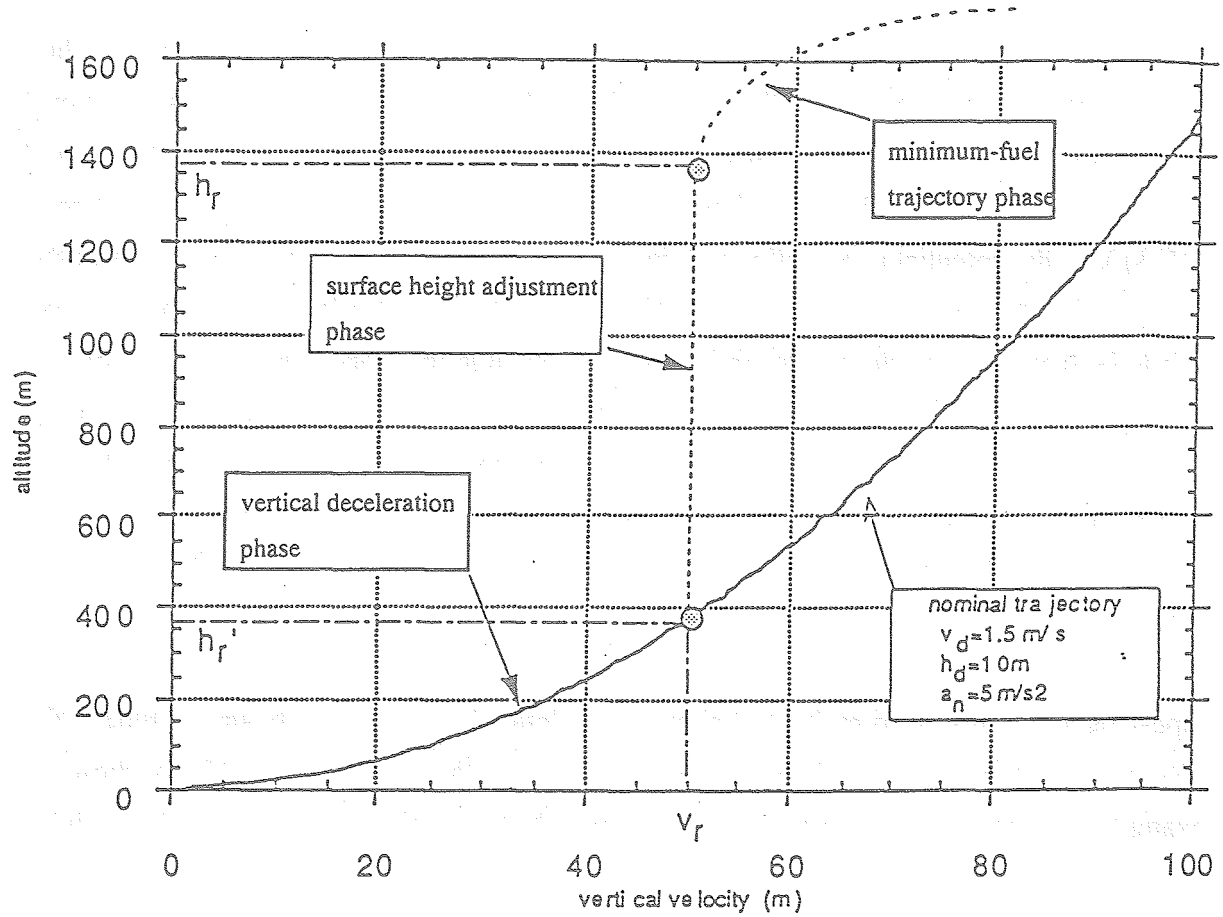

Figure 4.3.5 Nominal Trajectory in Vertical Deceleration Phase

Setting the acceleration v_r also determines h_r', which thereby determines the initial conditions of this phase. However, these conditions must be devised so that two phases, surface height adjustment and minimum-fuel trajectory, yield the optimal ΔV.

Here we will briefly discuss the guidance approach in this phase. Difference between the nominal velocity shown in formula (4.1) and the actual velocity should be solved by using the acceleration command (formula 4.2).

$$a_c = a_n + K_a(t)\left[v_a - \sqrt{2(a_n - g_L)(h - h_d) + v_d^2}\right] \qquad (4.2)$$

a_c; command acceleration

v_a; actual velocity

$K_a(t)$; guidance gain

For details, see the reference 4.3-1. The guidance gain Ka yields a function that linearly increases over time.

③ Surface height adjustment Phase

As mentioned earlier, the lander descend by keeping constant thrust against 1 lunar-G during this phase. This subsection will devise the difference of altitude. As seen from Figure 4.3-2, the maximum difference is to be ±1 km. Thus, difference of altitude to be considered is to be 0 km at the minimum and 2 km at the maximum; the nominal value is to be 1 km. As shown in Figure 4.3-5, this phase will continue from altitude h_r and velocity v_r to h_r' and velocity v_r. Therefore, by assuming the h_r at a point 1 km or more above h_r' (v_r), it will become possible to adjust the difference of ±1 km. Figure 4.3-6 shows velocity and altitude profile with consideration to the differences. This Figure outlines each landing case; nominal, highest point (+1 km) , and the lowest point (-1 km).

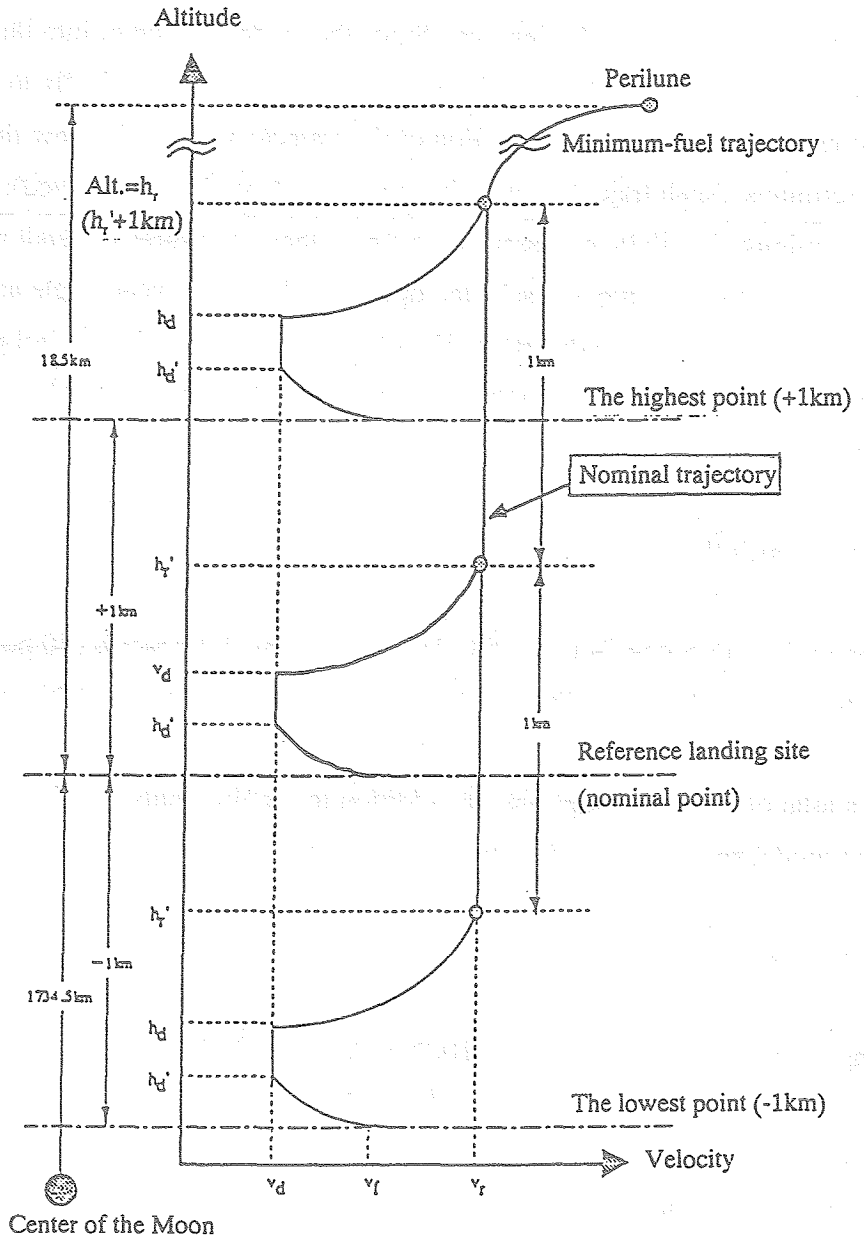

Figure 4.3-6 Velocity-Altitude Profile (with consideration to differences)

④ Minimum-fuel Trajectory

For derivation of the initial conditions (h_r, v_r, etc.) of the final descent trajectory, it will be first necessary to devise the flight conditions (ΔV, etc.) of the minimum- fuel trajectory so that the entire trajectory is validated. Therefore, we will here consider the flight conditions for the minimum-fuel trajectory.

The potential final conditions for the minimum-fuel trajectory are shown in section of 4.2. Given necessity of tradeoff study on velocity (v_r) and altitude (h_r) when determining the entire trajectory, this subsection will assume that both velocity and altitude are zero (0). Instead, the flight conditions will be derived from the optimal sweep angle (θ) and time-to-go (Ttg). When the optimal values for both sweep angle and time-to-go are selected, the roll axis of the lander will be laterally tilted by about 60 degrees. Since the lander will enter into the vertical descent phase immediately after this phase, the roll axis should be oriented vertically to the surface. Some measures should be taken; the selection of the trajectory that will allow the axis to orient vertically at the terminus (such trajectory will, however, not have fuel minimized); attitude control by RCS at the terminus. It will be necessary to examine these measures in detail and conduct tradeoff study. At the present time, the selected optimal values for sweep angle and time-to-go are temporarily conditioned to determine the trajectory in the minimum fuel phase. For details on the simulated derivation of the optimal values, see reference 4.3-2. Here the outline and results are described.

Parameters as follows:

Sweep angle	17.8 deg. $\geqq \theta \geqq$ 10.0 deg.	0.2 deg. increments (40 points)
Time-to-go	400 sec. $\geqq$ Ttg $\geqq$ 656 sec.	2 sec. increments (129 points)

yield a total of 5,160 assumptions. In addition to requirements mentioned in 4.2, such as the motion model and initial conditions, the followings are required.

1) Thrust requirements

Range of variable thrust:	1000 N $\geqq$ F $\geqq$ 500 N
Variable ratio :	dF/dt $\leqq$ 0.0

2) Altitude requirements

The terminal altitude must be minimum.

Since the landing reference surface is assumed to be 1,738 km from the center of the Moon, the flight altitude is to be 15 km - 0 km above the surface.

The results of analysis are summarized below.

- There is no solution for the time-to-go less than 480 sec. because of the additional requirements.

- Fuel consumption is minimum at both conditions; minimum time-to-go (480 sec.) and 14 degrees sweep angle. This solution is roughly the same trajectory where thrust is constantly 1,000N.

Consequently, the time-to-go and sweep angle are to be 480 seconds and 14 degrees, which leads to be ΔV 1,738 m/s.

⑤ Conditioning of v_r and h_r

The conditions devised so far are shown in Figure 4.3-7. The final velocity and altitude in the minimum-fuel trajectory are to be devised.

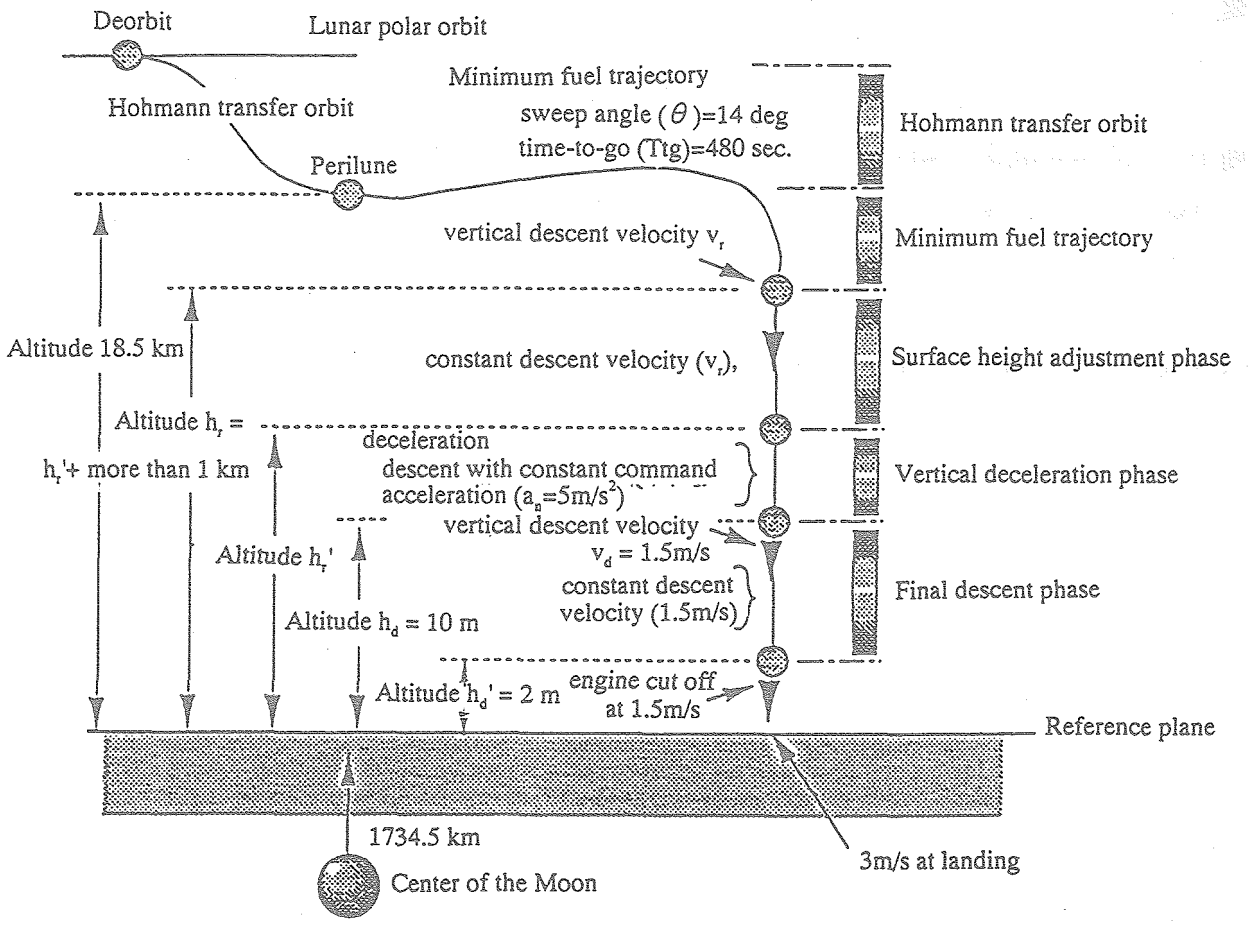

Figure 4.3-7 Determined Conditions of Reference Trajectory

The values of v_r and h_r must be selected to allow a safe landing on the modelled landing site mentioned previously and to ensure that ΔV from deorbit to the landing is minimum. As shown above in Figure 4.3-5, when v_r is assumed to be a certain value, then h_r' becomes fixed automatically. Figure 4.3-8 plots relation between h_r and the total ΔV from deorbit to the nominal landing point on the conditions that h_r' is to be the minimum altitude, and v_r is to be remaining vertical velocity above landing point.

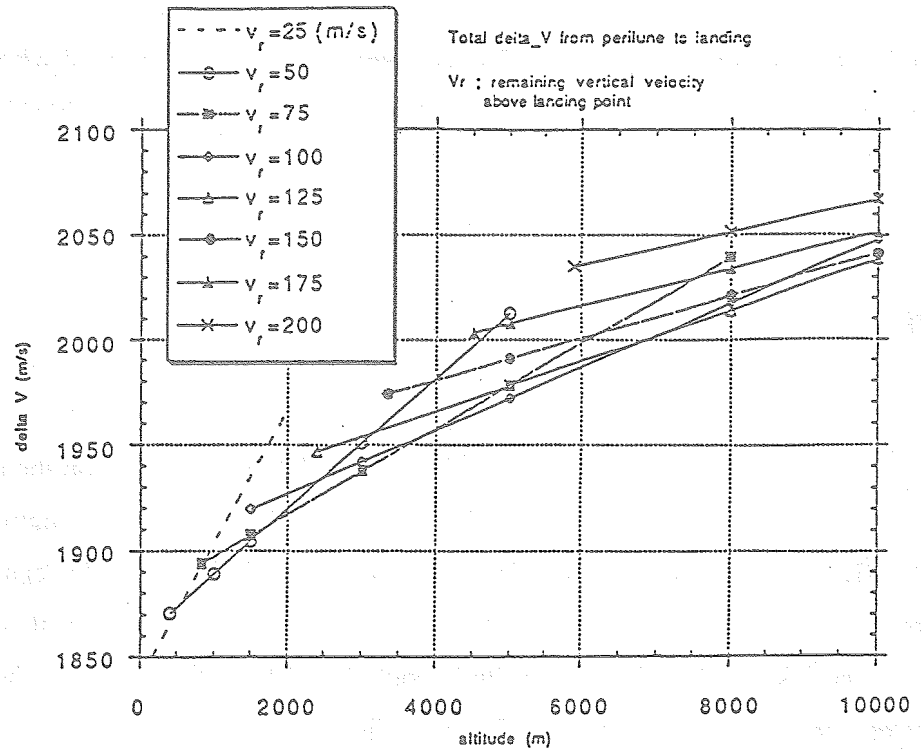

Figure 4.3-8 Relation between v_r, h_r and total $\triangle V$

The altitudes shown on this Figure are h_r ($h_r = h_r'$ on the left side of each line segment, see Figure 4.3-9). It is evident that when any altitude h_r is selected, there are relevant vertical velocities that minimize the total $\triangle V$ (from deorbit to landing) at that altitude.

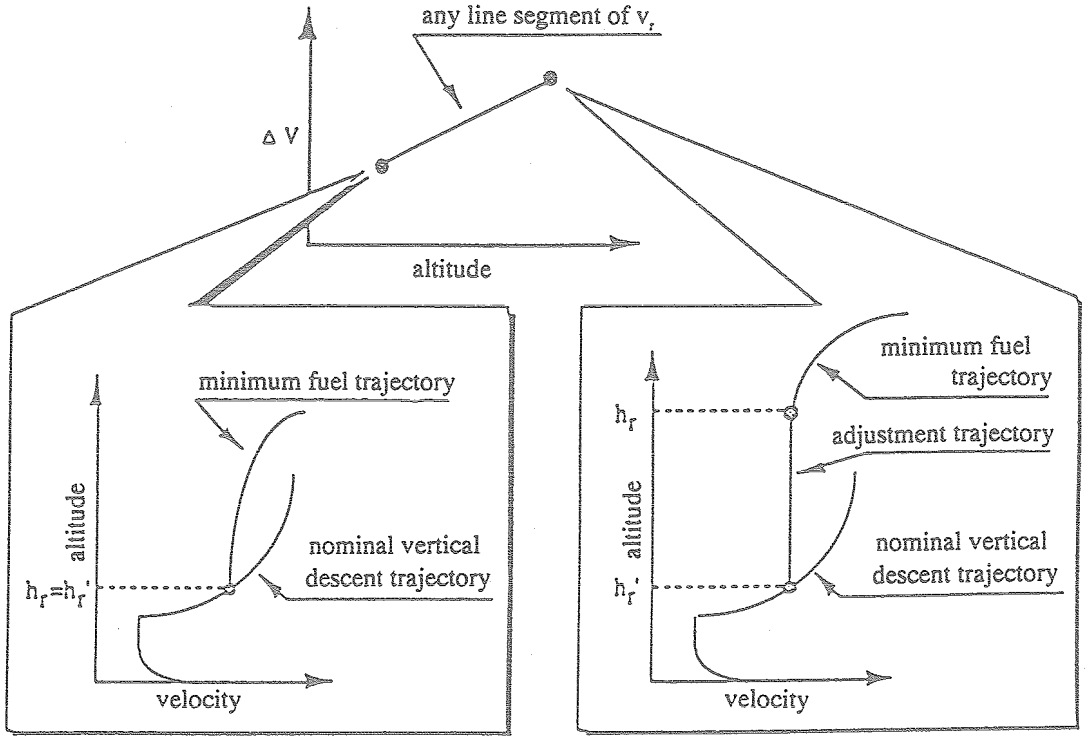

Figure 4.3-9 Velocity and Altitude Profile in Difference hr

From Figure 4.3-8, it appears that the total fuel consumption will be decreased when both of v_r and h_r are kept as small as feasible. However, certain requirements must be considered from view point of safety landing so that the optimal v_r and h_r will be derived. Two requirements may be considered.

1) Fuel margin
2) Altitude for surface height adjustment

In regard to (1), available $\triangle V$ is to be about 1939 m/s. This value is based on the conditions that the propulsion systems are to provide 2,020 m/s as the total $\triangle V$ of main engine and four percent of that figure should be excluded (3% for margin and 1% for loss). In regard to (2), the subsection of ③assumed the difference altitude to be 1 km or more. However, that altitude is here to be assumed 1 km. Therefore, the altitude could be added 1 km to that of Figure 4.3-8. These values can be plotted graphically as shown in Figure 4.3-10, which particularly focuses on the range from 0-3000 km and from 1840-1960 m/s, respectively.

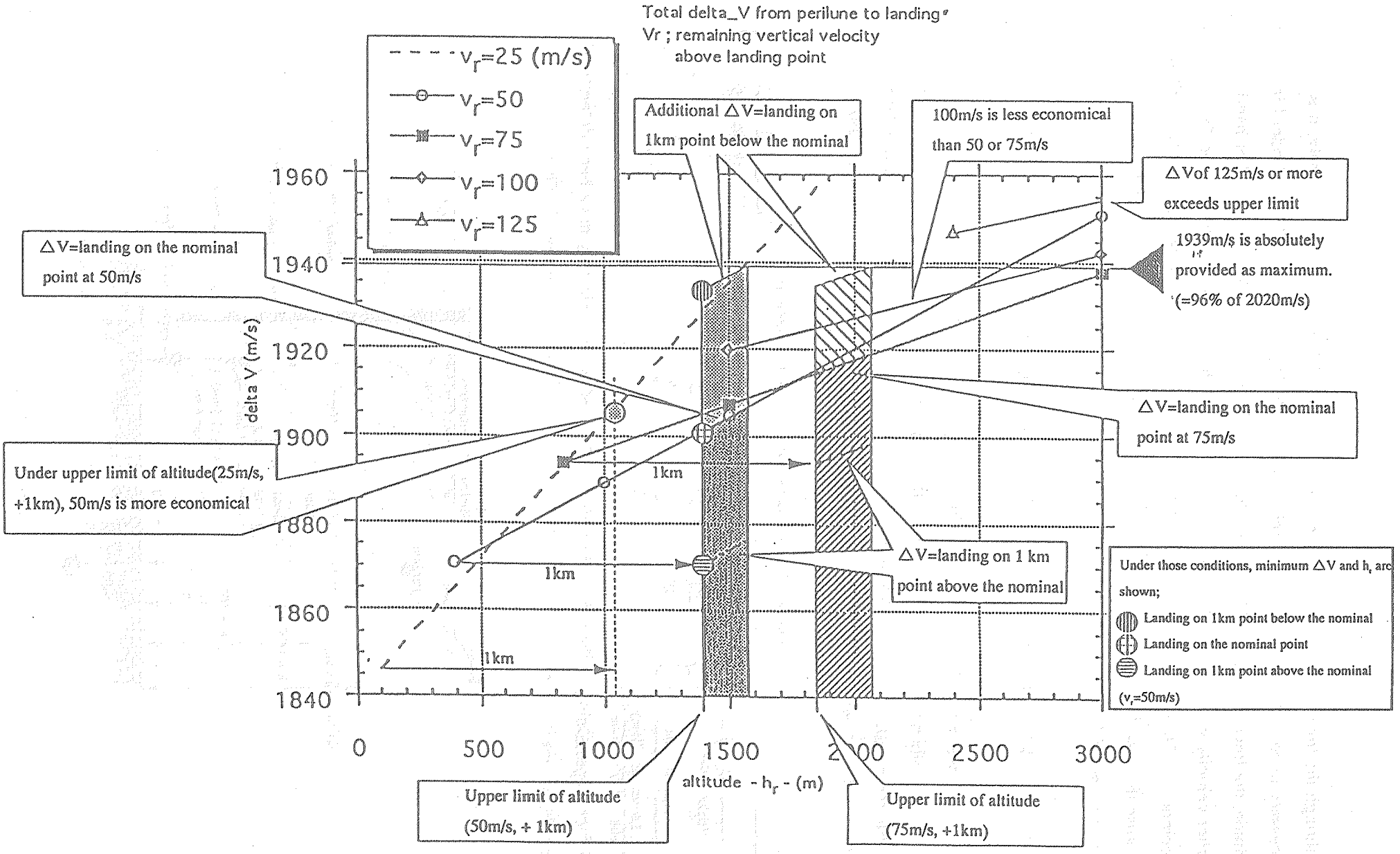

Figure 4.3-10 Total ΔV

Although the lower target values of h_r and v_r will make ΔV smaller proportionally, it is necessary to consider the constant velocity required during adjustment phase. Under higher target altitude, the lower velocity will result in the sharper increase in ΔV. On the other hand, the higher velocity will result in the larger ΔV because of the increased time required for deceleration. However, the increase in ΔV will be moderate, even with higher target altitude, because the time for the constant velocity descent becomes short. Consequently, there is likely to be a more suitable combination between h_r and v_r.

From Figure 4.3-10, the candidate values for v_r and h_r, which will land on 1km point above /below the nominal within the ΔV of 1939 m/s (96% of 2020 m/s) , are:

when v_r = 50 m/s, then h_r is in the range of 1400 m-1570 m.

when v_r = 75 m/s, then h_r is in the range of 1850 m-2060 m.

Taking the smallest value for ΔV within those ranges, v_r = 50 m/s, then h_r is around 1400 m. Table 4.3-2 illustrates ΔV and its related factors per each landing point in this condition.

Table 4.3-2 ΔV and Duration for Each Landing Point

	ΔV (m/s)	Duration (sec)	Mass at landing*(kg)
Highest point(+1km)	1868	500	185
Nominal point	1901	520	183
Lowest point(-1km)	1934	540	181

*) specific impulse=300 sec, initial mass=350 kg

All factors pertaining to the safe and minimum-fuel reference trajectory have been determined from the assumptions and conditions discussed above. Results are shown in Figure 4.3-11.

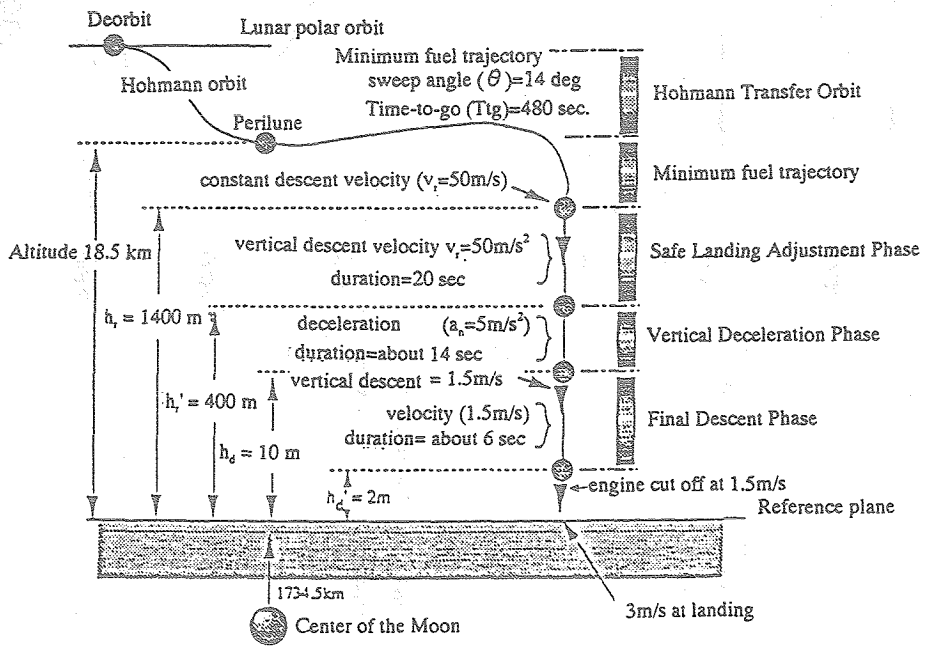

Figure 4.3-11 Conditions of Reference Trajectory

Figure 4.3-12 illustrates the approach for determining main conditions during the final descent phase. Examining Figure 4.3-11 together, it will help to understand the implication of each condition.

The above discussion provides complete coverage of determination approach for minimum-fuel and safe landing trajectory.

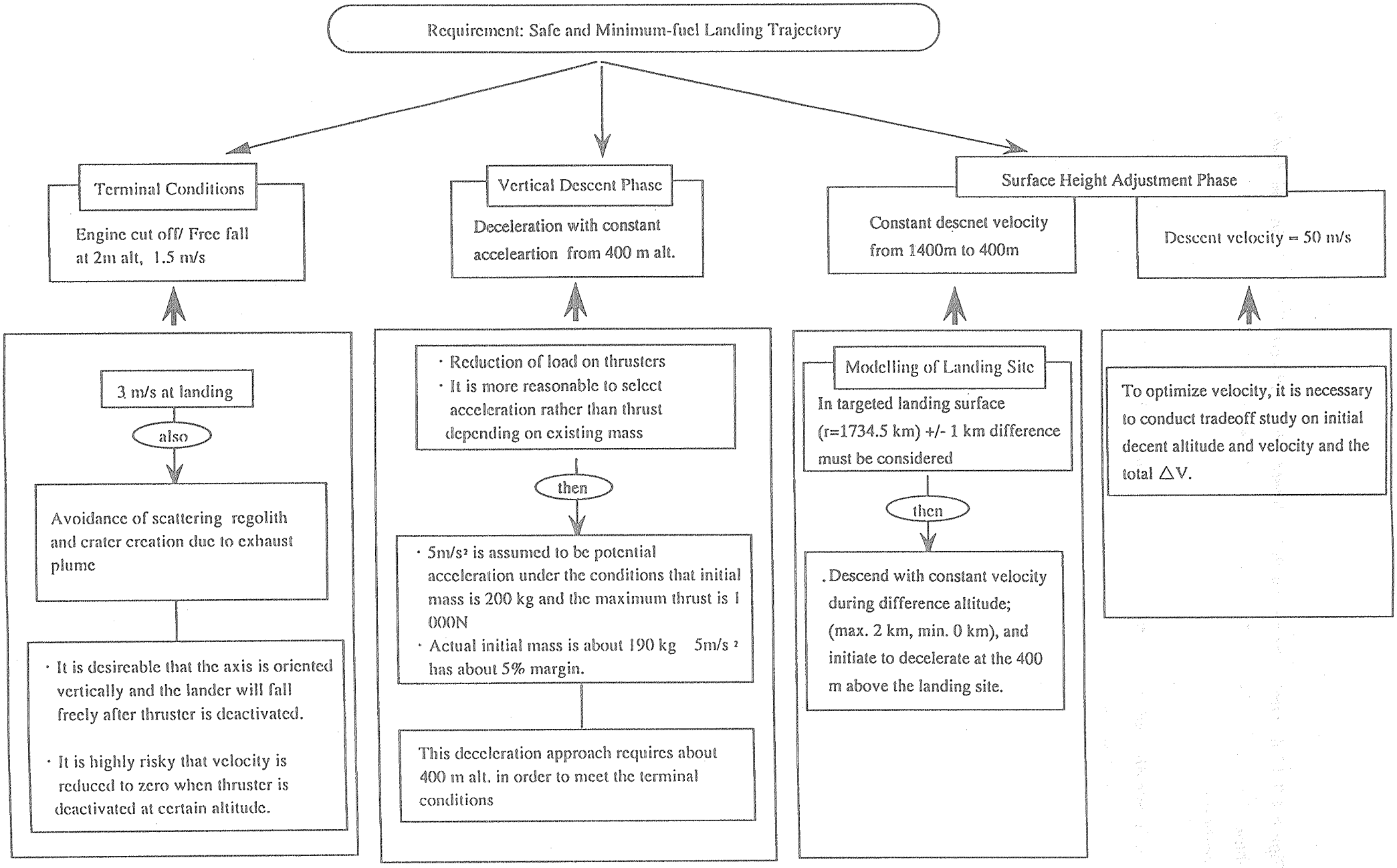

Figure 4.3-12 Outline of Conditions during Final Descent Phase

Reference

4.3-1 Edited by Cornelius T. Leondes, "Guidance and Control of Aerospace Vehicles", McGraw-Hill Book Company, Inc., (1963), pp.563-587

4.3-2 Mitsubishi Space Software Co., Nakajima, "Analysis of Lunar Landing Trajectory Based on Variable Thrust-1", Technical Memorandum PR22-0406-0001, 1995.1.23

4.3-3 NASDA Future Space Systems Laboratory, Kaneko, "Concept of Lunar Orbiter" Technical Memorandum GAF-94024, 1994.10.6

4.3-4 NASDA Future Space Systems Laboratory, Wada, "Reference for Design of Reference Trajectory of Lunar Lander" Technical Memorandum GAF-95006, 1995.1.27

4.3-5 NASDA Future Space Systems Laboratory, Takano, Ginoza, Wada, "Lunar Lander System Reference Model" Technical Memorandum GAF-94024, 1994.10.5

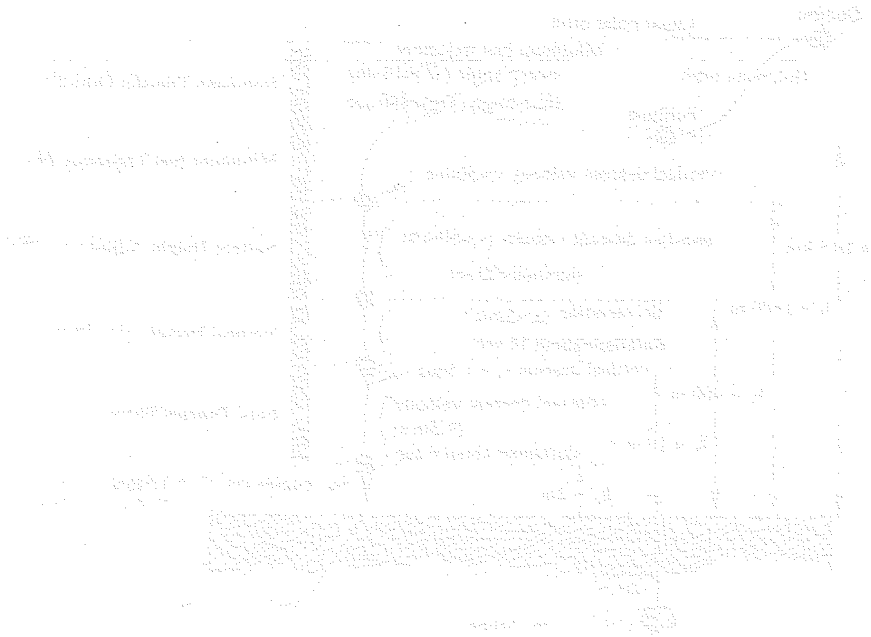

5. Conclusion

5.1 Summary

This paper has discussed each phase from lunar polar orbit to the landing on the surface. These phases were determined under a fundamental concept of a minimum-fuel and highly safe trajectory, and provided values to best meet conditions and assumptions which were made in this paper. Therefore, even when mass of the lander and its thrust slightly change, it will be feasible to determine the optimal landing trajectory by coordinating each value of these phases in accordance with measures given herein. Such trajectory will be also based on the following modelling which are developed for this study.

- **Landing site model**: The landing surface are to be 1734.5 km from the center of the Moon, and unknown altitude differences are to be ± 1 km. The sites are to be any mare on the near side on the moon. For lunar gravitational potential, Moon is assumed to be spherical, and consideration is given to only lunar-G to the lander. In addition, there will be no consideration of rotation of the Moon.
- **Lunar polar orbit**: The orbit will be circular, with a major semi-axis of 1838 km (assuming the lunar radius to be 1738 km, the altitude is to be 100 km). The inclination is 95 degrees. However, in view of the above landing site model, it is not necessary to consider that value.
- **Lander model**: The total mass is to be 350 kg, thrust is to be 1000 N (thrust variability:100-25 %), specific impulse is to be 300 sec., and the vertical downward velocity at the time of landing is to be 3 m/s or less.

Figure 5.1-1 shows an outline of the landing trajectory based on above model.

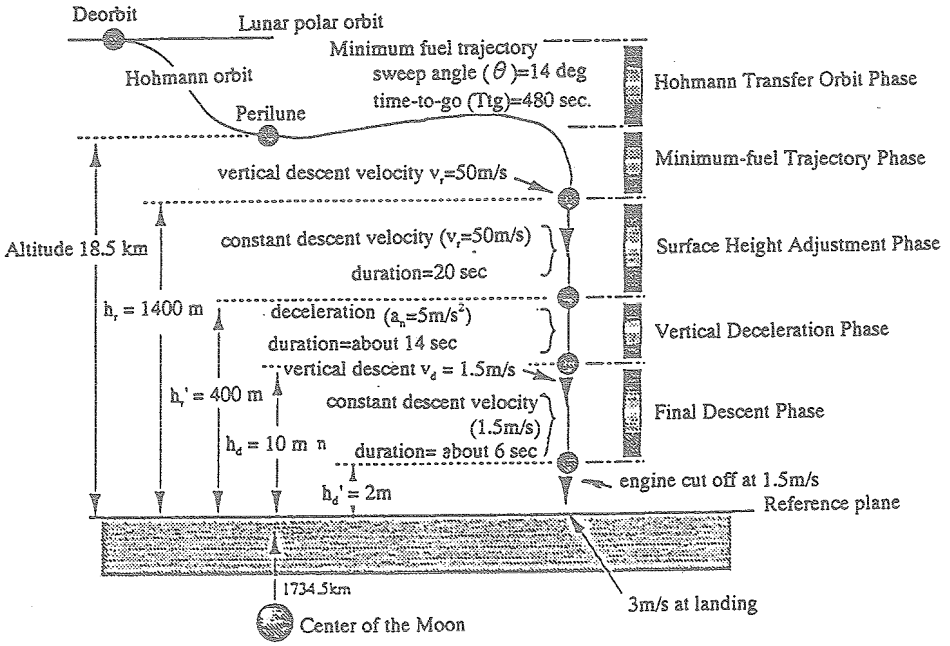

Figure 5.1-1 Outline of Reference Trajectory

The conceptual approach to the determination of reference trajectory is summarized below.

1) The minimum-fuel trajectory will be designed in accordance with the mass and thrust of the lander. In fact, it is necessary to simulate various vertical descent velocities immediately after passing the trajectory, however, this study simply assumes altitude and velocity to be both zero, which will be a similar to any trajectory with some velocities and altitudes. The design of the minimum-fuel trajectory requires a certain number of simulations. To optimize the final conditions for the minimum-fuel trajectory phase, in turn the initial conditions for the final descent trajectory, it is necessary to reversibly devise each condition of the subphases in the final descent phase.

2) When there is no change to the required velocity at the time of landing, there will be no need to change the initial conditions of the final descent phase (altitude h_d, velocity v_d). Therefore, all the conditions of the vertical deceleration phase can be devised so as to achieve a vertical velocity of 1.5 m/s at the altitude of 10 m.

3) The constant acceleration (a_n) of the vertical descent phase is devised. This value must has appropriate margin (for guidance), which is derived from the mass budget of the lander at the time of the beginning of this phase as well as the potential thrust. Based on this acceleration, the nominal trajectory is determined to meet the initial conditions for the final descent phase. From profile of altitude and velocity in this trajectory, it is necessary to select some options of vertical velocity (v_r) and altitude (h_r) in the terminus of the minimum-fuel trajectory, and h_r' in the initial altitude of vertical descent phase (altitude difference between h_r and h_r' is 1 km at the minimum).

4) Combining the minimum-fuel trajectory derived in (1) and the options for v_r-$h_r(h_r')$ selected in (3) yields ΔV from deorbit to the landing. Then, the selection of v_r and $h_r(h_r')$ is made so as to minimize ΔV. It is also necessary to consider fuel consumption for each landing case; nominal, 1 km point above the nominal, and 1 km below the nominal. It particularly notes that selection of v_r-$h_r(h_r')$ must be made to ensure that fuel consumption at the lowest landing point remains within the range of residual fuels. The resultant orbit is to be the optimal trajectory under this study.

Following this orbit design approach, it becomes feasible to determine reference trajectory to achieve the safe and economic landing at a point where altitude difference is within ± 1 km from the nominal. For the optimal reference trajectory of the lander (350 kg, 1000 N/thrust variability: 25-100%), it takes about 66 minutes to deorbit and then to land at the nominal point.

More specifically, the powered descent for deceleration lasts about 520 seconds, the total $\triangle V$ is to be about 1901 m/s, and the fuel consumption (when specific impulse is to be 300 seconds) will be about 167 kg. Table 5.1-1 illustrates $\triangle V$ and its related factors per each landing point.

Table 5.1-1 $\triangle V$ and Duration for Each Landing Point

	$\triangle V$ (m/s)	Duration (sec)	Mass at landing*(kg)
Highest point (+1km)	1868	500	185
Nominal point	1901	520	183
Lowest point (-1km)	1934	540	181

*) specific impulse=300 sec, initial mass=350 kg

In addition, Table 5.1-2 shows the features, flight time, and fuel consumption for each phase of the nominal landing.

Table 5.1-2 Summary of Nominal Landing

Phase	Feature	Altitude/Velocity	Flight time/Fuel Consumption
Hohmann Transfer Orbit	Deorbit from lunar orbit and fly to perilune	Perilune=15 km (r=1738 km). Perilune=18.5 km (r=1734.5 km), velocity= about 1692 m/s	Time=about 57 min Consumption=about 2.4kg △V=about 20m/s
Minimum-fuel Trajectory	Transfer to the targeted point in accordance with concept of minimum fuel consumption	At the targeted point, altitude=1.4 km velocity=50m/s (vertical)	Time=about 480 sec Consumption=about 157.1kg △V=about 1768m/s
Final Descent			
Surface Height Adjustment	Descend vertically with constant velocity against 1 lunar-G, and ensure safe landing	At the targeted point, altitude=400 m velocity=50m/s (vertical)	Time=about 20 sec Consumption=about 2.0kg △V=about 32m/s
Vertical Deceleration	Descend vertically at constant acceleration of $5m/s^2$	At the targeted point, altitude=10 m velocity=1.5m/s (vertical)	Time=about 14 sec Consumption=about 4.6 kg △V=about 72m/s
Final Descent	Descend vertically with constant velocity against 1 lunar-G, and deactivate thrusters at a given altitude	Deactivate thrusters at 2m alt. with 1.5m/s kept → freely fall to the surface	Time=about 6 sec Consumption=about 0.6 kg △V=about 9m/s
Entire Trajectory	Achieve the trajectory with safety and economical efficiency, combining minimum fuel and vertical descent	Velocity at landing Vertical=less than 3m/s Horizontal=less than 1.2m/s (target is 0m/s)	Time=about 66 min (including 520 sec for powered descent) Consumption=about 166.7kg △V=about 1901m/s

5.2 Comparative Study

5.2.1 Minimum-fuel Trajectory

This section will make a comparative study, from the theoretical and practical aspects, of the bilinear tangent law used as the guidance law in the previous fiscal year and the E-guidance used here.

〈Theoretical Aspect〉

The main feature of the bilinear tangent law is that guidance of the lander is controlled by changing the direction of thrust rather than its force. E-guidance, on the other hand, controls both the force and direction of thrust.

Figure 5.2.1-1 illustrates the derivation flow of the two guidance laws. The initial procedure is to choose functional for the fuel consumption per unit time and then to convert the functional into an equivalent value by using the equations of motion and the formula which defines specific impulse.

$$\dot{m} \rightarrow \frac{1}{2} a_T^2$$

In other words, the evaluation function is converted into its equivalent input energy. Next, the equations of motion is applied to Hamilton's equations of motion, and solved under the assumptions that

(1) specific impulse is constant, and

(2) gravitational acceleration is constant in orbit.

Consequently, the E-guidance formula is derived.

$$a_T = 6\frac{r - r_D - v_D(T_D - t)}{(T_D - t)^2} + 4\frac{v - v_D}{T_D - t} - g_0$$

Furthermore, from the evaluation function is rewritten with the addition of the hypothesis; (3) the force of the thrust is constant in orbit, and following the same procedure as before will yield the bilinear tangent law.

The resultant formula for thrust acceleration yields the vector functions of the current conditions (r, v, t) in addition to the terminal conditions (r_D, v_D, T_D) in the case of E-guidance. In contrast, the bilinear law is contingent only on the current time (t) in addition to the terminal conditions (r_D,

v_D, T_D). It is also the same for the formula for fuel consumption.

In view of the above, E-guidance has, in comparison to the bilinear law, the advantages of
a) placing fewer requirements on specific impulse, and
b) specifying more conditions.

Item (b) in particular helps to shorten calculation times, which will be of benefit to onboard computer.

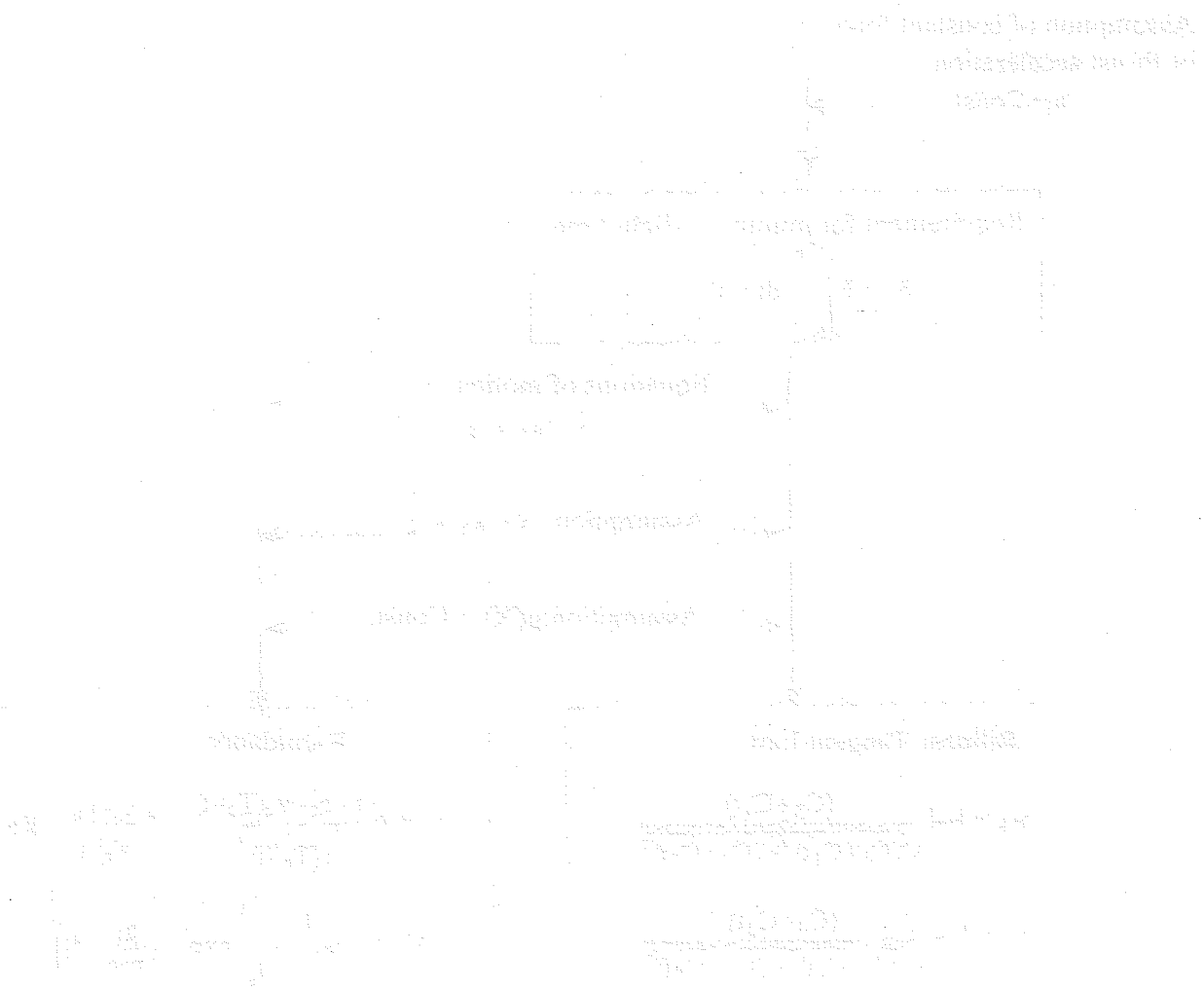

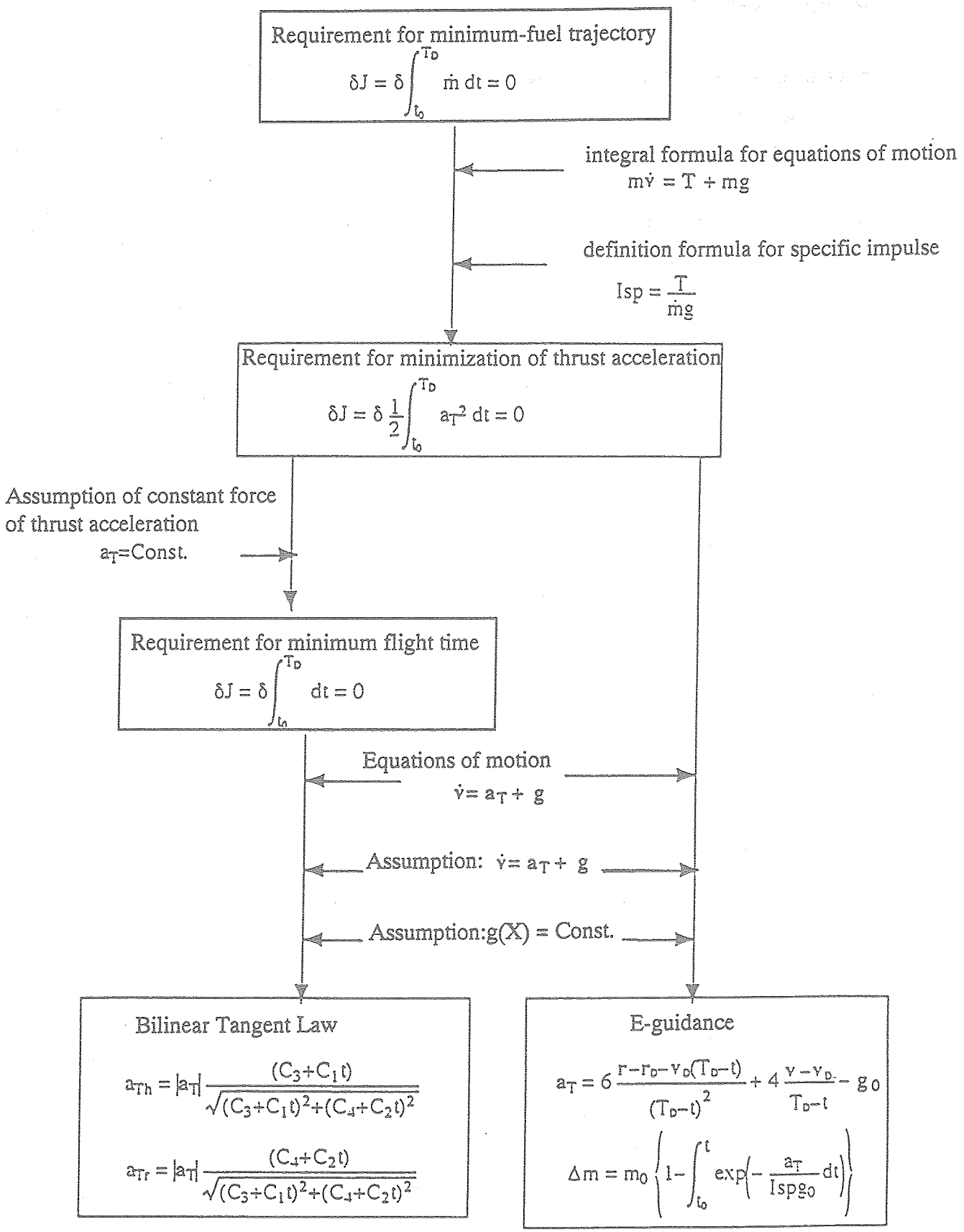

Figure 5.2.1-1 Derivation Flow of Both Guidance Laws

〈Practical Aspect〉

Let us compare the two guidance laws in terms of (1) fuel consumption and (2) orbit profile.

Based on Figure 5.2.1-2 to-6, Table 5.2.1-1 shows characteristics when the lander descends from the initial altitude of 15 km in accordance with each of two laws, and achieves zero values for altitude and velocity. As seen from Table, there is virtually no difference in regard to fuel consumption. Therefore, both laws have the same achievement in regard to the issue of fuel. Furthermore, both virtually yield the same flight time.

The difference is revealed in calculation time. E-guidance requires a shorter time for calculations, which is beneficial to onboard computer.

Another difference is that E-guidance is easier to achieve the targeted characteristics because of its feedback control systems, or closed loop systems. This makes E-guidance very favorable for the guidance.

Table 5.2.1-1 Comparison of Results

	Bilinear Tangent Law	E-guidance
Initial Mass (kg)	350	350
Thrust (N)	1000	---
Specific Impulse (sec)	320	320
Flight Time (sec)	476.565	476.565
Sweep Angle (deg)	14.119	14.119
Final Mass (kg)	197.908	197.908

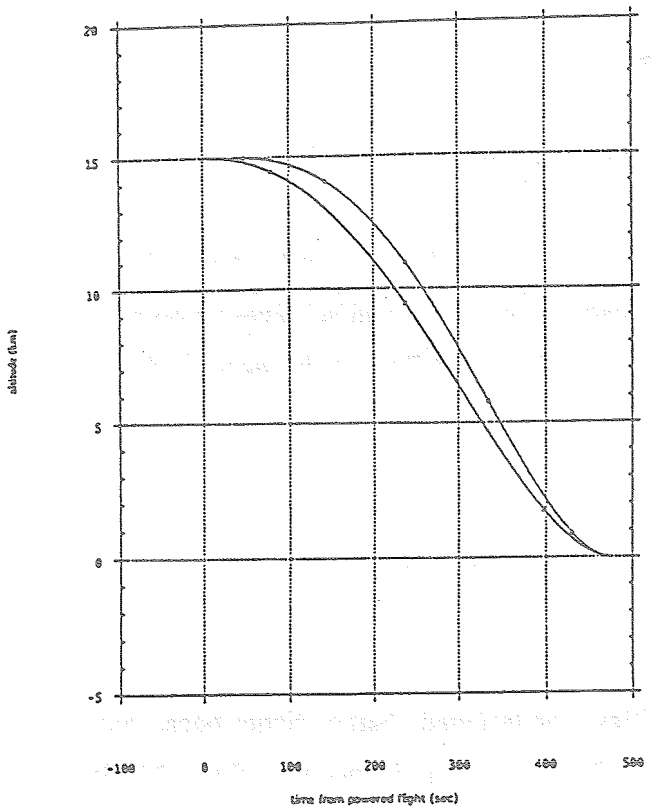

Figure 5.2.1-2 Flight Time and Altitude

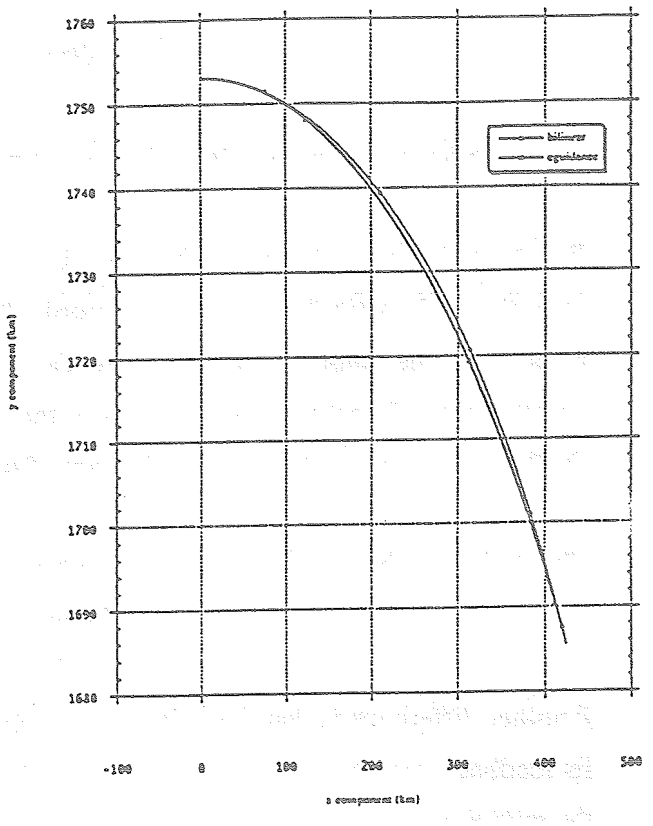

Figure 5.2.1-3 Altitude of Coordinate Systems in In

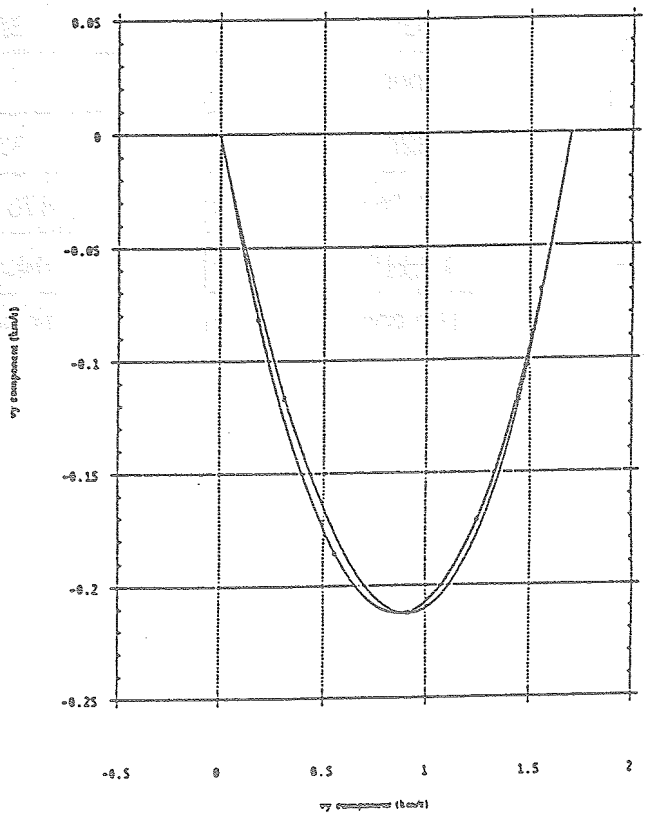

Figure 5.2.1-4 Velocity of Coordinate Systems in Inertial

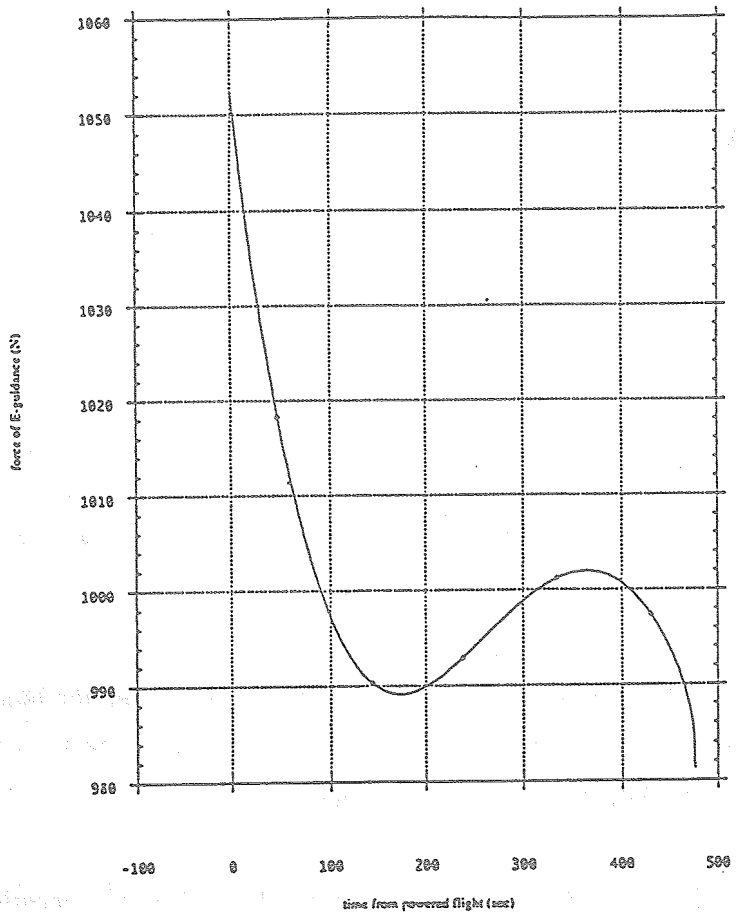

Figure 5.2.1-5 Flight Time and Thrust in E-guidance

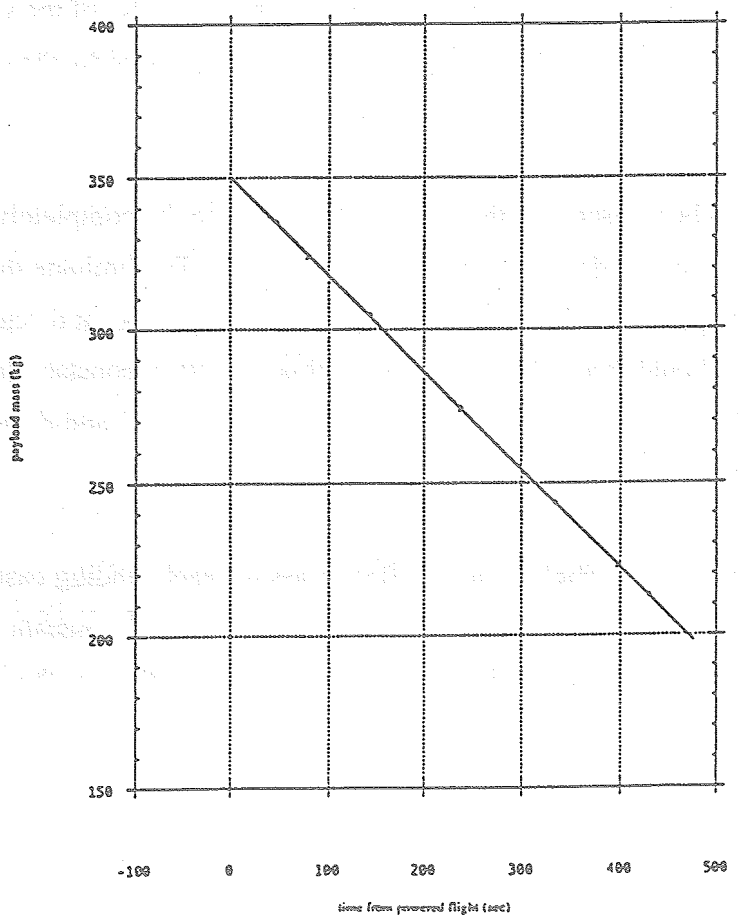

Figure 5.2.1-6 Flight Time and Payload Mass

5.2.2 Final Descent Trajectory

The final descent trajectory phase consists of the following three subphases.

1) Surface height adjustment,
2) Vertical deceleration, and
3) Final descent.

Outlines of each subphase have been provided and will not thus be further discussed here. Selection of this descent path has the following advantages.

- This path tolerates altitude difference of ±1 km. In other words, when the lander has arrived at the target point of the minimum-fuel trajectory phase, it will be possible to adjust landing site from approximately 400 m - 2,400 m altitude.

- The guidance law is simpler. In addition, the landing will be highly safe because the lander will descend at a low velocity just before landing at the target.

- The navigation sensors will collect data with higher precision because of the vertical descent. It is necessary to take sufficient protective measures on flame induced by the exhaust plume of the main engine.

However, the concern has been risen that this descent path may not be completely economical because it includes a phase of continued thrust against 1 lunar-G. To eliminate this concern, tradeoff study will be conducted on the final descent phase; vertical descent discussed in this paper and descent under E-guidance. The former is hereinafter called 'constant acceleration descent' (this is a combination of constant acceleration against 1 lunar-G and deceleration by keeping 5 m/s^2 constant).

The tradeoff is conducted on $\triangle V$, flight time and final mass for each landing case; the highest, nominal, and lowest point. The premises are that terminal conditions of constant acceleration descent (1.5 m/s at 2 m alt.) are applied. Figure 5.2.2-1 depicts an outline of the process of comparison.

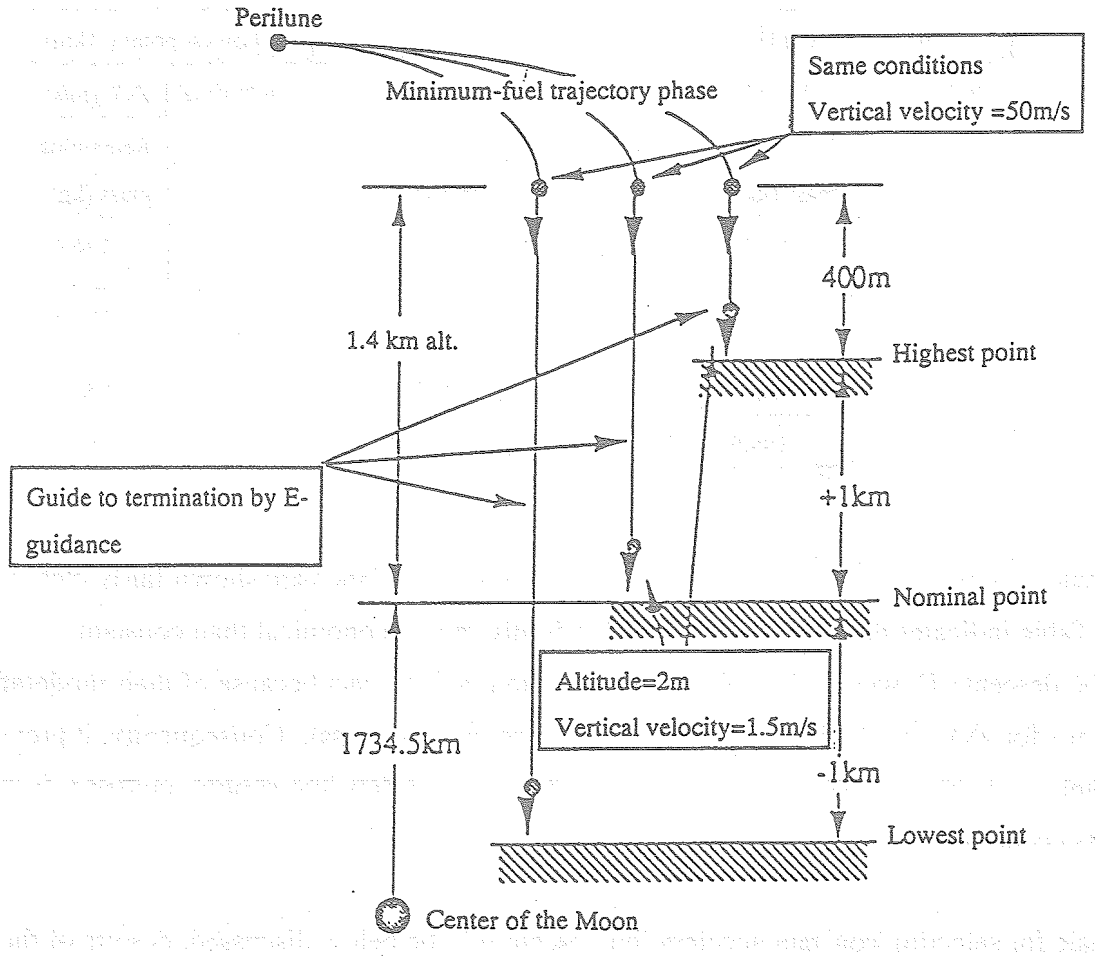

Figure 5.2.2-1 Vertical Descent under E-guidance

Table 5.2-1 shows the various values for flight time and $\triangle V$ for each landing case under constant acceleration descent and E-guidance. The initial and terminal conditions of this phase will be as follows.

Initial conditions

Mass: 190.56 kg

Velocity: vertically down at 50 m/s

Altitude: 1.4 km (assuming lunar radius is to be 1734.5 km), altitude difference of ± 1 km at the landing point),

Final conditions

Velocity: vertically down at 1.5 m/s

Altitude: 2 m from any of the landing elevations

Time-To-Go (in the case of E-guidance): optimal values devised for each landing site (See Table 5.2-1)

Table 5.2.1 Tradeoff Between Constant Acceleration Descent and E-guidance

	Highest point (+1km)		Nominal point (±1km)		Lowest point (-1km)	
	Flight time* (sec)	ΔV (m/s) / Remaining mass (kg)	Flight time* (sec)	ΔV (m/s) / Remaining mass (kg)	Flight time* (sec)	ΔV (m/s) / Remaining mass (kg)
Constant Acceleration Descent	20	81.44 / 185.4	40	114.1 / 183.2	60	146.6 / 181.3
E-guidance	15	72.7 / 185.9	35	105.5 / 183.8	52	133.2 / 182.1

*) For E-guidance, Time-to-Go is applied to minimize the fuel consumption

The differences between constant acceleration descent and E-guidance are shown fairly clearly in Table. Table indicates that E-guidance is only slightly more economical than constant acceleration descent. However, the differences have no major impact because of their moderate level (10 m/s for ΔV and 0.8 kg at the maximum for remaining mass). Consequently, it proved that constant acceleration descent with the first priority put on safety and simpler guidance is in no way less economical.

The rationale for selecting constant acceleration descent will be below discussed, despite of the fact that E-guidance features less fuel consumption. It will be reasonable to select E-guidance if we are in pursuit of economy. Therefore, it needs to prove the effectiveness of constant acceleration descent.

Figure 5.2.2-2 shows the thrust patterns for each landing point when using E-guidance.

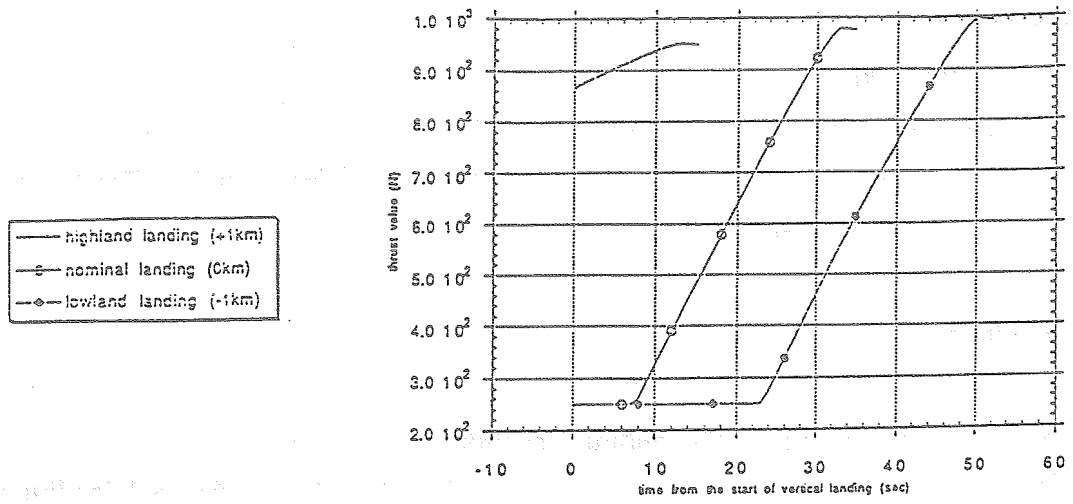

Figure 5.2.2-2 Thrust Pattern under E-guidance

From this Figure, descent velocity is initially increased by throttling down on thrust (reduction in flight time because of faster falling), and higher velocity is then controlled by increasing thrust gradually. In this thrust pattern, it needs engine to be cut off for free fall at the early stage, and to be ignited again for control at the final stage where the flight profile is optimized.

Such thrust profiles are likely to have risks of requiring the maximum thrust immediately before reaching at the terminal target. In other words, if there are errors (particularly delay) in the time required for the maximum thrust due to incorrect computation and measurement of navigation and other sensors, it will be difficult for the lander to fully complete its deceleration, which would place it in extreme danger. Furthermore, the required thrust may in certain cases exceed upper limited value (the situation shown in the Figure below) and crash into the lunar surface (example in Figure 5.2.2-2 is not in such situation).

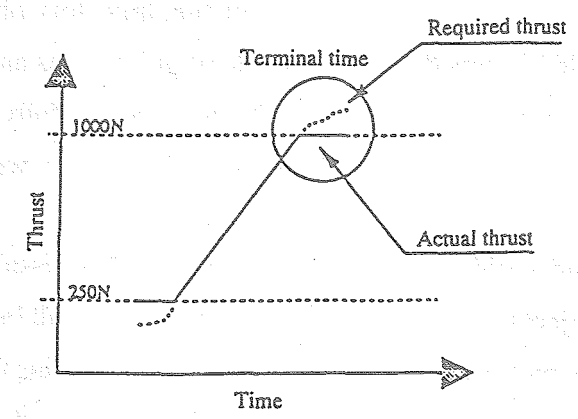

Figure 5.2.2-3 Required and Actual Thrust at Terminal Time

Figure 5.2.2-4 uses the nominal landing as an example to show what thrust profiles would be like under constant acceleration descent.

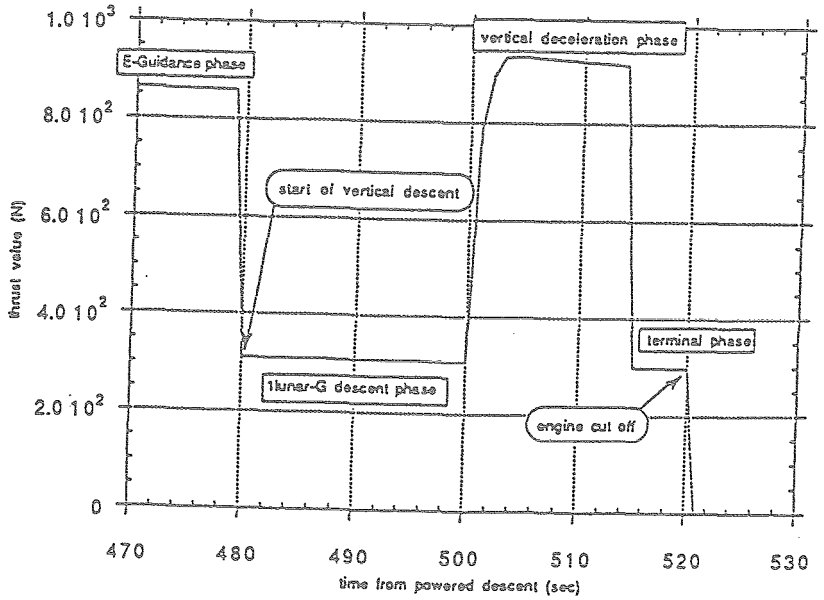

Figure 5.2.2-4 Thrust Profile at Constant Acceleration Descent

The time in this Figure is measured from the powered descent from the point of perilune (minimum-fuel trajectory phase), and vertical descent starts from 480 seconds. The values of thrust are specified so as to be within the upper limit of 1000 N and lower limit of 250 N. Moreover, there appear to be none of the risks that would be seen under E-guidance because sufficient margin for guidance to the terminal target is kept.

In view of the above discussion, constant acceleration descent examined in this paper is no less economical than the minimum-fuel vertical descent under E-guidance; moreover its orbit is likely to allow a safe and efficient landing on destination.

This paper does not discuss lateral guidance during the vertical descent, nor obstacle detection and avoidance. In regard to lateral guidance, it has been assumed here that horizontal velocity could be reduced to 0 (zero) at the final stage of minimum-fuel trajectory phase, however, in fact horizontal velocity should be considered. Since lateral guidance is an essential component to reduce horizontal acceleration to 0 (zero), it will be necessary to fully examine at which phase lateral guidance should be applied and which type of guidance law would be appropriate.

For obstacle detection and avoidance system, it depends on the mission and payload. In addition, it is largely subject to what extent obstacle avoidance will be needed (only for demonstration of landing technology or for mission after the landing). Based on the requirements, there will be discussions on the allowable values for the additional mass and fuel needed to perform obstacle detection and avoidance. In any case, it will be necessary to give

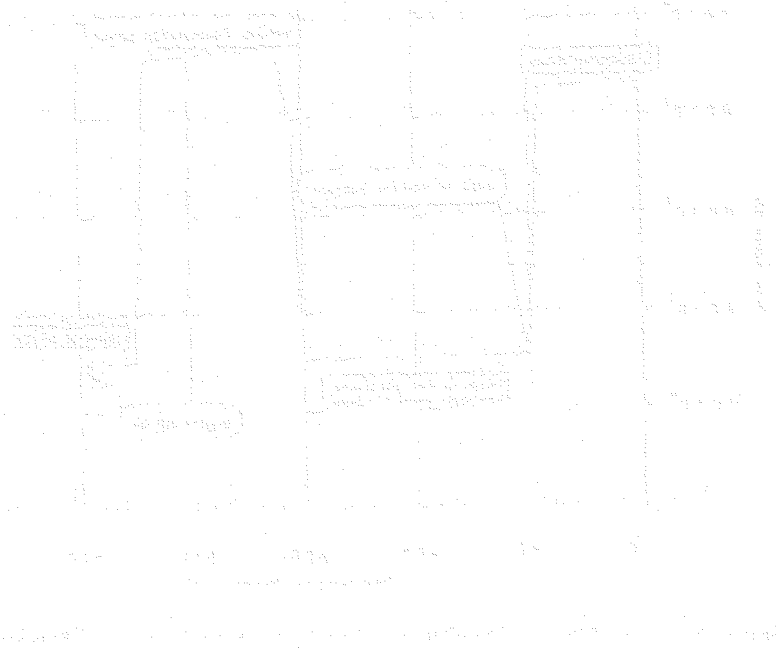

5.3 Future Studies

5.3.1 Discussion of Formulas (1)

As mentioned in section 4.2, the following requirements are not taken into account when the formulas for E-guidance are derived.

(1) Requirement for force of thrust

$$T_{min} \leqq T \leqq T_{max}$$

(2) Requirement for altitude

$$h(T_D) = h_{min} \qquad (h \geqq h_{min})$$

(3) Requirement for terminal attitude

Vertical at termination

$$\varphi(T_D) = \tan^{-1} \frac{v_r}{v_h}\Big|_{T_D} = \frac{\pi}{2}$$

Determination of the nominal orbit needs to monitor the computed orbits and select out the appropriate which meets those requirements and minimizes fuel consumption.

Nonetheless, it is desirable that there should be no oversights and errors generated in human search process. One alternative, for example, is first to replace the expressions by

$$T - \left(\frac{T_{max} - T_{min}}{2} \sin u_1 + \frac{T_{max} + T_{max}}{2}\right) = 0$$

$$h_1 = h - h_{min} \sin u_2 = 0$$

$$\varphi_1 = \varphi - \frac{\pi}{2} = 0$$

Thus, we have the Hamilton's equation

$$H = \frac{1}{2} a_T^2 + \lambda_1 \cdot v + \lambda_2 \cdot (a_T + g) + \lambda_3 \left\{T - \left(\frac{T_{max} - T_{min}}{2} \sin u_1 + \frac{T_{max} + T_{max}}{2}\right)\right\}$$

$$+ \lambda_4 \left(\varphi - \frac{\pi}{2}\right) + \cdots$$

and then we need to solve the corresponding equations of motion,

$$\dot{\lambda} = -\frac{\partial H}{\partial x}$$

$$\frac{\partial H}{\partial a_T} = 0$$
$$\frac{\partial H}{\partial u_i} = 0$$

Since those equations should be solved numerically rather than analytically, it leads to increases in calculation time and, on the other hand, decreases in human errors and enhancement of reliability.

These requirements are also met from practical point of view. As can be seen in Figure 4.2.4-8, approximately 70% of powered flight time are to be at maximum thrust, and the duration is not under the control of E-guidance. It is therefore necessary to follow a different guidance law in order to maintain the objective of minimum-fuel consumption. The previously mentioned formula meets that requirements.

5.3.2 Discussion of Formulas (2)

When deriving E-guidance by using the canonical equations,

$$a_T = 6\frac{r - r_D - v_D(T_D - t)}{(T_D - t)^2} + 4\frac{v - v_D}{T_D - t} - g_0$$

it is assumed that the gravitational acceleration is constant. A strict solution can be obtained when solving the equation without this assumption; however, the derivation will not be made here because of the difficulty of the analysis. That will be an issue to be solved in the future.

5.3.3 Landing Site Model

For landing site modelling, it is definitely the first priority to obtain as much detailed data as is currently feasible. As mentioned previously in this paper, the selection of the landing site should be made in terms of mission and operational requirements rather than orbital characteristics alone. The early identification of those requirements will allow the site to be modeled in more detail, in turn the trajectory to be developed with higher precision (in other words, this will allow fuel consumption to be estimated with greater accuracy). As one example, the altitude difference at the landing site is currently thought to be ± 1 km; however, if it were possible to narrow this difference down to several hundred meters, that would reduce fuel consumption in the worst case flight scenario and would reduce the mass of the lander.

5.3.4 Landing Trajectory

The landing trajectory is here referred to flight path from the perilune initiating powered descent to the landing. However, the entire trajectory should properly include lunar orbit and deorbit. Figure 5.3.4-1 simply illustrates analysis flow to determine the trajectory. It is clear from this Figure that this study is an extremely limited one, when viewed from the overall landing technology systems. Below is a brief set of items for further study.

1) From deorbit to powered descent

- Development of the deorbit sequence
- Identification of errors at deorbit (the precision of deorbit and the performance of sensors for navigation and guidance)
- Identification of orbit transfer errors induced by the lunar gravitational potential
- Identification of dispersion at the initial point of powered descent

2) From the powered descent to landing

- Development of the landing point (landing site modelling and allowable disparities)
- Development of the landing trajectory
- Identification of errors during powered descent (continued thrust, the precision of attitude control, and the performance of sensors for navigation and guidance)
- Identification of dispersion at the landing point

3) Orbit calculations and analysis of errors for the entire trajectory

- Identification of the landing trajectory (including dispersion at the initial powered descent point) and of dispersion at the landing point
- Feasibility study on the landing model
- Corrections and updates for the performance of sensors for navigation /guidance, and the lander, and the landing trajectory

These items will reveal the need for further studies in detail.

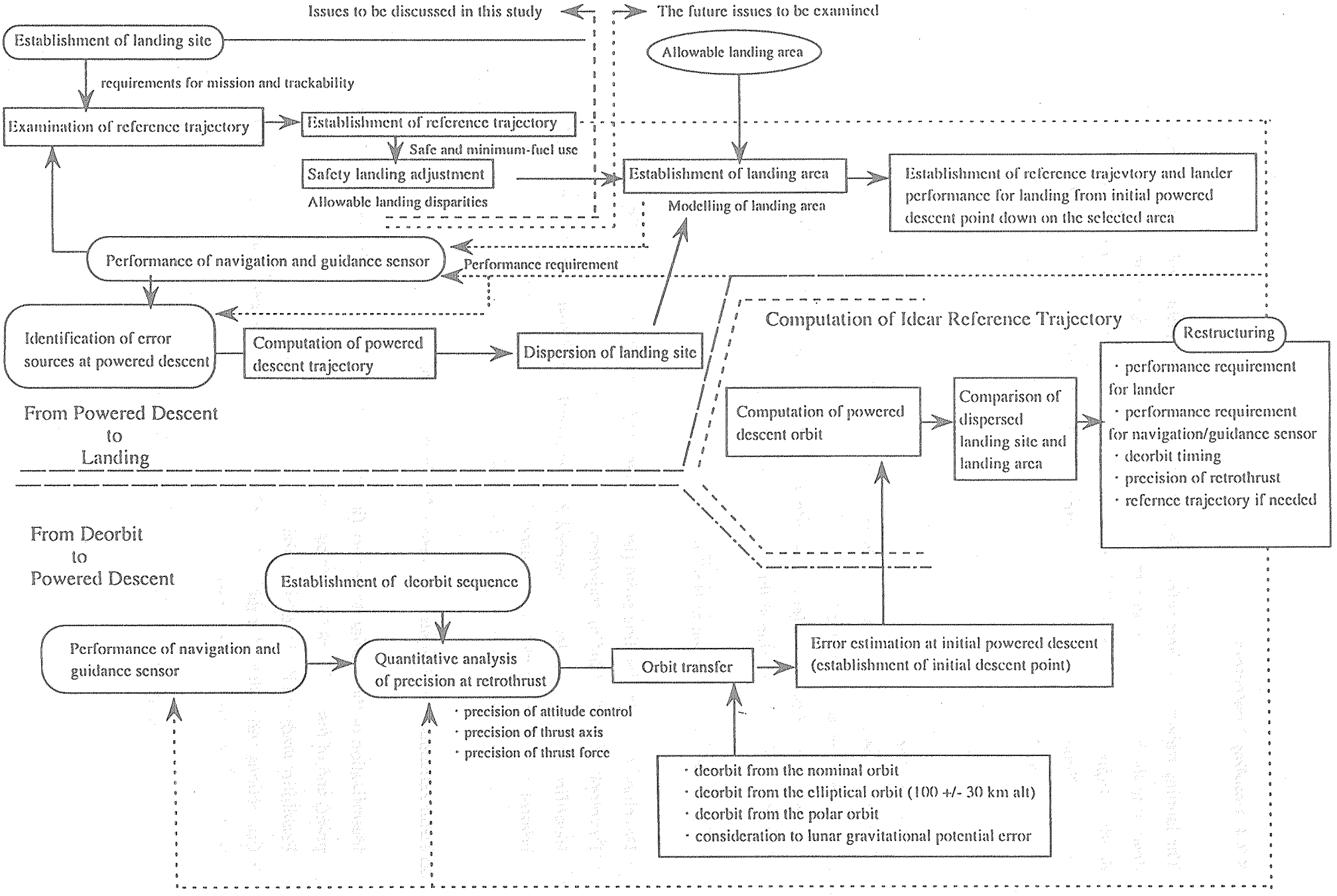

Figure 5.3.4-1 Trajectory Analysis Flow

Below are discussed the further issues related to reference trajectory in this paper.

(1) Hohmann Transfer Orbit

As mentioned previously, it is necessary to develop the separation and retrothrust sequence, and evaluate effects of errors on subsequent orbits. In addition, it is necessary to evaluate the orbit transfer errors induced by the lunar gravitational potential and the flight path, and differences in the terminal conditions.

(2) Fuel-minimal Trajectory Phase

This phase has already been optimized, based on E-guidance; however, this may change if it later becomes possible to identify a better guidance law. It will be necessary at the present stage to retain some flexibility to adopt any other guidance law. In any guidance law, it is necessary to extract factors related to differences in the terminal conditions and to make estimate of additional fuel to be required when the lander deviate from the nominal orbit.

(3) Surface Height Adjustment Phase

This phase has an issue of control attitude; the lander will be laterally tilted by about 60 degrees and should shift thrust axis to 0 degree at the initial stage of this phase. There would be no problem if RCS controls the attitude of the lander instantly. However, the maneuver in fact requires a certain amount of time, during which the conditions of the lander change second-by-second and its orbit slips out of the reference trajectory. Moreover, reduction of the thrust from around 750 N to 300 N requires an certain amount of time. It is thus inevitable to examine how to minimize such time and control attitude successfully.

The recent analyses provided a method to orient the axis where it should be at the final stage of minimum-fuel (the initial stage of this phase) by coordinating the flight time of the minimum-fuel trajectory and the sweep angle (although this will not be economical in terms of fuel). This method would contribute to eliminating the difficulty of attitude control, however tradeoff study should be conducted on difference of fuel consumptions required for RCS and this method.

(4) Vertical Deceleration Phase

In this phase of vertical deceleration in accordance with the equations discussed previously in section 4.2, the optimal value for guidance gain Ka should be developed. This study used an

empirical value based on several simulations. However, there is no guarantee that this actually is the optimal value, so this empirical value must be set logically and systematically as much as feasible. Other guidance laws may also conceivably be applied for greater economy. This issue is further to be examined.

(5) Final Descent Phase

This phase should fully consider anti-regolith characteristics of the lander and its orbit, as pointed out in this paper. The quantitative analyses are mainly made on relation between scattering regolith and creation of craters and thrust, altitude, and descent velocity through CFD (one of numerical fluid simulations) and experiments using regolith simulant. Moreover, the detailed tradeoff study should be conducted so as to optimize the target altitude of the final conditions in the vertical descent phase (h_d').

5.3.5 Other Technologies (lateral guidance, obstacle detection and avoidance)

The major component of descent orbit herein is vertical guidance rather than lateral guidance. However, there actually may be a remaining lateral velocity, and thus it is necessary to examine another guidance law to achieve optimal values. This lateral guidance is inevitably to reduce the horizontal velocity to 0 (zero), and full consideration is given to questions such as at which phase lateral guidance should be conducted, and what type of guidance law would be appropriate.

In addition, this paper excludes detection and avoidance system for the craters and obstacles. It will be possible to examine more suitable detection and avoidance system through the landing site modelling and understanding of more topographic details. Under the present situations, study on detection and avoidance system should be performed to identify the appropriate system for various type of mission and payload by using hypothetical models of the craters and obstacles. However, the determination of the system is largely interrelated to requirements for control attitude and obstacles detection in the current concept of the lander. Based on the requirements, it will be further discussed how much additional mass and fuel are to be required and tolerable. Hovering to avoid obstacles should be strictly avoided because it would lead to an increase in $\triangle V$ (hovering at an altitude of 100 m would increase $\triangle V$ by about 100 m/s). If hovering is adopted during this final descent orbit, the vertical deceleration phase or the final descent phase is to be considered (surface height adjustment phase would not be appropriate because the flight time could not be determined). It will be necessary to examine guidance algorithm as well as required time. Therefore, time and effort must be devoted to determine the feasibility of this system in the future.

NASDA Technical Memorandum (NASDA-TMR-950013T)
Date of Issue : March 25, 1996
Edited and Published by :
National Space Development Agency of Japan
2-4-1, Hamamatsu-cho, Minato-ku,
Tokyo, 105-60 Japan

Inquiries and suggestions on the Report
should be addressed to :
Technical Information Division
External relations Department
2-4-1, Hamamatsu-cho, Minato-ku,
Tokyo, 105-60 Japan
FAX : +81-3-5402-6516
* This report is an English version of NASDA-TMR-950013

NASDA

NATIONAL SPACE DEVELOPMENT AGENCY OF JAPAN